2016

High Affinity Block of ICl,swell by Thiol-Reactive Small Molecules

Sung H. Park
Virginia Commonwealth University

HIGH AFFINITY BLOCK OF $I_{Cl,swell}$ BY THIOL-REACTIVE SMALL MOLECULES

A dissertation submitted in partial fulfillment of the requirement for the degree of
Doctor of Philosophy at Virginia Commonwealth University School of Medicine
by

Sung Hoon Park

Studies toward M.Sc., University of San Francisco, 2007-2010
B.Sc., University of California, Los Angeles, 1996

Director: CLIVE M. BAUMGARTEN, PH.D.
Interim Chairman of Physiology and Biophysics
Professor of Physiology and Biophysics,
of Internal Medicine (Cardiology),
and of Biomedical Engineering

Medical College of Virginia
Virginia Commonwealth University
Richmond, Virginia
July, 2016

Acknowledgement

First off, let me just thank God for turning me back toward what I love the most. Yes, it is Science! Secondly, anyone who says that electrophysiology, especially whole cell patch-clamping, is easy is clearly confused. I respect all those who practice electrophysiology in any shape or form; however, in my opinion, the deepest enlightenment can be found in forming high giga ohm to tera ohm seals prior to forming whole cell configuration. Yes, I have seen tera ohm seals! So I would have never thought driving cross country from Agoura Hills, California and arriving in Richmond, Virginia back in August 22, 2010 was for the purpose of forming giga ohm seals to measure $I_{Cl,swell}$, which is something I have never even heard of until I set foot in Dr. Clive M. Baumgarten's Laboratory. Just when I was losing hope after several rotations here at Medical College of Virginia, I reluctantly discovered whole-cell patch clamping. Measuring current *in vitro* did not come easy, but in this case diligence paid off with the end result leading to the ultimate discovery of a high affinity tag for $I_{Cl,swell}$.

So I dedicate this work to my family and friends who stood by me through this long road to Ph.D. I especially would like to personally thank my wife, Jihee, for enduring through my tantrums and giving birth to my two beautiful daughters, Romie Chae-Ah and Rorie Chae-Young Park. And of course I could never have done this alone without the help of my parents, So Ja (Sue) and Young Kwon Park, who have provided unending support through hardship. I want to thank my mom (Sue) for flying more than 7000 miles from Dae Jeon, South Korea to witness my Thesis Defense which took place on July 20,

2016. Let me also thank my mother in-law, Young Ae Lee, who also flew more than 7000 miles from Jinju, South Korea to take care of my young ones during these enduring times and making iodide rich traditional seaweed soup for my wife following the birth of Rorie on June 5, 2016 at 10:14 AM. And I want to thank my father in-law for his generous gift congratulating me and my family. There are so many people to thank, but the list would not be complete without mentioning Deacon Ahn, Dae Wook's family along with his wife Lee, Shin Young who took precious time out of her schedule to look after Romie and also providing generous portions of seaweed soup that lasted us for so long. I also thank Mina (my wife's friend), Deacon Grant Lee and his wife Christina, and Elder Roh and his wife for also providing healthy portions of seaweed soup and plenty of Korean food to keep us busy. And to my best buddy, Jung Han Kim, Ph.D. and his wife, I extend my special thanks. Let me not forget, Jung Hoon for his friendship and helping me with obtaining all the goodies and coffee for the actual defense.

With that I want to express my deepest gratitude to Dr. Clive M. Baumgarten for his unending mentoring through his open door policy which has led to many interesting discoveries. It has been an awesome run and I am forever indebted to Clive Baumgarten. His corrections seem endless and sometimes it drove me to the brink of pulling my hair out; nonetheless, I have become a better scientist and an improved writer from his mentoring. I want to also thank Dr. Diomedes Logothetis and Dr. Lou DeFelice for their moral support through the completion of my project. It was really their instrumental hand which placed me under Clive Baumgarten. I cannot thank you guys enough for your mentoring. Thanks to all of you, the world of ion channels makes a little more sense now. But I have so much more to learn about this fascinating world. And last but not least, I wish to also extend thanks to my committee for taking the time to read my thesis and provide valuable feedback. And thank you Medical College of Virginia for providing a physical roof over my head both at home and at work during my fascinating research experience.

And let me just end this with a dream that a Master's student, Noah Belkhayat had regarding my thesis. So one day Noah walks into the lab and says that in his dream he finds a Master's Thesis sitting around. Apparently Noah asks me about this nicely written Master's Thesis in this dream sequence and I happen to tell him the following: "That's my Master's Thesis. I thought Dr. Baumgarten was not going to let me leave with a Ph.D. so I wrote a Master's Thesis instead." I am really glad that Noah's dream never came true and was not some omen because I am walking out of the lab more refined and ready to take on any project whether it be science or not. I was not upset at all about Noah's dream. To the contrary, I truly had a good laugh and now I will never forget it. In a way, this episode of Noah is quite complimentary to me and Dr. Clive M. Baumgarten as summed up by Noah's acknowledgement:

> Without a doubt, I am forever indebted to Sung Park. As I write this, SHP sits just over my shoulder, working and working and working and working and working away. As I had no prior research experience, he put me through the paces and taught me to be diligent. He was a major contributor to the basis of my thesis, even though he says "All the credit goes to the man who did the experiment, not the guy who thought about it." I tend to disagree, so count the number of times I mention him as a reference. He constantly reminds me we have joined an elite club, "THIS IS BAUMGARTEN LAB!"

Of course, for those of you who experienced the 2006 epic fantasy film ***300***, you might hear a little bit of King Leonidas played by Gerald Butler in all this. What I really meant was that whole cell patch-clamping takes time and due diligence where one must show up every day and work hard. I believe we only scratched the surface of $I_{Cl,swell}$. The true molecular basis in my opinion is still up for grabs. Perhaps this current Thesis can shed some major light on this subject with ebselen-*para*-yne.

Table of Contents

List of Figures and Tables

List of Figures in Appendix

List of Abbreviations

Abbreviation	Full Name
9AC	9-anthracene carboxylic acid
Ag85c	*Mycobacterium tuberculosis* antigen 85 complex
AngII	angiotensin II
AntiA	antimycin A
AQP4	aquaporin 4
AT_1R	angiotensin II receptor, type 1

BEST1……bestrophin 1

BK……...big conductance K^+ channel

CaCC……Ca^{2+}-activated chloride channel

cAMP……..cyclic adenosine monophosphate

CFTR(inh)-172…4-[[4-Oxo-2-thioxo-3-[3-trifluoromethyl)phenyl]-5-thiazolidinylidene]methyl]benzoic acid

CLC……...chloride channel

CNE-2Z……...nasopharyngeal carcinoma cells

CPAE……calf bovine pulmonary artery endothelial cell

Cx43……connexin 43 gap junction α-1 protein

DCPIB……4-[(2-Butyl-6,7-dichloro-2-cyclopentyl-2,3-dihydro-1-oxo-1*H*-inden-5-yl)oxy]butanoic acid

Diaz……..diazoxide

DIDS……4,4′-diisothiocyanotostilbene-2,2′-disulfonic acid

DI TNC1……Diencephalic astrocyte, *Rattus norvegicus* cell line

DNDS……..4,4′-dinitrostilbene-2,2′-disulfonic acid

DPC……diphenylamine-2-carboxylic acid

DR3305……..ebselen

Ebs……2-phenyl-1,2-benzisoselenazol-3(2H)-one (ebselen)

Ebs-biotin……biotinylated ebselen

Ebs-*p*-yne……..ebselen-*para*-yne

EbO……...ebselen oxide

EGF……...epidermal growth factor

EGFR……...epidermal growth factor receptor

ET-1……endothelin-1

ET_AR……endothelin receptor type A

FAK……...focal adhesion kinase

GFAP……glial fibrillary acidic protein

GLAST……..glutamate aspartate transporter

GLT-1……glutamate transporter

GPx……glutathione peroxidase

hCFTR……human cystic fibrosis transmembrane conductance regulator

HEK293……..……human embryonic kidney cells

HeLa……..immortalized cell line derived from cervical cancer cells

IAA-94……..indanyloxyacetic acid-94

I_{Ca}……calcium current

$I_{Cl,Ca}$……Ca^{2+}-activated Cl^- channel

$I_{Cl,PKA}$……protein kinase A-dependent Cl^- current

$I_{Cl,swell}$…… swelling-activated chloride current

$I_{Cl,vol}$…… volume-activated chloride channel

I_K…… Ca^{2+}–sensitive K^+ current

I_{K1}…… inwardly rectifying potassium current

I_{Ks}…… slow delayed rectifying K^+ current

I_{Na}…… sodium current

K_{ATP}…… ATP-dependent K^+ channel

Kir…… inwardly-rectifying K^+ channel

LRRC8A……..leucine-rich repeat-containing protein 8A encoded by the *LRRC8A* gene

MDR-1……P-glycoprotein or multidrug resistance protein

MTSEA……2-Aminoethyl methanethiosulfonate hydrobromide

MTSES……..2-Sulfonatoethyl methanethiosulfonate sodium salt

MTSET…….. 2-(Trimethylammonium)ethyl methanethiosulfonate, bromide

NAC…… N-acetyl-L-cysteine

NEM…….. N-Ethylmaleimide

NIH/3T3…… fibroblasts

NOX…… NADPH oxidase

NPPB…… 5-nitro-2-(3-phenylpropylamino) benzoic acid

PI-3K…… phosphoinositide-3-kinase

pI_{Cln}…….. phospholemman

PIP_2…… phosphatidylinositol 4,5-bisphosphate

PKC…….. protein kinase C

PP2…….. protein phosphatase 2

PRD…… proline rich domain

PZ51……...ebselen

RNS…… reactive nitrogen species

ROS…… reactive oxygen species

SAC…… stretch-activated channel

SITS…….. 4-acetamido-4′-isothiocyanostilbene-2,2′-disulfonic acid

SPI-1005…….. ebselen

Src…… proto-oncogene c-*Src*

SRIXE……. synchrotron radiation induced X-ray emission spectroscopy

SV40 T…….. Simian vacuolating virus 40 large T antigen

SWELL1……. leucine-rich repeat-containing protein 8A encoded by the *LRRC8A* gene

TBI…… traumatic brain injury

TcdB…… Clostridium difficile major virulence factor toxin B

Thr101…….. pan-NADPH oxidase inhibitor, specific for NOX2

TMD……. transmembrane domain

TMEM16A…….. anoctamin 1

TTX…….. tetrodotoxin

UDP-glucose 4-epimerase……... uridine diphosphate-glucose 4-epimerase

VRAC……. volume-regulated anion channel

VSOAC……... volume-sensitive organic osmolyte anion channel

VSOR…….. volume-sensitive outwardly rectifying Cl^- channel

xCT…….. cysteine-glutamate heteroexchanger

Abstract

HIGH AFFINITY BLOCK OF $I_{Cl,swell}$ BY THIOL-REACTIVE SMALL MOLECULES

By Sung Hoon Park

A dissertation submitted in partial fulfillment of the requirement for the degree of Doctor of Philosophy at Virginia Commonwealth University School of Medicine

Medical College of Virginia
Virginia Commonwealth University, 2016

Director: CLIVE M. BAUMGARTEN, PH.D.
Professor of Physiology and Biophysics,
of Internal Medicine (Cardiology),
and of Biomedical Engineering

Ebselen (Ebs) is considered as a glutathione peroxidase (GPx) mimetic and primarily thought to function by scavenging intracellular reactive oxygen species (ROS). Previous to our work, Deng et al. (2010a) demonstrated complete block of $I_{Cl,swell}$ with 15 μM Ebs following endothelin-1 (ET-1) induced activation of the current in cardiomyocytes. This block was presumed to take effect mainly via the quenching of ROS. Nonetheless, our work with DI TNC1 astrocytes strongly emphasizes that Ebs might function by an alternative mechanism based on its kinetic profile in blocking $I_{Cl,swell}$. Our experiments showed that 45 nM Ebs can fully block $I_{Cl,swell}$ thus suggesting an apparent IC_{50} <5 nM. Based on this result, we predicted Ebs to possess a high k_{on} with a low k_{off} close to zero. As predicted, Ebs failed to washout in the timescale covered by our patch-clamp experiments. The block was also distal to H_2O_2, previously considered as the most proximate regulator of $I_{Cl,swell}$. And based on further evidence demonstrating irreversible block of $I_{Cl,swell}$ distal to H_2O_2 with Ebs congeners, complete suppression of native $I_{Cl,swell}$ with MTS reagents, and failure of Ebs to block $I_{Cl,swell}$ from the cytosol, we concluded that Ebs and its congeners can covalently modify important –SH groups required for current activation while functioning as sulfhydryl reagents. Complete irreversible block of $I_{Cl,swell}$ with 110 μM cell impermeant MTSES in native DI TNC1 astrocytes contrasts sharply to SWELL1 (Qiu et al., 2014) or LRRC8A (Voss et al., 2014), the latest molecular entity presumably responsible for $I_{Cl,swell}$, where 3.33 mM MTSES failed to demonstrate block of $I_{Cl,swell}$ in the wild-type stably expressing SWELL1 (Qiu et al., 2014). Our data with Ebs, its congeners, and MTS reagents indicate the existence of a common extracellular binding site which involves a selenenylsulfide (Se-S) bond that critically modulates $I_{Cl,swell}$. We, therefore, synthesized a derivative of Ebs called ebselen-*para*-yne (Ebs-*p*-yne), which provided an even higher affinity for blocking $I_{Cl,swell}$ with a presumed IC_{50} ~picomolar range. Ebs-*p*-yne is a promising novel molecule that may serve as a tag in identifying the molecular fingerprint ultimately responsible for $I_{Cl,swell}$. Furthermore, we can take advantage of click chemistry to ultimately pull out the channel or channel

component which has remained elusive for greater than two decades.

CHAPTER 1

INTRODUCTION

1.1 Origin of $I_{Cl,swell}$ and Phenotypic Expression

Several years after pioneering experiments studying the effects of electrogenic mobility of radiolabeled cations and anions due to cell volume changes in Ehrlich ascite tumor cell line and human lymphocytes (Grinstein et al., 1982; Hoffman, 1978; Hoffman et al., 1984; Sarkadi et al., 1984 a and b), two groups used electrophysiological techniques to independently record the volume-sensitive Cl^- currents in epithelial 407 cells and human lymphocytes for the first time (Hazama and Okada, 1988; Cahalan and Lewis, 1988). This current is now referred to as the swelling-activated chloride current ($I_{Cl,swell}$) and is also known as the volume-activated chloride channel ($I_{Cl,vol}$), volume-regulated anion channel (VRAC), volume-sensitive organic osmolyte anion channel (VSOAC), or volume-sensitive outwardly rectifying (VSOR) Cl^- channel. These names refer to the same current or 'entity' and arise from various research contributions. Henceforth we will refer to it as $I_{Cl,swell}$. $I_{Cl,swell}$ turns on in response to cell swelling and various stimuli and plays a crucial role in regulatory volume decrease, electrical activity in heart, programmed cell death, and even ischemic preconditioning (Baumgarten et al., 2005). $I_{Cl,swell}$ also responds to stretch and has shown important relevance in mechano-sensitive signaling (Baumgarten and Clemo, 2003).

$I_{Cl,swell}$ is ubiquitously expressed in diverse tissues across multiple species, including man. For example, a few years after its initial description, $I_{Cl,swell}$ was identified in freshly isolated adult canine cardiac myocytes (Tseng, 1991 and 1992). It plays critical roles in mouse and human cholangiocytes or bile duct epithelial cells where cell volume regulation is vital to survival (Chen et al., 2010), nasopharyngeal carcinoma cells (CNE-2Z) where channel expression is highest during G_1 phase and is lowest at S phase with subsequent increase in M phase (Chen et al., 2002), fibroblasts derived from periodontal ligament in humans (Chung and Kim, 2002), trout red blood cells (Egee et al., 1997), rat articular chondrocytes (Ponce et al., 2012), endothelial cells from bovine pulmonary artery (Szucs et al., 1996), interstitial cells of Cajal (Park et al., 2005), pancreatic duct cells

(Verdon et al., 1995), and glial cellls in the brain (Mongin, 2015). Even though broadly distributed among various tissue, the molecular identity or the genetic signature of the channel has been elusive and several claims have been overturned (Baumgarten and Clemo, 2003; Baumgarten et al., 2005). Aspects of the current elicited by hypotonic challenge are tissue specfic, and one cannot exclude the possibility that distinct proteins or multiple channel isoforms contribute to the current empirically identified as $I_{Cl,swell}$. Most recently, a protein refered to as SWELL1 (Qiu et al., 2014) or LRRC8A (Voss et al., 2014) was putatively identified as the basis for $I_{Cl,swell}$ by two groups.

1.2 Biophysical Characteristics and Physiological Relevance of $I_{Cl,swell}$

Some of the features of $I_{Cl,swell}$ differ in comparison to other Cl^- currents. $I_{Cl,swell}$ displays outwardly-rectifying Cl^- current or inward Cl^- ion flux upon stepping to postive potentials in both physiological and symmetrical Cl^- gradients. Outward-rectification in symmetrical Cl^- gradient is only observed in $I_{Cl,swell}$, whereas other Cl^- channels display a linear current-voltage relationship in symmetrical Cl^- solutions. $I_{Cl,swell}$ displays time-independent behavior over most of the physiologic voltage range with partial inactivation as voltage steps toward more positive potentials and reverses at the Cl^- equilibrium potential (E_{Cl}) predicted by the Nernst Equation. Nevertheless, multiple anions permeate through the channel following the permeability sequence $SCN^- > I^- \geq NO_3^- > Br^- > Cl^- > Asp^-$, a low-field strength anion selectivity resulting with an Eisenman type I sequence (Mongin, 2015). Moreover, the selectivity between anions is relatively modest.

Studies show that $I_{Cl,swell}$ observed in normal mammalian cardiac myocytes is independent of Na^+, K^+, or Ca^{2+} ions since replacing these cations with non-permeant cations fails to dissipate the current, and $I_{Cl,swell}$ is recorded in the presence of the intracellular Ca^{2+} chelator EGTA or BAPTA (Baumgarten and Clemo, 2003; Baumgarten et al., 2005); nonetheless, diseased embryonic chick myocytes do show intracellular Ca^{2+}

dependency blockable by removing Ca^{2+} from bath solution (Hall et al., 1997). Others suggest that Ca^{2+}-nanodomains may be critical for proper activation of this current (Akita et al., 2011). $I_{Cl,swell}$ persistently activates under iso-osmotic conditions in hypertrophic ventricular myocytes freshly isolated from dogs with tachycardia-induced cardiomyopathy. In turn, exposing these diseased myocytes to osmotic swelling fails to further increase the current, and osmotic shrinkage blocks the current compared to non-diseased canine cardiomyocytes where $I_{Cl,swell}$ only activates following osmotic challenge (Clemo et al., 1999).

One of the first electrophysiological recordings of $I_{Cl,swell}$ in the brain comes from an astrogliomal C6 cell line that accumulates inositol during chronic hypertonic stress. Upon cell swelling, whole-cell conductance increases rapidly to 1.5-2 nS/pF and displays an outwardly-rectifying anion selectivity with enhanced inositol and taurine efflux. Further investigations show that certain organic osmolytes efflux through $I_{Cl,swell}$ (Jackson and Strange, 1993) altering neuronal output and release astrocytic signaling molecules or gliotransmitters for active neuron-astrocyte communication (Haydon and Carmignoto, 2006; Parpura et al., 2012). There is also evidence supporting the role of increased Cl^- conductivity through $I_{Cl,swell}$ accompanying a shift in membrane potential (E_M) in cases of mild, moderate to severe traumatic brain injury (TBI) when K^+ ions elevate extracellularly reseting the K^+ ion equilibrium potential (E_K). In turn E_M shifts to a value between E_{Cl} and E_K. The establishment of this new electromotive driving force now favors both K^+ influx accompanied by Cl^- influx through $I_{Cl,swell}$. The resulting net influx of KCl follows electroneutrality and is accompanied by an osmotic water movement into the cells.

1.3 Pharmacology of $I_{Cl,swell}$

Initial studies of $I_{Cl,swell}$ utilized anion channel blockers that were not selective. For example, members of the stilbene family such as DIDS (4,4′-diisothiocyanotostilbene-

2,2′-disulfonic acid), DNDS (4,4′-dinitrostilbene-2,2′-disulfonic acid) and SITS (4-acetamido-4′-isothiocyanostilbene-2,2′-disulfonic acid) were found to block the anion current evoked by swelling. In canine cardiomyocytes taken from the atria (Sorota, 1994) and primary astrocyte cell culture taken from Sprague-Dawley rats (Parkerson and Sontheimer, 2004), the block of $I_{Cl,swell}$ with DIDS demonstrates voltage-dependence with greater inhibition of the outwardly-rectifying current than the inward current. Block by DNDS and SITS are also voltage-dependent (Sorota, 1994; Hagiwara et al., 1992; Shuba et al., 1996). DIDS does not block $I_{Cl,PKA}$, an isoprenaline-activated protein kinase A (PKA)-dependent-Cl^-current (Hume et al., 2000; Jentsch et al., 2002), a chloride current often confused with $I_{Cl,swell}$. DIDS, however, is a potent blocker of $I_{Cl,Ca}$ (Ca^{2+}-activated Cl^- channel), monovalent cation and ATP-dependent K^+ channel (K_{ATP}), and Na^+- and Cl^--dependent bicarbonate transporters (Baumgarten and Clemo, 2003). In addition to stilbene derivatives, Sorota (1994) lists several other compounds that are tested in canine atrial cardiomyocytes for pharmacological activity: niflumic acid, NPPB (5-nitro-2-(3-phenylpropylamino) benzoic acid, IAA-94 (indanyloxyacetic acid-94), 9AC (9-anthracene carboxylic acid), dideoxyforskolin, and extracellular cAMP. Under whole cell patch-clamp condition after demonstrating Cl^- ion selectivity and Ca^{2+} ion independence, niflumic acid, NPPB, and IAA-94 are identified as full blockers of $I_{Cl,swell}$ in canine heart cells with off-target effects on cation channels at the same concentration used to block $I_{Cl,swell}$ whereas 9AC, dideoxyforskolin, and extracellular cAMP are characterized as partial blockers of $I_{Cl,swell}$ providing 50%, 80%, and 10% inhibition, respectively (Sorota, 1994). In comparison to DIDS, DNDS, and SITS, niflumic acid and NPPB inhibit the channel in a voltage-independent manner (Parkenson and Sontheimer, 2004). Using both hippocampal astrocytes from neonatal rats and astrocyte cultures with gap junction protein (Cx43) knockout genetically modified in mice, Ye et al. (2009) also provides important pharmacology of NPPB, IAA-94, and tamoxifen discussing the relative cross-inhibition of Cx43, referred sometimes as connexin hemichannels, and $I_{Cl,swell}$. Finally

DPC (diphenylamine-2-carboxylic acid) inhibits $I_{Cl,swell}$ in embryonic chick myocytes (Zhang et al., 1993), glibenclamide (antidiabetic drug and K_{ATP} channel blocker) blocks both $I_{Cl,swell}$ and $I_{Cl,PKA}$ in cardiomyocytes (Sakaguchi et al., 1997; Yamazaki and Hume, 1997), genistein (protein tyrosine kinase inhibitor) suppresses both $I_{Cl,swell}$ and stretch-activated Cl^- current in heart (Browe and Baumgarten, 2003), and PP2 (selective blocker of focal adhesion kinase (FAK) and Src (proto-oncogene c-*Src*) fully inhibits the stretch-activated Cl^- current, which most likely is due to $I_{Cl,swell}$ (Browe and Baumgarten, 2003).

A higher affinity blocker of $I_{Cl,swell}$ with improved selectivity between anion channels is tamoxifen, an estrogen receptor antagonist utilized clinically in the treatment of breast carcinoma (Kistner and Smith, 1960; Herbst et al., 1964; Cole et al., 1971; Ward, 1973). Tamoxifen provides complete block of $I_{Cl,swell}$ at 10 μM in cardiac tissue (Vandenberg et al., 1994; Duan et al., 1997) and does not block $I_{Cl,PKA}$ or any of the inwardly-rectifying Cl^- channels. On the other hand, off-target effects of tamoxifen include block of the ligand-gated cation channels, L- and T- type Ca^{2+} channels, the big conductance BK K^+ channels, I_{Ks} or the delayed rectifier, tetrodotoxin (TTX)-sensitive Na^+ channels, and cardiac gap junction proteins in multiple preparations (Vandenberg et al., 1994; Duan et al., 2000; Allen et al., 1998; Dick et al., 1999 and 2002; Smitherman and Sontheimer, 2001; Verrecchia and Herve, 1997). The mechanism of how tamoxifen blocks $I_{Cl,swell}$ is unclear and may not involve block of nuclear estrogen receptors. Nevertheless, tamoxifen is a prodrug and its cellular metabolism increases its affinity for and block of the estrogen receptor.

DCPIB, a non-diuretic acylaryloxyacid analogue of ethacrynic acid, has become the standard selective inhibitor of $I_{Cl,swell}$. In drug discovery studies, this agent initially was shown to block swelling of astrocytes *in vitro* and in the cat cerebral cortex *in vivo* (Bourke et al., 1981; Cragoe et al., 1982) identifying a potential clinical application, but the underlying mechanism of action was not identified. The novel role of DCPIB in selective inhibition of $I_{Cl,swell}$ was not recognized until Decher et al. (2001) demonstrated

that DCPIB (10 μM) fully inhibited $I_{Cl,swell}$ in a voltage-independent manner in guinea-pig atria and prevented the shortening of action potential duration (APD). They also showed that DCPIB blocks $I_{Cl,swell}$ in calf bovine pulmonary artery endothelial (CPAE) cells with an IC_{50} of 4.1 μM, and DCPIB almost fully blocks the swelling-activated Cl^- current in *Xenopus* oocytes while showing no significant effect on $I_{Cl,Ca}$ in CPAE cells, CLC family of Cl^- channels, heterologously expressed human cystic fibrosis transmembrane conductance regulator (hCFTR) in *Xenopus* oocytes, and several of the anion and cation conductance found in guinea-pig heart including $I_{Cl,PKA}$, I_K, I_{Ks}, I_{K1}, I_{Na}, and I_{Ca} (Decher et al., 2001). A recent study of glutamate transport pathways in glial cells shows that DCPIB blocks Cx43, glutamate transporter (GLT-1), and cysteine-glutamate heteroexchanger (xCT); however, DCPIB fails to suppress GLAST (glutamate aspartate transporter) often found in astrocytes and vesicular glutamate release in synaptosomes from rat forebrain (Bowens et al., 2013). More recently, the latest work by Deng et al. (2016) strongly suggests that DCPIB can also bind to inwardly rectifying K^+ (Kir) channels with relatively weak affinity for PIP_2 whereas DCPIB fails to block Kir isoforms such as I_{K1} which is known to demonstrate higher affinity for PIP_2.

1.4 Molecular Identity of $I_{Cl,swell}$

Although DCPIB is identified as the most selective in blocking $I_{Cl,swell}$, none of the aforementioned blockers including DCPIB are considered high affinity and suitable to employ as tool for protein isolation. Once bound, they all unbind and show full reversibility upon washout. Therefore, without available high affinity irreversible blockers of $I_{Cl,swell}$ and perhaps overly influenced by the name "swelling-activated chloride channel," investigators used osmotic swelling as a tool to peruse the molecular identity of the channel. In more than a decade of experiments, this lead to claims that $I_{Cl,swell}$ was due to P-glycoprotein (MDR-1), pI_{Cln}, phospholemman, CLC3, TMEM16A (anoctamin 1), and

bestrophin 1 (BEST1), but in each case, the proposed molecular identity for $I_{Cl,swell}$ was refuted (Hume et al., 2000; Jentsch et al., 2002; Nilius et al., 1997; Kunzelmann, 2015). For example, both anoctamin 1 and BEST1 require Ca^{2+} for activation and fall into the category of calcium-activated chloride channels (CaCC), but $I_{Cl,swell}$ appears to be Ca^{2+}-independent and critical biophysical properties are distinct from those of anoctamin 1 and BEST1. Among the molecular candidates listed, perhaps CLC3 provided the strongest case for being labeled as $I_{Cl,swell}$. This Cl^- channel was identified as cardiac $I_{Cl,swell}$ based on functional expression of a guinea pig cardiac clone in NIH/3T3 fibroblasts (Duan et al., 1997, 1999). According to Duan et al. (1997), expression of guinea pig CLC3 lead to swelling-activated Cl^- currents sharing the same biophysical properties of $I_{Cl,swell}$ and its modulation by PKC and serine/threonine phosphatases. However, Jentsch et al. (2002) discredited the role of CLC3 in eliciting $I_{Cl,swell}$, as CLC3 is normally clustered to intracellular membranes and its up-regulation does not necessarily give rise to $I_{Cl,swell}$. Li et al. (2000) also argues that increased expression of CLC3 prompts currents with inconsistent permeability sequence where $Cl^- > I^-$ accompanied by incorrect pharmacological response than $I_{Cl,swell}$. Even though CLC3 antisense appeared to minimize $I_{Cl,swell}$ in ciliary epithelium (Wang et al., 2000), *Xenopus* oocytes and HeLa cells (Satterwhite et al., 2002), it was difficult to exclude the possibility that CLC3 was a regulator of $I_{Cl,swell}$ rather than the channel itself, and CLC-family proteins were shown to serve as proton-Cl^- exchangers (Scheel et al., 2005). Finally, knockout of CLC3 failed to affect neuronal $I_{Cl,swell}$ (Stobrawa et al., 2001), and Hume, Duan and coworkers (Yamamoto-Mizuma et al., 2004) found $I_{Cl,swell}$ also persisted in cardiac and smooth muscle myocytes, although aspects of its regulation were altered.

Of the approaches taken to identify $I_{Cl,swell}$, swelling has been the most instrumental in activating the current as the channel name suggests as the ultimate means to verify the presence of $I_{Cl,swell}$. The latest molecular entity identified to adopt swelling as the primary approach is SWELL1 by Qiu et al. (2014) or LRRC8A by Voss et

al. (2014). Even though their approach taken is novel, swelling is still a prerequisite prior to halide (I^-) quenching (Qiu et al., 2014; Voss et al., 2014). Although swelling plays an important role in current activation, it is just one factor among a number of existing critical regulators identified to date that shape $I_{Cl,swell}$ signaling cascade as comprehensibly defined by Baumgarten and co-workers (Deng et al., 2010a; Browe et al., 2004 and 2006; Ren et al., 2008; Ren and Baumgarten, 2005; Du et al., 2004). Key components of the signaling cascade are summarized by Deng et al. (2010a). Fig.1 shows that in rabbit ventricular myocytes, osmotic swelling is upstream of angiotensin II (AngII), endothelin-1 (ET-1), and epidermal growth factor (EGF) which represent three specific peptide molecules known to elicit $I_{Cl,swell}$ each by activating AT_1 receptors (AT_1R), ET_A receptors (ET_AR), and EGF receptors (EGFR), respectively (Deng et al., 2010a; Browe et al., 2004 and 2006; Ren et al., 2008). ET-1 elicited $I_{Cl,swell}$ is downstream of AngII and upstream of EGF and phosphoinositide-3-kinase (PI-3K) signaling cascades; therefore, suppressing EGFR or PI-3K blocks $I_{Cl,swell}$ after its activation by ET-1 whereas antagonizing AT_1R remains ineffective (Fig. 1). Direct blockade of NOX (Active NOX2) shown in Fig. 1 inhibits $I_{Cl,swell}$ in the presence of osmotic swelling, AngII, ET-1, and EGF, which places NOX downstream of all four upstream signaling cascades. Reactive oxygen species (ROS) production by NOX help elicit $I_{Cl,swell}$ but blocking mitochondrial Complex I completely inhibits $I_{Cl,swell}$. Directly augmenting ROS release at Complex III also leads to $I_{Cl,swell}$ and shows insensitivity to NOX inhibitors. This places mitochondria downstream of NOX in the signaling cascade (Fig. 1). Lastly, exogenous H_2O_2 has been known to fully elicit $I_{Cl,swell}$ despite blockade of all the aforementioned upstream activators; therefore, H_2O_2 acts to turn on DCPIB sensitive $I_{Cl,swell}$ at or near the channel itself (Fig. 1). This makes H_2O_2 the most proximate to $I_{Cl,swell}$ and furthest from osmotic swelling in the signaling cascade known to date. The $I_{Cl,swell}$ regulatory signaling cascade is, therefore, very complex involving a number of critical regulators from osmotic swelling down to H_2O_2. Thus, swelling alone cannot ultimately serve as a basis for conclusively

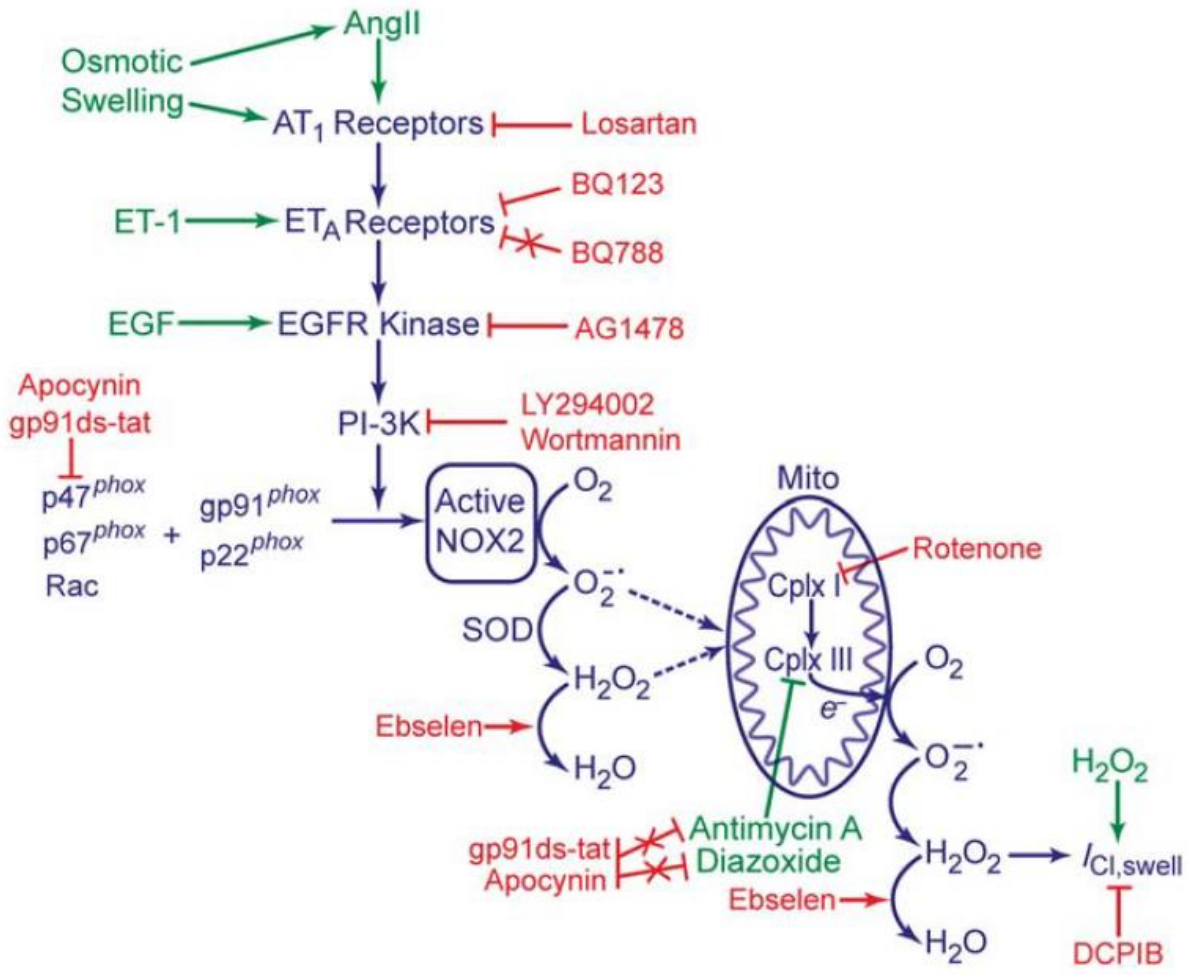

FIG. 1: $I_{Cl,swell}$ signaling cascade in heart. Exogenous stimuli such as osmotic swelling, AngII, ET-1, EGF, and H_2O_2 lead to $I_{Cl,swell}$. Osmotic swelling and AngII activated $I_{Cl,swell}$ through AT_1Receptors, ET-1 through ET_AReceptors, and EGF through EGF Receptors; in addition, these 3 receptors were up stream of PI-3K and NOX2. Superoxide or H_2O_2 generated most likely by NOX2 stimulated mitochondrial ROS production via Cplx III. Antimycin A and diazoxide augmented Cplx III ROS generation independent of NOX2. Ebselen effectively scavenged H_2O_2 from NOX2 and/or mitochondria. Green represents stimulation and red shows suppression [21]. Activation ($\rightarrow$), inhibition ($\perp$), and excluded pathways (X) are indicated.

identifying the channel.

1.5 Identification of Ebselen (Ebs): High Affinity Blocker of $I_{Cl,swell}$

Ebselen (2-phenyl-1,2-benzisoselenazol-3(2H)-one; also called PZ51, DR3305, and SPI-1005) is a selenoorganic small molecule which has been known for more than two decades as a glutathione peroxidase (GPx)-mimetic (Sies, 1993; Nakamura et al., 2002; Sakurai et al., 2006). Some common targets of Ebs range from hydrogen peroxide and small organic hydroperoxides to cholesterol hydroperoxides (Sies, 1993), and Ebs also is active against free radicals and singlet oxygen (Sies, 1993). Based on its GPx-mimetic activity, Ebs is utilized as a ROS scavenger, and Ebs at 15 μM is sufficient to provide complete block of $I_{Cl,swell}$ and the role of mitochondrial ROS was confirmed by flow cytometry (Deng et al., 2010a, 2010b). However, Ebs was recently reported to suppress NOX2 activity in broken cell preparations (Smith et al., 2012).

Based on the ability of Ebs to act as a GPx-mimetic and its ability to suppress $I_{Cl,swell}$ (Deng et al., 2010a, 2010b), we utilized Ebs in preliminary experiments on $I_{Cl,swell}$ following ROS augmentation at Complex III in the DI TNC1 astrocyte cell line. To our surprise, 15 μM Ebs suppressed $I_{Cl,swell}$ with fast kinetics, suggesting it possessed much greater than expected affinity, and we found that block was irreversible within the time scale of patch clamp studies. Together, these findings lead us to postulate that Ebs might be useful as a high affinity irreversible $I_{Cl,swell}$ blocker and as a tool to directly isolate the target responsible for current block. Experiments designed to characterize the action of Ebs and its congeners identified several compounds that fully and irreversibly suppressed $I_{Cl,swell}$ at concentrations as low as 5 nM. Moreover, evidence suggests that covalent binding of Ebs and its congeners to critical sulfhydryl groups modulate the conductance of the channel. Finally, the site of block $I_{Cl,swell}$ by Ebs and its congeners must be distal in the signaling cascade that activates the channel because block could not be overcome

by exposure to exogenous H_2O_2, the most distal regulator of $I_{Cl,swell}$ previously identified.

CHAPTER 2

METHODS

2.1 DI TNC1 Astrocyte Cell Culture

DI TNC1 cell line was originally established by Radany et al. (1992) by transfecting primary astrocytes from diencephalon of a 1 day-old Sprague Dawley rat with a DNA construct that contains the oncogenic early sequence of SV40. It is positive for glial fibrillary acidic protein (GFAP) and aquaporin 4 (AQP4; astrocyte water channel) negative. DI TNC1 cells are phenotypically equivalent to type 1 astrocytes and lack specific epitopes characteristic of type 2 astrocytes, and over 90% of transfected cells show the presence of SV40 T antigen upon immunostaining (Radany et al., 1992). DI TNC1 cells (American Type Culture Collection; ATCC CRL-2005, passages 3-17) were grown on Corning CELLBIND (60 x 15 mm) pretreated culture dishes using DMEM (Corning Cellgro, 10-013-CV) supplemented with 10% v/v fetal bovine serum (FBS) (Sigma-Aldrich, F2442), and 1% v/v penicillin/streptomycin (Cellgro 30-002-CI). The cells were grown at 37 °C under 5% CO_2 and 95% O_2. After cells reached 80-90% confluency, a brief wash with 5-7 mL of Dubecco's phosphate buffered saline without calcium and magnesium (Thermo Scientific, HyClone SH30028.02) followed by incubation with 3-5 mL of 0.25% trypsin-EDTA (Gibco/Thermo Fisher Scientific, 25200056) for 10-20 min at 37 °C was performed to dislodge the cells while gently tapping the culture dish. Additional DMEM (5-8 mL) was then used to wash the cells into 15 mL conical centrifuge tubes prior to centrifugation at 2500 rpm for 3-5 min on a table top centrifuge. Supernatant was removed to isolate the pellet prior to resuspension in 8-12 mL of DMEM. About 1-2 mL were plated for the next passage, and the rest were incubated at 37 °C for 1 h in 5% CO_2 prior to use. After recovery, DI TNC1 astrocytes were resuspended in appropriate experimental bath solution. We also used HEK293 cells, gift of Dr. Gea-Ny Tseng, in some experiments and the cells were subjected to similar culturing conditions.

2.2 Experimental Solutions and Drugs

Solutions were designed to isolate the Cl^- current. The isosmotic bath solution (1T; 320 mOsm/kg; T denotes times isosmotic) contained (in mmol/L): 90 N-methyl-D-glucamine-Cl, 3 $MgCl_2$, 10 HEPES, 10 glucose, 5 CsCl, 0.5 $CdCl_2$, and mannitol was used to adjust bath solution osmolarity (pH 7.4; adjusted with CsOH). Hyposmotic (0.8T) bath solution contained less mannitol. Standard pipette solution contained: 110 NMDG-glucuronate, 20 TEA-Cl, 0.15 $CaCl_2$, 10 Cs_2EGTAH_2, 10 HEPES, 5 Mg-ATP, and 0.1 Tris-GTP (pH 7.2; CsOH). Symmetrical Cl^- pipette solution contained: 82 CsCl, 28 Cs-Aspartate, 20 TEA-Cl, 0.15 $CaCl_2$, 8 Cs_2EGTAH_2, 10 HEPES, 5 Mg-ATP, and 0.1 Tris-GTP (pH 7.2; CsOH).

Stock solutions of ebselen (Ebs; 17 mM, Cayman), ebselen-*p*-yne (Ebs-*p*-yne; 15 mM, M. Hartman and P. Dupart, Dept. of Chemistry, VCU), ebselen-biotin (Ebs-biotin; 15 mM, M. Hartman and P. Dupart, Dept. of Chemistry, VCU), ebselen oxide (EbO; 15 mM, Sigma), Thr101 (19 mM, Calbiochem), DCPIB (10 mM, Tocris), diazoxide (Diaz; 40 mM, Sigma), antimycin A (AntiA; 10 mM, Sigma), and VAS2870 (5.5 mM, Enzo) purged under argon were prepared in DMSO and stored in -20 °C in aliquots until use. Stock solutions of MTSES (110 mM, Toronto), MTSET (110 mM, Toronto), and MTSEA biotin (50 mM, Toronto) were dissolved in water and prepared fresh on the day of the experiment. Hydrogen peroxide (H_2O_2; 500 mM, Fisher Scientific, 7722-84-1) was also prepared fresh on the day of use. Chemical structures for Ebs, Ebs-*p*-yne, EbO, and Thr101 can also be found in Fig. 1 of the Appendix. Structure of Ebs-biotin is shown in Fig. 5 of the Appendix. Structures of diazoxide, antimycin A, DCPIB, Ebs and its congeners, and VAS2870 are as follows:

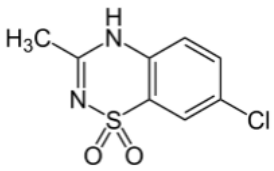

Diazoxide

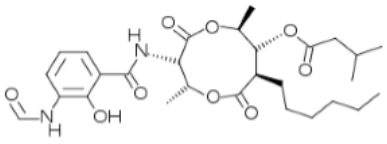

Antimycin A

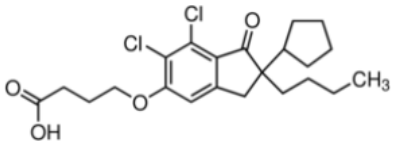

DCPIB

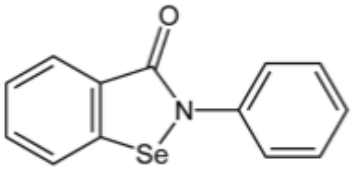

Ebselen (Ebs)

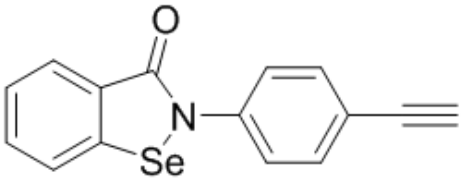

Ebselen-*para*-yne (Ebs-*p*-yne)

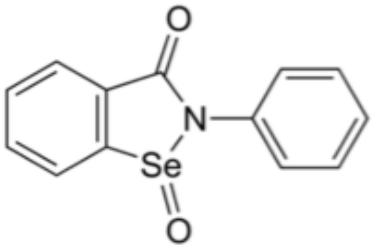

Ebselen Oxide (EbO)

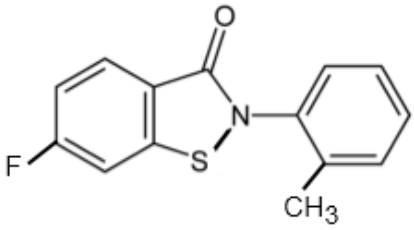

Thr101

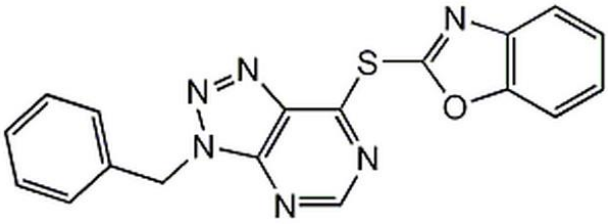

VAS2870

2.3 Whole Cell Patch-Clamp and Electrophysiological Recordings

After 1 h recovery at 37 °C under 5% CO_2, DI TNC1 cell resuspensions in 1T or 0.8T were gently pipetted onto the glass-bottomed patch chamber on the stage of an

inverted light microscope (Nikon) equipped with 40x LWD Hoffman modulation optics and coupled to a high resolution video camera (CCD72, Dage-MTI) for visualizing the cells. After settling, the cells were suprafused with 1T or 0.8T bath solution at 2-3 mL/min while recording at room temperature of 18-21 °C. The patch pipettes were pulled from 7740 thin-walled borosilicate capillary tubing (Sutter) and fire-polished to a tip diameter of approximately 1-3 μM with a bath solution resistance of 3-5 MΩ. Membrane currents were recorded under whole cell mode using an Axopatch 200B amplifier and Digidata 1322A data acquisition system (Axon). A 3 M KCl agar bridge was used as the ground electrode. Seal resistances of 10-50 GΩ were typically obtained prior to applying negative pressure. Access resistances were 4-10 MΩ before compensation (typically 40-60%). All measured membrane potentials were corrected for the liquid junction potential (LJP). DI TNC1 cells were then dialyzed 2-5 min prior to recording membrane currents.

Voltage-clamp protocol and data acquisition were established by pClamp 8.2 (Axon). Successive 500 ms pulses were made from a holding potential of -60 mV to test potentials from -100 to +60 mV in +10 mV increments. Membrane currents were low-pass filtered at 2 kHz and digitized at 5 kHz, and selected current traces were low-pass filtered at 500 Hz for presentation. *I-V* relationships were generated from corresponding membrane current traces. Data were recorded without correcting for leak currents and expressed as pA/pF (current density) to normalize variations in cell size to capacitive membrane area. Current amplitudes for both activation and block were measured relative to zero current rather than the initial current recorded upon breaking into a cell. This approach slightly overestimated the swelling-activated chloride current and underestimated the fraction of current that was blocked because leak current could not be independently measured and, therefore, was not subtracted. For clarity, in some instances data are plotted and expressed as fractional block by normalizing to current density after activation of $I_{Cl,swell}$.

2.4 Intracellular Application of Drugs by Back-Filling

Patch experiments performed under isosmotic conditions (1T) utilized intracellular diazoxide (Diaz [in]; 53 μM) or antimycin A (AntiA [in]; 10 μM) included in the pipette solution to activate $I_{Cl,swell}$. Selected experiments were done using a hypoosmotic challenge with 0.8T to activate $I_{Cl,swell}$. In some of these studies, either ebselen (Ebs [in]; 30 μM) or DCPIB (DCPIB [in]; 30 μM) were included in the pipette solution. To be able to collect data before dialysis of the cell by pipette solution was complete, patch-pipettes were dipped in appropriate drug-free pipette solution for 30-90 s utilizing capillary action to pull in a ~1-2 mm column of drug-free pipette solution prior to back-filling the pipette with proper drug-containing media. Diffusion of drug within the tip of the pipette allowed sufficient time to mount the pipette, form a gigaseal, break-in, and begin recording membrane currents while currents were still near their control values.

2.5 Reversibility of DCPIB

Demonstration of the reversible nature of block by DCPIB, the most selective blocker of $I_{Cl,swell}$ known to date, can be found in Fig. 8 of the Appendix.

2.6 Total Number of Channels Per DI TNC1 Astrocyte

Based on reported open probability, P_o, of 0.68 and unitary conductance, γ, of 28 ± 1 pS of $I_{Cl,swell}$ at strongly positive potentials by Duan et al. (1997) and incorporating our experimentally observed macroscopic currents, ~1000 - 3000 pA at +60 mV with an E_{Cl} of -41 mV, we can estimate the total number of $I_{Cl,swell}$ channels, N, in an astrocyte. The unitary current, *i*, is given by:

$$i = \gamma\ (E_{test} - E_{Cl})$$

where E_{test} is the test potential, +60 mV, and the macroscopic $I_{Cl,swell}$, I, is given by:

$$I = i\ N\ P_o$$

Substituting for *i* yields and then solving for N:

$$I = \gamma\ (E_{test} - E_{Cl})\ N\ P_o$$

$$N = I\ [\gamma\ (E_{test} - E_{Cl})\ P_o]^{-1}$$

gives ~520-1560 channels per DI TNC1 astrocyte. Even at low nanomolar concentrations, blockers applied in flowing bath solutions are in excess of the number of potential binding sites and can be considered to remain constant during the experiment.

2.7 Model of $I_{Cl,swell}$ Block by Ebs and Its Cogeners

One caveat in describing block by Ebs and Ebs-*p*-yne is whether block is irreversible or very slowly reversible. We ascertained the rate constants for block of current assuming 1:1 bimolecular pseudo-first order kinetics and that binding to the receptor was proportional to current block. Experimentally we found that block by Ebs and its congeners could be well-described by a single exponential and was irreversible over the time course studied.

The scenario can be described by drug (D) bound to its receptor (R):

$$R + D \underset{k_{-1}}{\overset{k_1}{\rightleftarrows}} RD \xrightarrow{k_2} R\text{-}D$$

where k_1 and k_{-1} are forward and reverse rate constants for formation of a reversible intermediate, RD, and k_2 is the rate constant for irreversible conversion of RD to R-D, (e.g., formation of a covalent bond). We cannot, however, independently identify the RD state or distinguish whether just R-D or both RD and R-D block $I_{Cl,swell}$. To simplify the analysis, we described the kinetics of current block (rather than drug-receptor binding) based on fits to a single exponential function, giving a time constant, τ, and its inverse, a rate constant, K (see p. 56).

Given the possibility that Ebs and its congeners may eventually reverse provided enough time, for purposes of comparison, we estimated an apparent IC_{50} for current block based on the concentration giving full block. This approach previously was used by others. For example, two studies of the action of Ebs to bacterial proteins report an IC_{50} of ~100 nM for Ebs binding to Ag85c (Favrot et al., 2013) and IC_{50} of ~6.9-17.2 nM for Ebs binding to TcdB (Bender et al., 2015) even though these authors argued Ebs binding lead to irreversible covalent modification of the target proteins.

2.8 Statistics

In order to decrease variability, each cell was used as its own control. Data are reported as mean ± SEM; n denotes the number of cells for current density or rate constant (K) of block determination. One-way repeated-measures ANOVA were performed and all pairwise comparisons made by the Holm–Sidak method. For calculating K under conditions of apparent irreversible block, time courses were fit to a pseudo-first order exponential decay (SigmaPlot) assuming 1:1 bimolecular interaction of drug and its receptor after accounting for the time required for equilibration of drug in the tissue bath.

The kinetics of block by Ebs (Control) were compared to those of EbO and Thr101 using block of 20-80% of the current because the rapid block by Ebs was difficult to fit to an exponential function. Because normality test on the raw data failed, instead we analyzed the natural log of the data, which passed normality testing. We compared EbO and Thr101 to Ebs (Control) by a one-way ANOVA and the Holm-Sidak method.

CHAPTER 3

RESULTS

3.1 Identification of $I_{Cl,swell}$ in DI TNC1 Astrocytes

Fig. 2 demonstrates typical outwardly-rectifying Cl^- currents characteristic of $I_{Cl,swell}$ in DI TNC1 astrocytes during 0.8T hypo-osmotic challenges with physiological (*A-C*) and symmetrical Cl^- gradients (*D-F*). Panel *A* and *D* represent current traces generated when -100 to +60 mV voltage steps were applied for 500 ms in 10 mV increments. Panel *B* and *E* are the corresponding *I-V* relationships and cell capacitances. Panel *C* and *F* present summary data illustrating fractional block of the steady-state swelling-induced current in 0.8T at +60 mV by 10 μM DCPIB, a selective inhibitor of $I_{Cl,swell}$ (Decher et al., 2001).

As expected for $I_{Cl,swell}$ (Baumgarten and Clemo, 2003), the currents elicited in 0.8T outwardly rectified in both physiological and symmetrical Cl^- solutions and were blocked by DCPIB. The current activated by 0.8T at +60 mV was 33.3 ± 6.9 pA/pF (n = 4) in physiological Cl^- and 34.8 ± 10.0 pA/pF (n = 5) in symmetrical Cl^-. With a physiological Cl^- gradient, the observed E_{rev} was between -35 and -38 mV, which is close to the calculated value of the Nernst equilibrium potential for Cl^- (E_{Cl}), -41 mV, after correcting for the liquid junction potential. With a symmetrical Cl^- gradient, E_{rev} was almost exactly 0 mV as predicted for E_{Cl}. Addition of DCPIB (10 μM, 5-15 min) blocked 87.5 ± 3.2% (n = 4) (*C*) and 92.5 ± 1.3% (n = 5) (*F*) of the swelling-activated Cl^- current at +60 mV (for both, $P < 0.001$). Although outward rectification was observed with both physiological and symmetrical Cl^- gradients, the rectification was greater under physiological than symmetrical conditions, as previously reported for $I_{Cl,swell}$ (Vandenberg et al., 1994; Duan et al., 1997). Thus, current elicited by osmotic swelling of DI TNC1 astrocytes shared the biophysical and pharmacological characteristics of $I_{Cl,swell}$.

Two technical issues should be noted. First, the current density of $I_{Cl,swell}$ can vary with the passage number. For example, $I_{Cl,swell}$ in another group of astrocytes was 240.3 ± 63.5 pA/pF (n = 4) at +60 mV in 0.8T, a much greater current density than that shown in Fig. 2. Nevertheless, DCPIB very strongly blocked 99.0 ± 0.3% of $I_{Cl,swell}$ in these cells

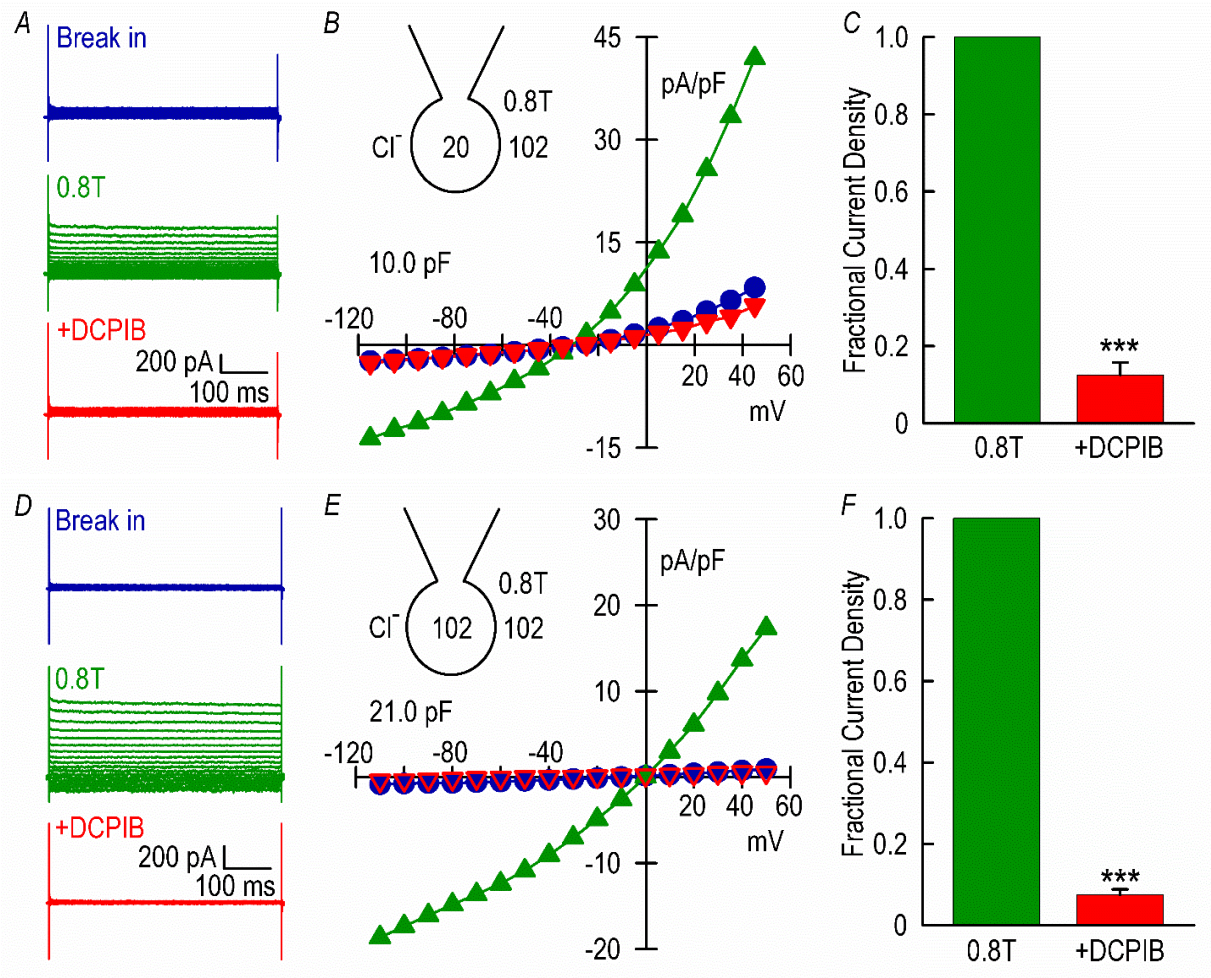

FIG. 2: Activation of outwardly rectifying $I_{Cl,swell}$ and block by DCPIB (10 μM, 5-10 min) following hypo-osmotic challenge with physiological (*A-C*) and symmetrical (*D-F*) Cl^- gradients in DI TNC1 astrocytes. ***A and D***. Current traces upon stepping for 500 ms to -100 mV to +60 mV in 10 mV increments from a holding potential of -60 mV under conditions that isolate the Cl^- current. ***B and E***. Current-voltage (*I-V*) relationships at break in (blue), after steady state current activation with 0.8T hypo-osmotic bath solution (green), and after block with DCPIB (red) in 0.8T; plots of *I-V* relationships were corrected for measured liquid junction potential. ***C and F***. Block of 0.8T-induced current by DCPIB at +60 mV. DCPIB blocked 87.5 ± 3.2% (n = 4, $P < 0.001$) and 92.5 ± 1.3% (n = 5, $P < 0.001$) of swelling-induced current in physiological (***C***) and symmetrical (***F***) Cl^- solutions, respectively. Physiological Cl^- solutions contained 20 mM Cl^- inside the patch pipette and 102 mM Cl^- in bath solution, and symmetrical Cl^- solutions contained 102 mM Cl^- in both (*see insets, B and E*). Current densities were calculated based on measured membrane capacitance. Repeated measures ANOVA were based on current densities and are presented as fractional current densities and fractional block for clarity.

as well (n = 4, P < 0.001). Second, as mentioned in Methods, current amplitudes for both activation and block were measured relative to zero current rather than the initial current recorded upon breaking into a cell. The approach adopted slightly overestimated the swelling-activated current and underestimated the fraction of current that was blocked because leak current could not be independently measured and was not subtracted. Failing to subtract leak likely explains why DCPIB appeared to block a greater fraction of $I_{Cl,swell}$ when the swelling-induced current density was greatest (i.e, 240 pA/pF vs 33 pA/pF). If instead we measured currents relative to the current at break in, we would have underestimated activation of $I_{Cl,swell}$ in the presence of partial current activation (pre-activation) under isosmotic conditions, as is sometimes the case, and overestimated the fraction of current blocked by DCPIB. Consistent with this idea, preliminary analyses measuring currents relative to that at break in sometimes resulted in >100% block by DCPIB.

Because astrocytes express various glutamate receptors and glutamate transporters (Seifert et al., 2006), we assessed whether these transport processes contributed to the measured Cl^- current. Application of external glutamate (1-3 mM) failed to affect the current attributed to $I_{Cl,swell}$ (n = 4, P = 0.490; *ns*; Appendix, Fig. 11). Similarly, CFTR(inh)-172 (20 μM), a highly selective inhibitor of CFTR, also failed to affect $I_{Cl,swell}$ (n = 6, P = 0.079; *ns*; Appendix, Fig. 12).

3.2 Effect of Ebselen (Ebs) on $I_{Cl,swell}$

3.2.1 Block of $I_{Cl,swell}$ by Ebs

Intracellular diazoxide (53 μM; Diaz [in]) elicited an outwardly-rectifying Cl^- current characteristic of $I_{Cl,swell}$ in physiological Cl^- gradient. Diaz, a K_{ATP} channel opener displaying sensitivity toward mitoK_{ATP} (Garlid and Halestrap, 2012), augments Complex III ROS production independent of NOX and leads to $I_{Cl,swell}$ activation (Deng et al.,

2010a; Queliconi et al., 2011). Fig. 3 demonstrates block of $I_{Cl,swell}$ following activation when diazoxide was back-filled in the patch pipette as described in Methods. Unless otherwise specified, experiments were performed under conditions isosmotic (1T) with equal pipette and bath osmolarity. Typical current traces, corresponding *I-V* relationships, summary data demonstrating fractional block at +60 mV by Ebs (15 μM) added to flowing bath solution, and a typical time-course for the full experiment are shown. Ebs blocked 93.9 ± 5.6% (n = 15, P < 0.001) of the Diaz [in]-induced current (Fig. 3). The block of $I_{Cl,swell}$ was relatively fast with complete block in 2-3 min after addition of Ebs.

3.2.2 Diazoxide-induced $I_{Cl,swell}$ failed to rundown

To rule out $I_{Cl,swell}$ rundown in the presence of Diaz [in] as the cause of current inhibition upon addition of Ebs, a control experiment tested whether activation of $I_{Cl,swell}$ by Diaz [in] was ephemeral or maintained for the duration of exposure (Fig. 4). After reaching steady-state activation at ~20 min, $I_{Cl,swell}$ remained persistently elevated for ~50 min. Rather than rundown, the summary data showed a small but statistically insignificant increase in current that may have resulted from uncertainty in the precise timing of reaching steady-state activation.

3.3 High Affinity Block of $I_{Cl,swell}$ by Ebs

3.3.1 Ebs blocked $I_{Cl,swell}$ with nanomolar affinity

The block of $I_{Cl,swell}$ in cardiac myocytes with 15 μM Ebs was previously demonstrated by Deng et al. (2010a) following activation with endothelin-1 (ET-1). The rapid onset of block by Ebs in DI TNC1 cells (complete block in 2-3 min; Fig. 3) suggested Ebs might act with high affinity for its target. After preliminary studies showed Ebs fully blocked Diaz [in]-induced $I_{Cl,swell}$ at 1.5 μM and 150 nM (both, n = 1), the response to

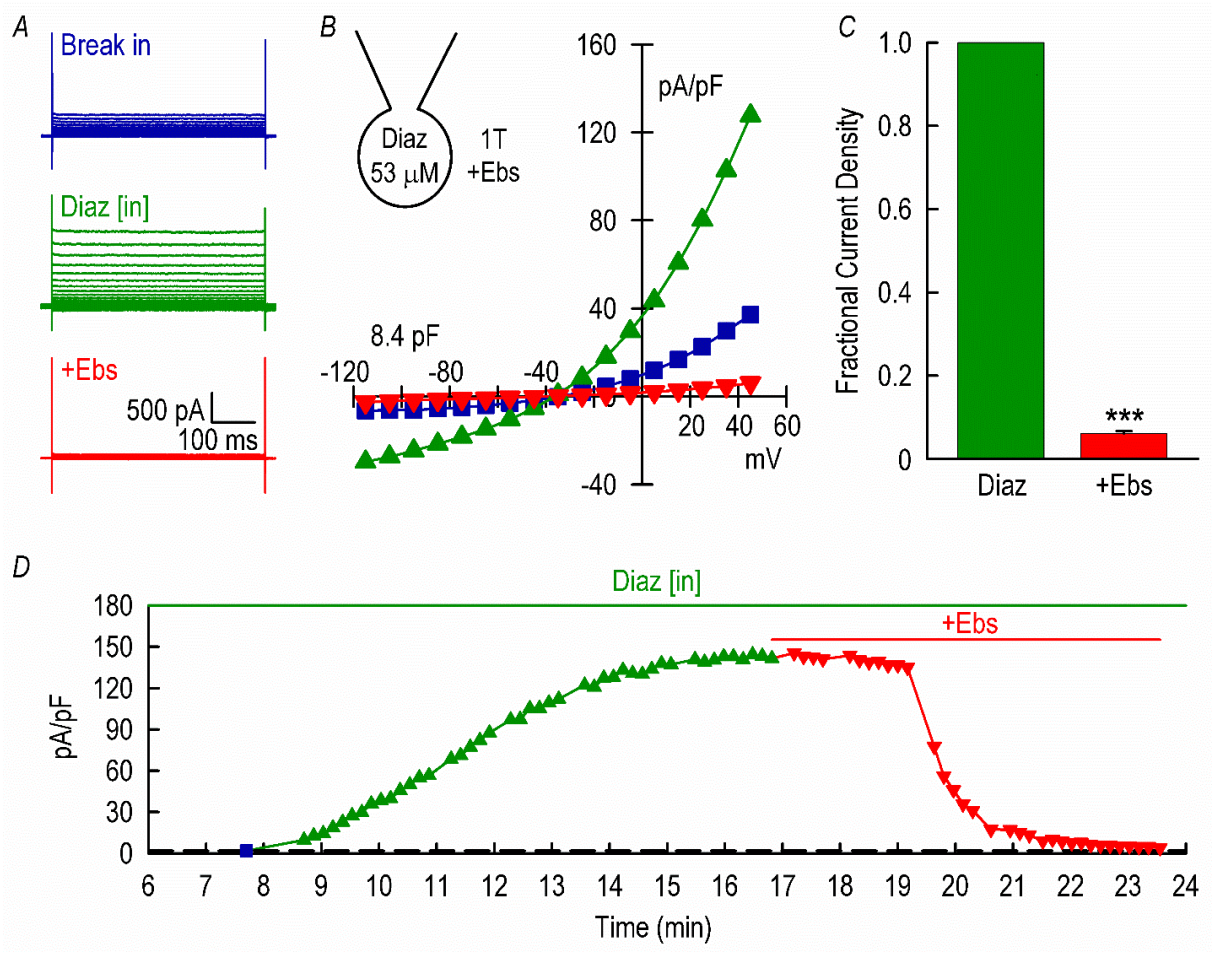

FIG. 3: Block of $I_{Cl,swell}$ by Ebselen (Ebs). $I_{Cl,swell}$ was activated under isosmotic (1T) conditions by back-filling patch pipette with 53 µM diazoxide (Diaz [in]; see inset) and was rapidly blocked by adding 15 µM Ebs in bath. Current traces (***A***) and *I-V* relationships (***B***) showing break in (blue), activation with Diaz [in] (green), and block with Ebs (red); time lag before onset of block represents transit time in perfusion system. ***C***. Block of Diaz-induced current by Ebs at +60 mV. Ebs blocked 93.9 ± 5.6% (n = 15, P < 0.001) of the Diaz-induced current (148.5 ± 20.4 pA/pF) in a physiological Cl^- gradient. ***D***. Time-course for Diaz-induced current activation, block by Ebs, and time of break in (blue square); symbols correspond to ***B***. Patch pipette was back-filled with Ebs at 0 min. Dash line indicates current upon break in.

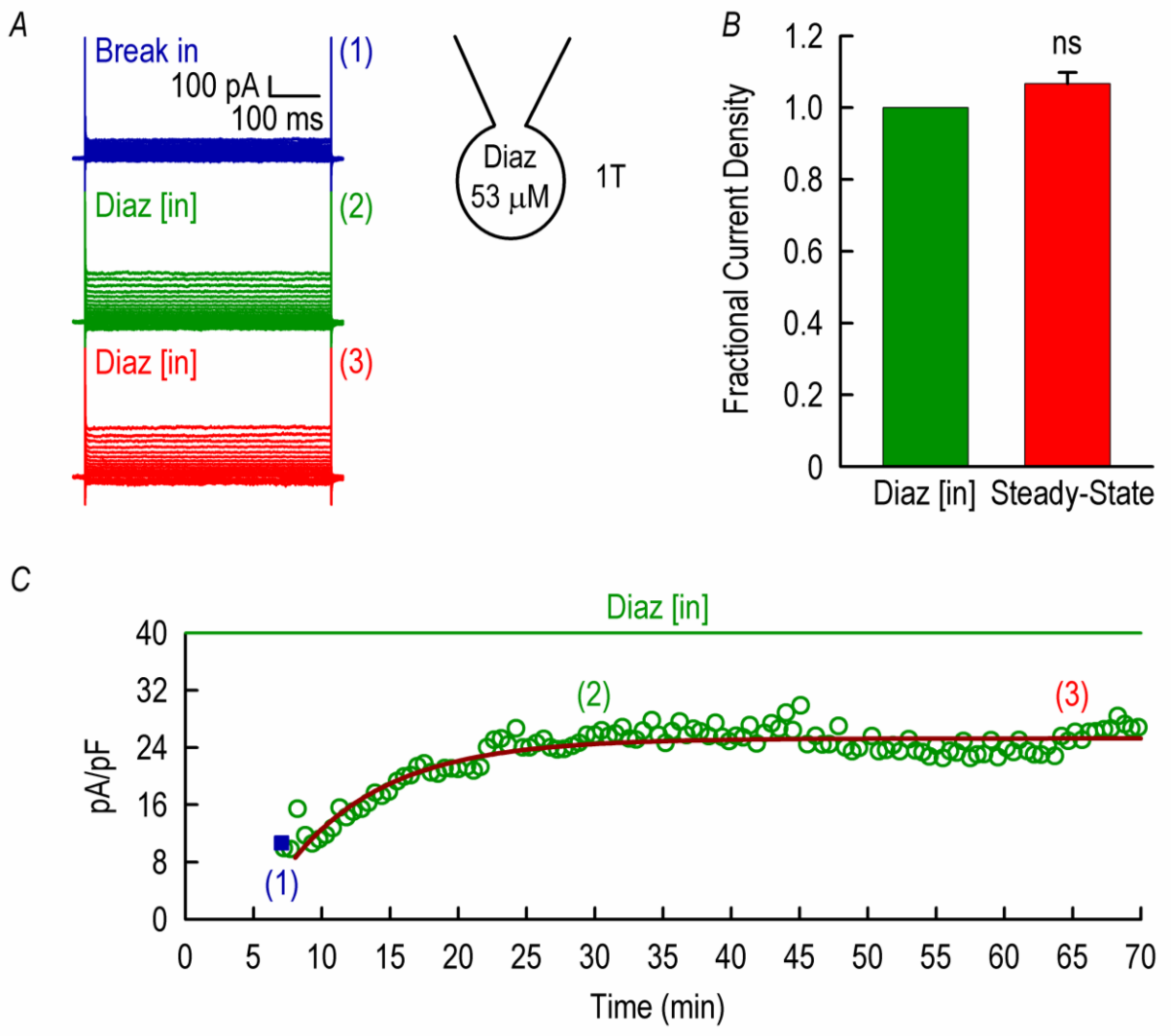

FIG. 4: $I_{Cl,swell}$ failed to rundown during prolonged activation (~1 hr). ***A***. Current traces at break in (blue), after full activation of $I_{Cl,swell}$ by Diaz [in] (green), and after prolonged activation (steady-state; red) recorded at times indicated by (1), (2) and (3) in ***C***. ***B***. Diaz-induced current after full activation (100.6 ± 33.3 pA/pF) at (2) and in steady-state (3) were not distinguishable (n = 6, P = 0.084; *ns*). ***C***. Time-course showing when corresponding current traces were taken.

45 nM Ebs was characterized in detail. Fig. 5 shows that 45 nM Ebs fully blocked $I_{Cl,swell}$ and that increasing superfusate Ebs to 15 μM did not significantly block additional current. Nevertheless, block by 45 nM Ebs demonstrated slower kinetics as expected. Assuming a simple 1:1 bimolecular reaction between Ebs and its receptor, full block at 45 nM suggests that that the IC_{50} for block of $I_{Cl,swell}$ by Ebs must be <5 nM.

3.3.2 Ebs failed to washout

The apparent Ebs IC_{50} of <5 nM and the time course of development of block suggest that the rate of dissociation of Ebs must be very slow or irreversible. Fig. 6 demonstrates that block of $I_{Cl,swell}$ by 15 μM Ebs failed to washout in 1T bath solution. Ebs blocked 94.1 ± 0.9% of the current, and 94.1 ± 1.5% remained blocked after 5-25 min of washout (n = 6, P = 0.987; *ns*). To rule out the possibility that the apparent irreversibility of Ebs block was due to an interaction between diazoxide in the pipette solution (Diaz [in]) and Ebs added to the bathing solution, an alternative approach was used to activate $I_{Cl,swell}$. Antimycin A inhibits the mitochondrial electron transport chain at Complex III, causes ROS to spill into the cytosol, and like diazoxide, activates $I_{Cl,swell}$ (Deng et al., 2010a). Fig. 7 illustrates the activation of $I_{Cl,swell}$ when the patch pipette was backfilled with antimycin A (10 μM; AntiA [in]), block by Ebs, and attempted washout of Ebs in 1T. Both Anti [in] (Fig. 7) and Diaz [in] (Fig. 6) elicited similar outwardly rectifying currents with the expected E_{Cl}. Furthermore, AntiA [in]-activated $I_{Cl,swell}$ was blocked by Ebs, 84.3 ± 2.9% (n = 4, P < 0.001), and block by Ebs failed to significantly washout in 1T after 20-60 min (n = 4, P = 0.085; *ns*). Therefore, block of $I_{Cl,swell}$ by Ebs appeared to be irreversible within the timescale of the patch clamp recording and did not depend on the agent used to elicit $I_{Cl,swell}$ in 1T.

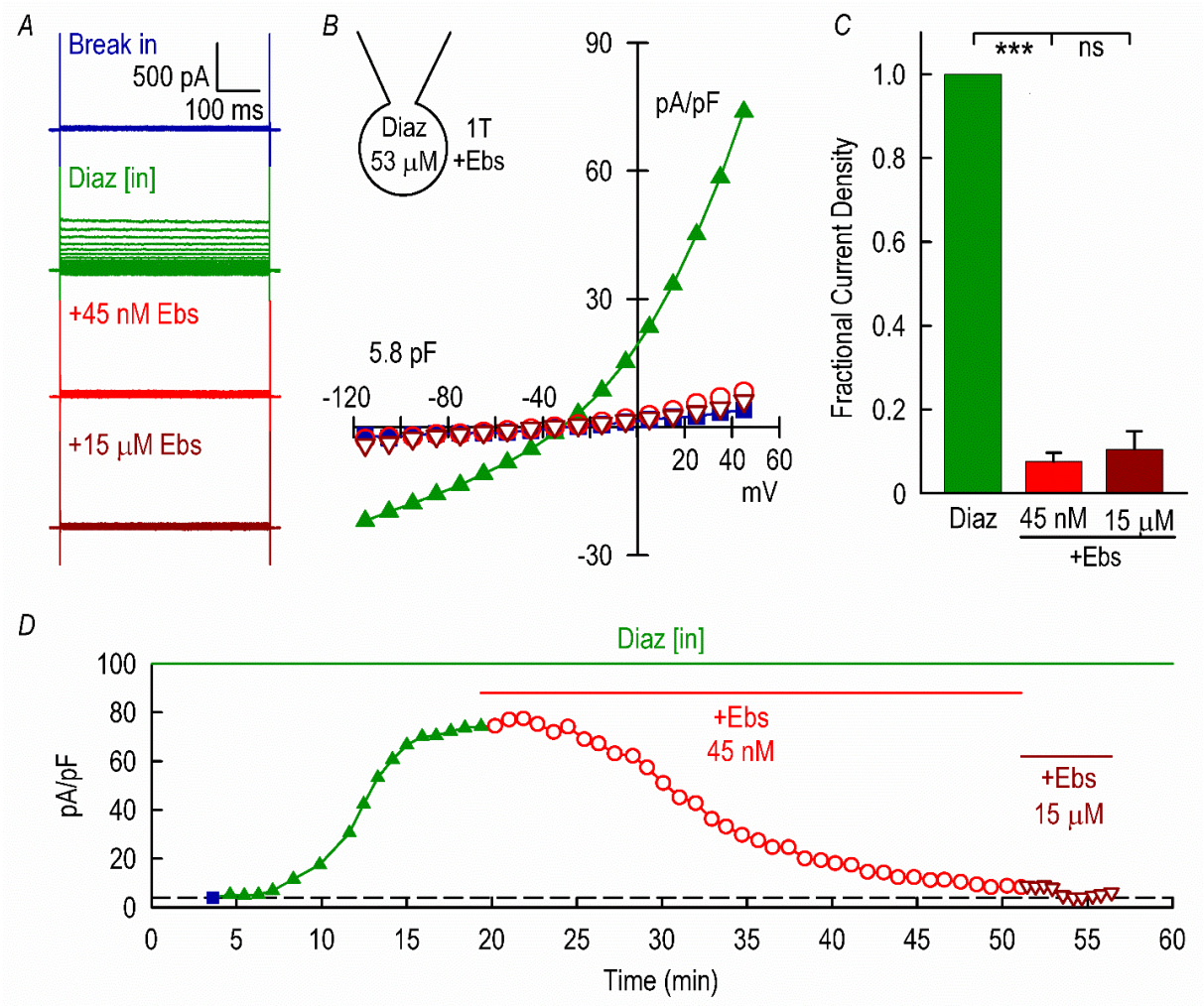

FIG. 5: Ebselen blocked $I_{Cl,swell}$ with high affinity. Diaz [in]-induced $I_{Cl,swell}$ was blocked by 45 nM Ebs. Current traces (***A)*** and *I-V* relationships (***B***) at break in (blue), after activation with Diaz [in] (green), and after block with 45 nM Ebs (red; open circle) and 15 μM Ebs (dark red; downward open triangle). ***C***. Fractional block of Diaz-induced current by Ebs. Ebs (45 nM) blocked 92.5 ± 2.2% (n = 3, P < 0.001) of the Diaz [in]-induced current (101.9 ± 20.9 pA/pF), and increasing Ebs to 15 μM failed to provide addition block (n = 3, P = 0.385; *ns*). ***D***. Time-course for current activation by Diaz [in], block by 45 nM and 15 μM Ebs, and time of break in.

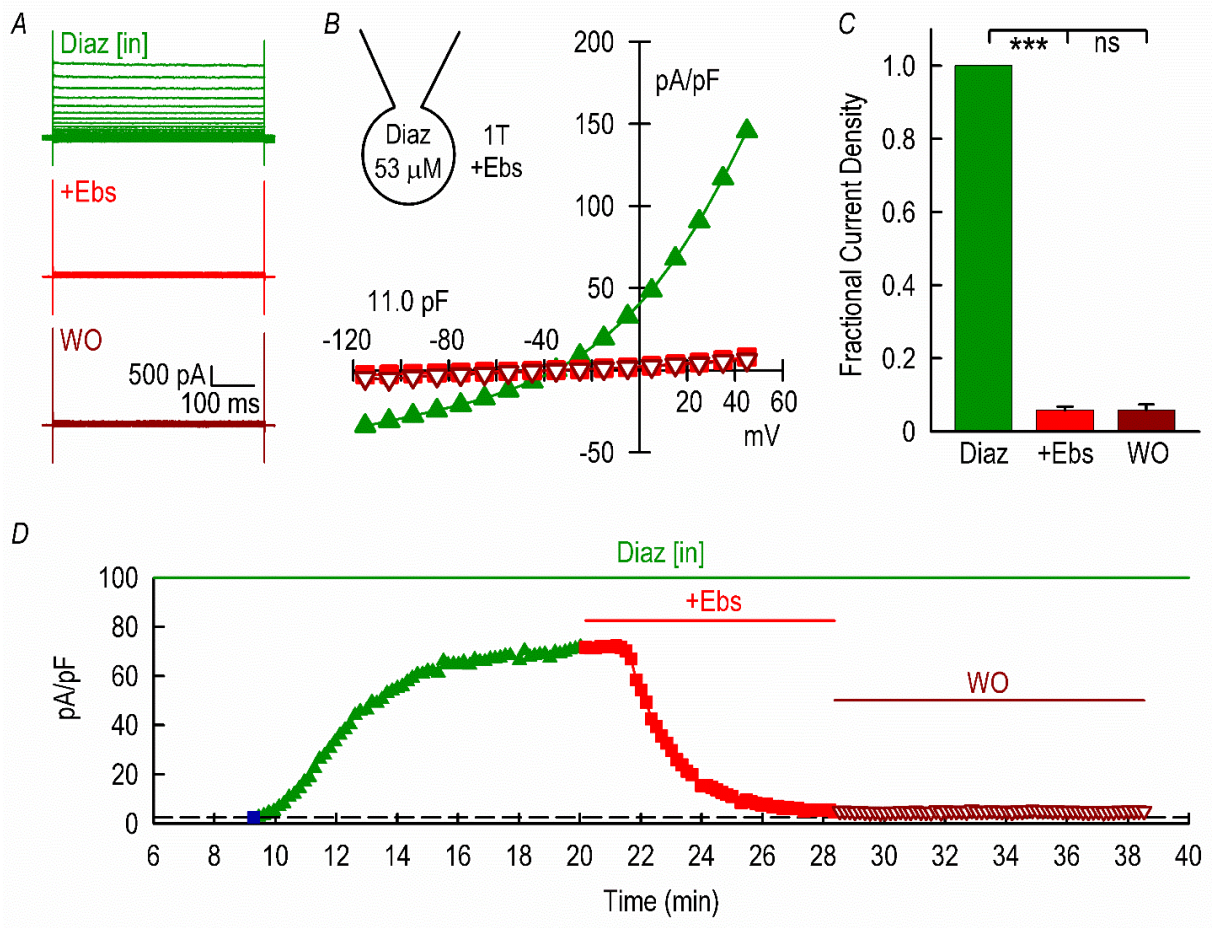

FIG. 6: Ebselen block of diazoxide-induced $I_{Cl,swell}$ failed to washout. $I_{Cl,swell}$ was activated with Diaz [in] and blocked by adding 15 μM Ebs to bath solution. $I_{Cl,swell}$ did not recover on washout (WO) in Ebs-free 1T bathing media. Current traces (***A***) and *I-V* relationships (***B***) showing activation of $I_{Cl,swell}$ with Diaz (green), block with 15 μM Ebs (red), and washout with 1T (dark red). ***C***. Ebs (15 μM) blocked 94.1 ± 0.9% (n = 6, $P < 0.001$) of the Diaz [in]-induced current (105.0 ± 15.1 pA/pF) and failed to washout in 1T (n = 6, P = 0.987; *ns*). ***D***. Time-course for activation, block and attempted washout; time of break in indicated by filled square (blue).

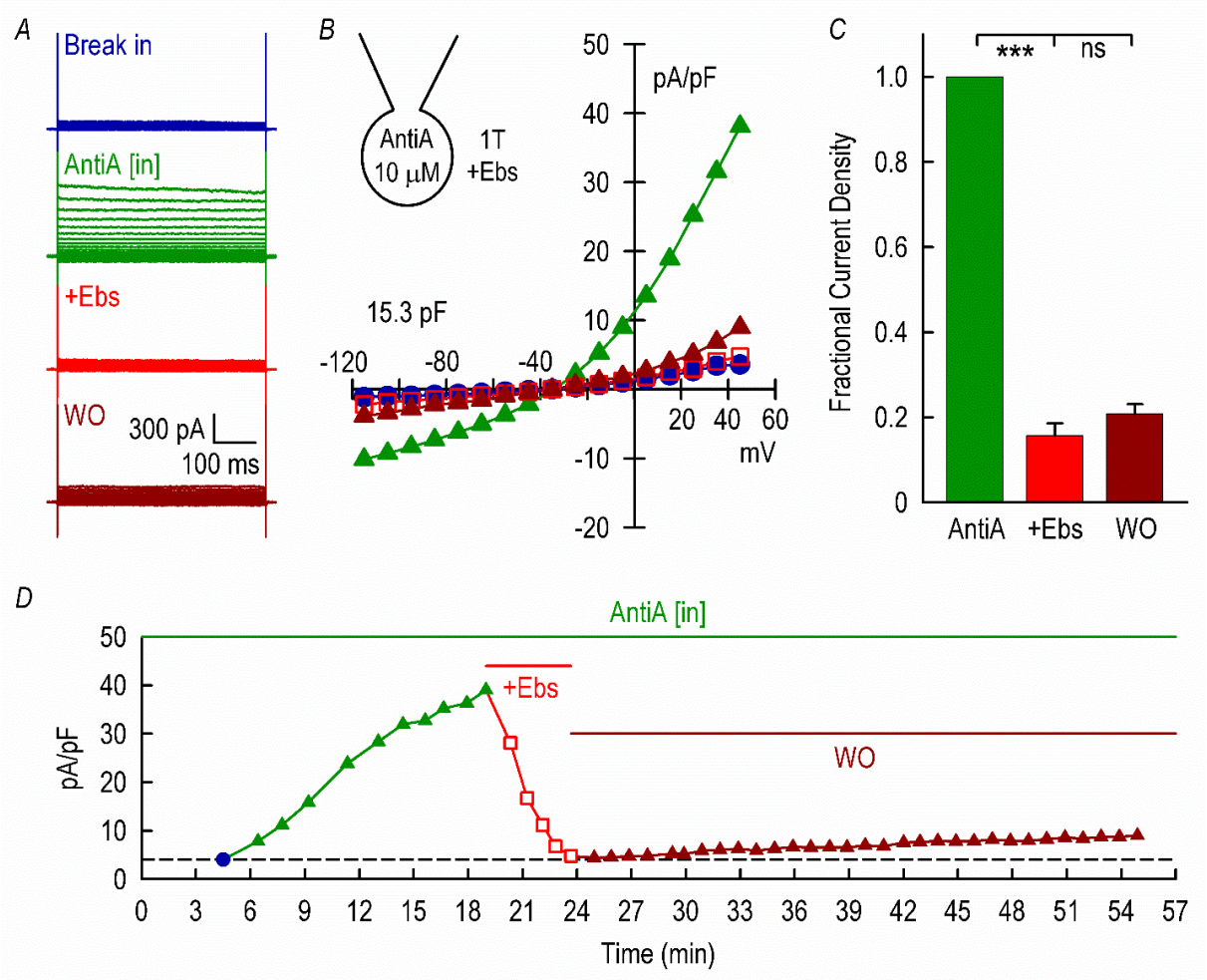

FIG. 7: Ebselen blocked antimycin A-induced $I_{Cl,swell}$ and failed to washout. $I_{Cl,swell}$ was activated by 10 μM antimycin A in pipette solution (AntiA [in]; see inset) and was rapidly blocked with 15 μM Ebs. Current traces (***A***) *I-V* relationships (***B***) showing break in (blue), after activation with AntiA [in] (green), block with Ebs (red), and attempted Ebs washout (WO) in 1T (dark red). ***C***. Fractional block of AntiA-induced current and washout. Ebs (15 μM) blocked 84.3 ± 2.9% (n = 4, P < 0.001) of AntiA [in]-induced current (54.9 ± 15.4 pA/pF) and block failed to significantly washout in 1T (n = 4, P = 0.085; *ns*). ***D***. Time-course for the current activation by AntiA [in], block by Ebs, attempted washout, and time of break in.

3.4 H_2O_2 Failed to Reactive $I_{Cl,swell}$ Following Ebs Block

The fact that Ebs blocked $I_{Cl,swell}$ elicited by activators of mitochondrial ROS production suggests that its site of action is distal in the signaling cascade that leads to activation of $I_{Cl,swell}$ by osmotic swelling and signaling molecules (Deng et al., 2010a). Because H_2O_2 is the most downstream activator of $I_{Cl,swell}$ identified to date (Deng et al., 2010a), we tested whether the site of block by Ebs is upstream or downstream of the current activated by H_2O_2. Fig. 8 demonstrates that Ebs blocked 92.5 ± 2.2% of AntiA [in]-induced $I_{Cl,swell}$, and 85.5 ± 6.3% remained blocked following Ebs washout (2-5 min) and subsequent H_2O_2 superfusion (15-20 min). Failure H_2O_2 to reactivate $I_{Cl,swell}$ after block by and washout of Ebs (n = 3, P = 0.322, *ns*) implies Ebs acts downstream to H_2O_2 in the signaling cascade. In contrast, if Ebs simply acts as a GPx mimetic and quenches ROS (Nakamura et al., 2002; Sakurai et al., 2006; Deng et al., 2010a, 2010b), one would expect reactivation of $I_{Cl,swell}$ by H_2O_2 applied after washout of Ebs.

This observation leads to several possibilities. Since H_2O_2 is a major form of ROS that crosses the plasma membrane barrier, Ebs could directly target an intracellular source of ROS or a proximate regulator responsible for $I_{Cl,swell}$. On the other hand, although H_2O_2-induced activation of $I_{Cl,swell}$ is documented in cardiac myocytes (Browe and Baumgarten, 2004; Ren et al., 2008; Deng et al., 2010a), HeLa cells (Shimizu et al., 2004) and HTC cells (Varela et al., 2004), to our knowledge the role of ROS and activation of $I_{Cl,swell}$ by H_2O_2 has not been documented in DI TNC1 astrocytes. Thus, one might argue that failure of H_2O_2 to overcome Ebs block reflects differences in signaling responsible for activating $I_{Cl,swell}$ rather than the site of Ebs block in the signaling cascade. To exclude this possibility, we tested whether H_2O_2 elicited $I_{Cl,swell}$ in DI TNC1 astrocytes in 1T bathing media. As shown in Fig. 9, exposure to 500 μM H_2O_2 evoked an outwardly rectifying current that was fully blocked by DCPIB. This confirms the conclusion that Ebs is downstream of H_2O_2 in the signaling cascade and is the most proximate modulator of $I_{Cl,swell}$ identified to date.

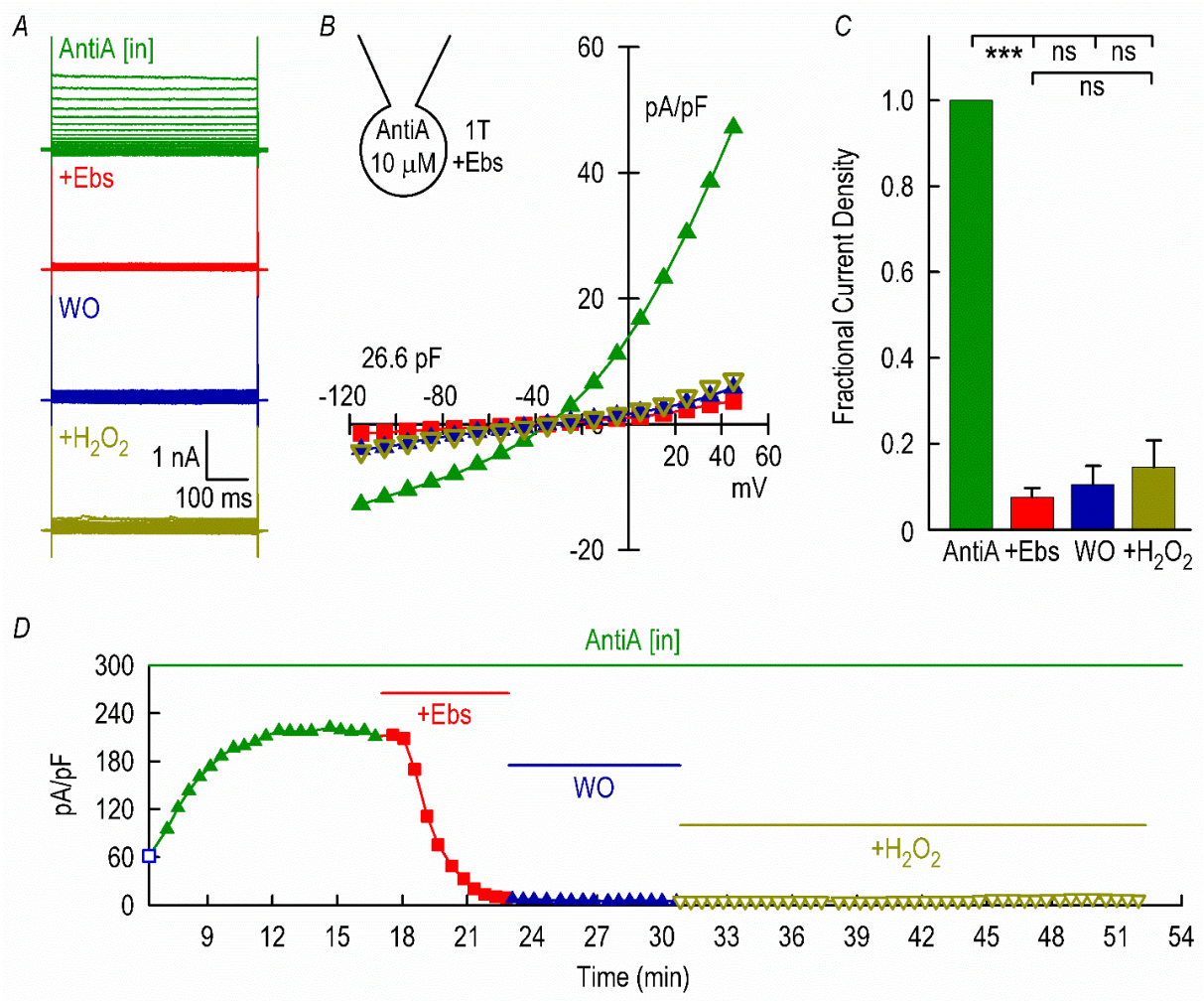

FIG. 8: H_2O_2 failed to activate $I_{Cl,swell}$ following block with Ebs. $I_{Cl,swell}$ was activated with AntiA [in], blocked with 15 µM Ebs, and Ebs was briefly washed out prior to adding H_2O_2. Current traces (***A***) and *I-V* relationships (***B***) showing activation with AntiA [in] (green), block with Ebs (red), washout of Ebs (WO, blue), and attempted $I_{Cl,swell}$ activation with H_2O_2 (dark yellow). ***C***. Fractional block of AntiA-induced current (100.2 ± 45.4 pA/pF) by Ebs, washout of Ebs from bath, and response to adding H_2O_2. Ebs blocked 92.5 ± 2.2% (n = 3, P < 0.001) of the normalized current, and block was unaffected by washout in 1T bath solution (n = 3, P = 0.471; *ns*). H_2O_2 (500 µM) failed to significantly reactivate $I_{Cl,swell}$ after block by Ebs (vs. Ebs, P = 0.322, *ns*; vs. WO, P = 0.566, *ns*; n = 3 for both). ***D***. Time-course for the experiment; time of break in indicated by open square (blue).

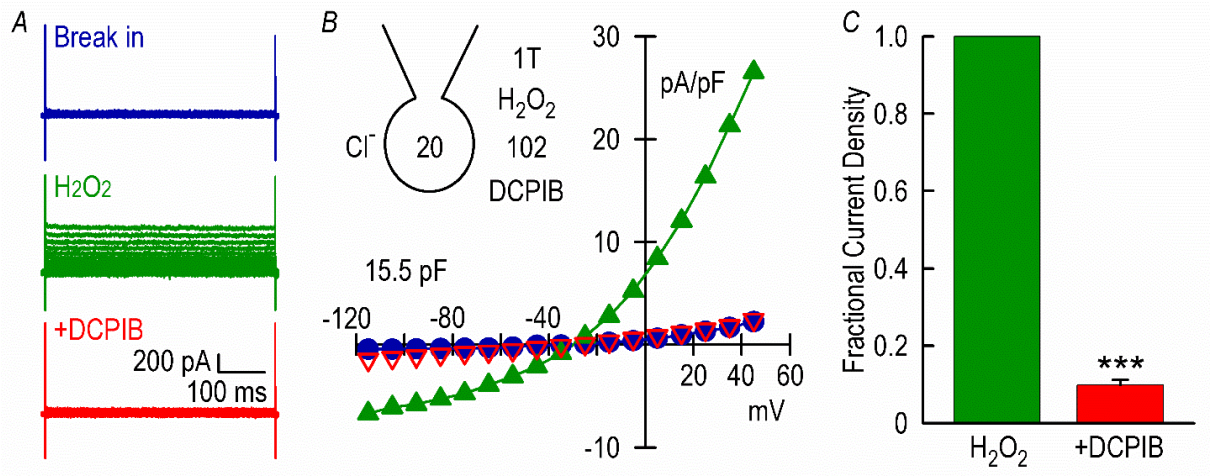

FIG. 9: Activation of outwardly rectifying $I_{Cl,swell}$ and block by DCPIB following H_2O_2 addition in physiological Cl^- gradient in DI TNC1 astrocytes. $I_{Cl,swell}$ was activated by H_2O_2 (500 μM, 10 – 15 min) and blocked with 10 μM DCPIB (10 μM, 5 - 10 min) in physiological Cl^- (see inset). Current traces (***A***) and *I-V* relationships (***B***) showing break in (blue), activation with H_2O_2 (green), and block with DCPIB (red). ***C***. Fractional block of H_2O_2-induced current (28.9 ± 5.2 pA/pF) by DCPIB; DCPIB blocked 90.2 ± 1.3% (n = 4, $P < 0.001$) of the normalized current.

3.5 Ebs Congeners Lacking GPx Activity Completely Blocked $I_{Cl,swell}$

3.5.1 EbO

As Ebs demonstrates chemical structural congeners (Schewe, 1995, Zhao et al., 2002; Sakurai et al., 2006), ebselen oxide (EbO), a congener readily produced by oxidation of Ebs in the presence of either H_2O_2 (Glass et al., 1988) or peroxynitrite (Daiber et al., 2000), was tested. Unlike Ebs, EbO is not a GPx-mimetic and lacks the antioxidative profile of Ebs (Lass et al., 1996). Since superoxide radical ($O_2^{-\bullet}$) or H_2O_2 produced by NOX can directly stimulate ROS production via Complex III (Deng et al., 2010a) and $O_2^{-\bullet}$ is known to generate peroxynitrite in the presence of NO (Pacher et al., 2007), block of $I_{Cl,swell}$ with EbO was tested under the assumption that Ebs may be converted to EbO during $I_{Cl,swell}$ activation.

3.5.1(a) Block of $I_{Cl,swell}$ with EbO

If Ebs blocks $I_{Cl,swell}$ by scavenging ROS, EbO should be ineffective because EbO lacks ROS scavenging activity (Lass et al., 1996). To the contrary, Fig. 10 shows that EbO (15 μM) blocked 92.6 ± 1.7% (n = 5, P < 0.001) of the current elicited by Diaz [in]. Moreover, block by EbO also appeared to be irreversible as 94.2 ± 1.8% of the current remained blocked after washout of EbO for 35-100 min (n = 5, P = 0.324; *ns*). On the other hand, the kinetics of block by 15 μM EbO was obviously slower than by 15 μM Ebs (Ebs: 1.6 ± 0.3 min, n = 5; EbO: 11.9 ± 2.2 min, n = 7; P < 0.001). Block with EbO required ~20 min (Fig. 10), whereas block by the same concentration of Ebs was complete in 2-3 min (Fig. 3). The fact that a non-GPx-mimetic analog of Ebs induced complete block of $I_{Cl,swell}$ with apparent irreversibility upon washout raises the possibility that Ebs and EbO act by a common mechanism that is independent of ROS scavenging.

3.5.1(b) EbO blocked downstream of H_2O_2

To determine whether EbO, like Ebs, acts at a site distal to H_2O_2, we attempted to

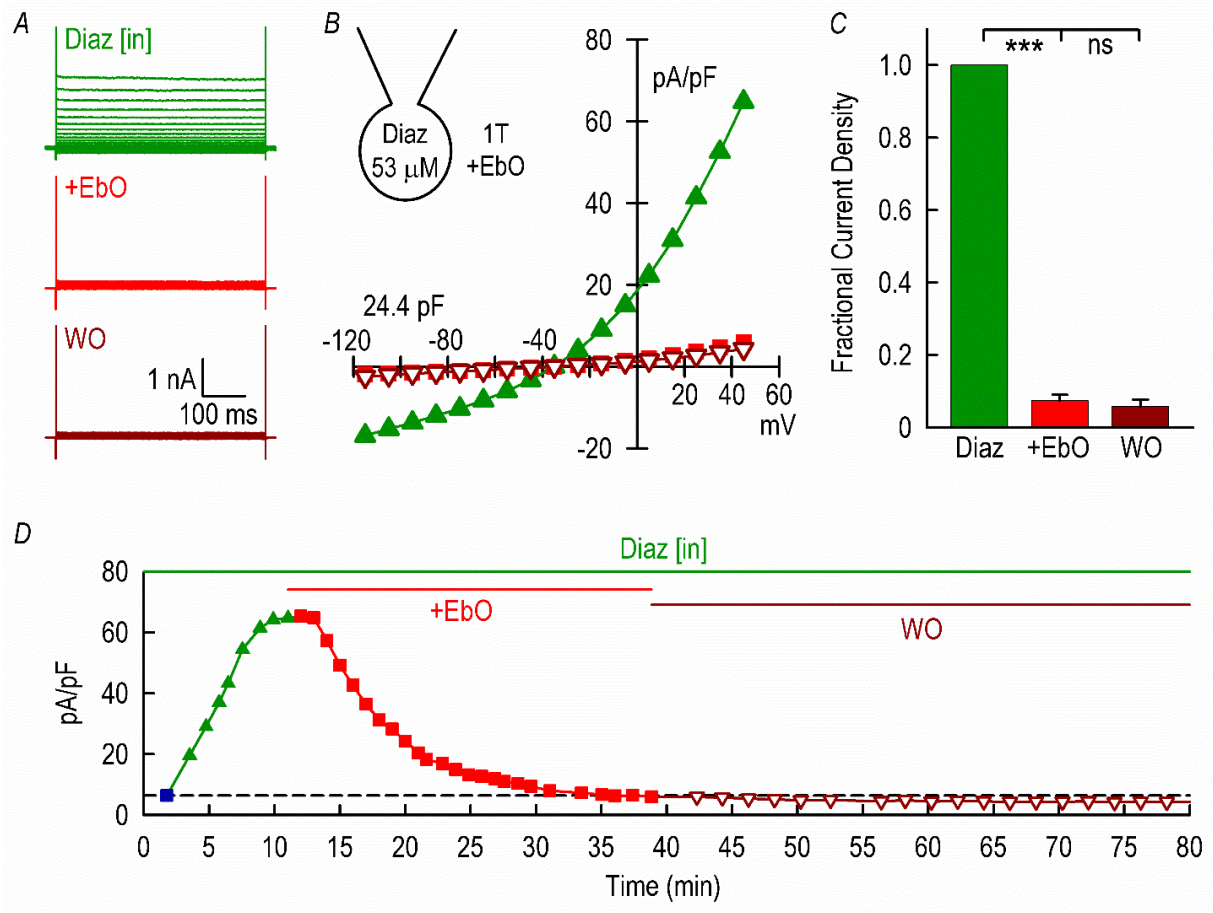

FIG. 10: Ebselen oxide (EbO) blocked $I_{Cl,swell}$ and failed to washout. $I_{Cl,swell}$ was activated with Diaz [in] and was blocked with 15 μM EbO. Current traces (***A***) and *I-V* relationships (***B***) showing $I_{Cl,swell}$ activation with Diaz [in] (green), block with 15 μM EbO (red), and attempted washout with EbO-free 1T bath solution (dark red). ***C***. Fractional block of Diaz-induced current (159.7 ± 62.4 pA/pF) by EbO and washout. EbO (15 μM) blocked 92.6 ± 1.7% (n = 5, P < 0.001) of the current and failed to washout in 1T (n = 5, P = 0.324; *ns*). ***D***. Time-course of the experiment; time of break in indicated by blue square.

reactivate $I_{Cl,swell}$ following block with EbO. After activating $I_{Cl,swell}$ with Diaz [in], EbO blocked 93.1 ± 1.4% (n = 4, $P < 0.001$) of the current and 95.0 ± 0.9% of block was maintained after failed attempts to reactivate $I_{Cl,swell}$ with H_2O_2 (vs. EbO, $P = 0.186$, *ns*; vs. WO, $P = 0.383$, *ns*; $n = 4$ for both) (Fig. 11). Therefore, block of $I_{Cl,swell}$ with EbO was downstream of H_2O_2 and these findings suggest both a common mechanism and common binding site.

3.5.2 Thr101

Thr101 is a NOX2-selective (Smith et al., 2012) congener of Ebs with a sulfur replacing selenium and an additional fluoride (F) and methyl (CH_3-) group. In contrast to Ebs but similar to EbO, Thr101 does not possess GPx activity (Leurs et al., 1989). One might argue that block of $I_{Cl,swell}$ by EbO in the previous experiment could be due to reduction of EbO back to GPx-mimetic Ebs by an unknown cellular processes. Therefore, to further challenge the importance of Ebs GPx mimetic activity in block of $I_{Cl,swell}$, we tested the ability of Thr 101 to block of $I_{Cl,swell}$ despite the Se to S substitution and the response to exogenous H_2O_2 after block. Because NOX2 is upstream from mitochondrial ROS production in the $I_{Cl,swell}$ signaling cascade (Deng et al., 2010a), activation of $I_{Cl,swell}$ by mitochondrial ROS is expected to bypass the effect of suppression of NOX2 by Thr101 on $I_{Cl,swell}$.

3.5.2(a) Block of $I_{Cl,swell}$ with Thr101

Fig. 12 shows Thr101 blocked 86.2 ± 4.1% ($n = 3$, $P < 0.001$) of Diaz [in]-induced $I_{Cl,swell}$. The kinetics of block by Thr101 was slow relative to Ebs (Ebs: 1.6 ± 0.3 min; Thr101: 23.1 ± 6.0 min; $n = 5$ for both; $P < 0.001$). Moreover, Thr101 failed to washout after 25-55 min, and 90.4 ± 3.6% of the current remaining blocked ($n = 3$, $P = 0.269$; *ns*). Thus block of $I_{Cl,swell}$ by Thr101 also appeared irreversible (Fig. 12). This demonstrates that Se is not required and GPx-like activity were not required to irreversibly block $I_{Cl,swell}$.

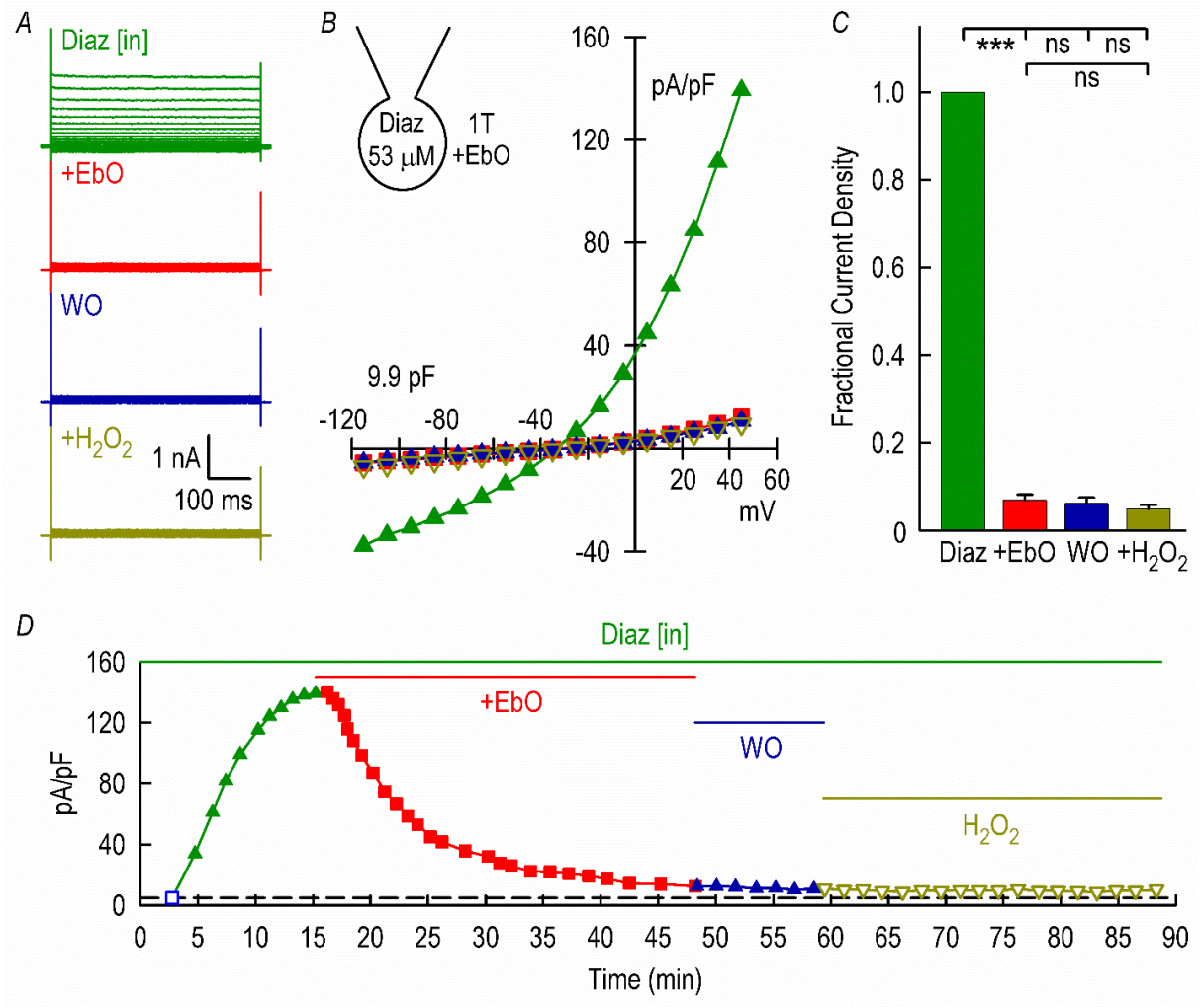

FIG. 11: H_2O_2 failed to activate $I_{Cl,swell}$ following block with EbO. $I_{Cl,swell}$ was activated with Diaz [in], blocked with 15 μM EbO, and EbO briefly washed out prior to adding H_2O_2. Current traces (***A***) and *I-V* relationships (***B***) showing activation with Diaz [in] (green), block with EbO (red), washout of EbO (blue), and attempted activation with H_2O_2 (dark yellow). ***C***. Fractional block of Diaz-induced current (99.2 ± 14.0 pA/pF) by 15 μM EbO, response to washout of EbO, and attempted activation of $I_{Cl,swell}$ with H_2O_2. EbO (15 μM) blocked 93.1 ± 1.4% (n = 4, $P < 0.001$) of the current and failed to washout in 1T ($n = 4$, $P = 0.471$; *ns*). Final treatment with H_2O_2 (500 μM) also failed to recover $I_{Cl,swell}$ compared to EbO block ($n = 4$, $P = 0.186$; *ns*) or washout ($n = 4$, $P = 0.383$; *ns*). ***D***. Time-course of experiment; time of break in indicated by open blue square.

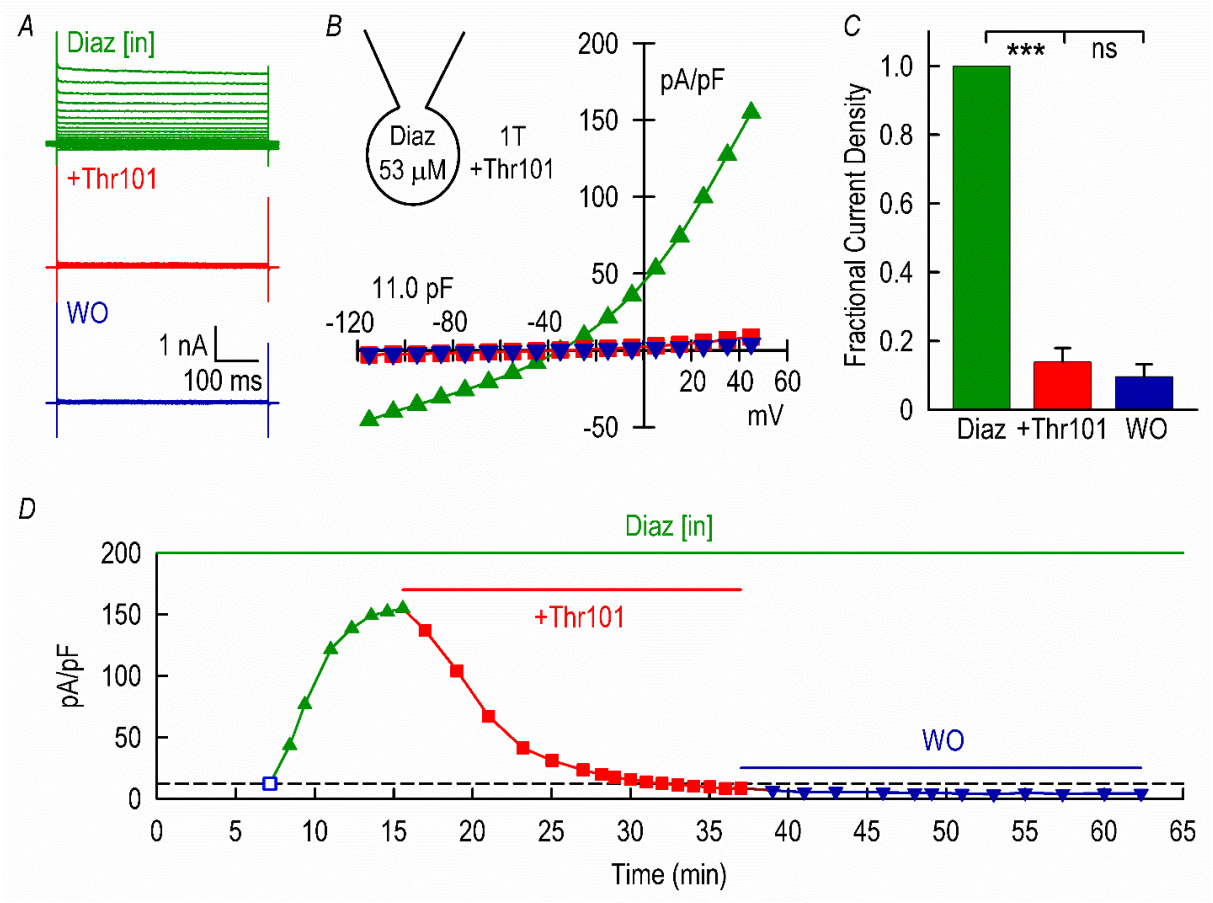

FIG. 12: Thr101 blocked $I_{Cl,swell}$ and failed to washout. $I_{Cl,swell}$ was activated with Diaz [in] and was blocked with 15 μM Thr101. Current traces (***A***) and *I-V* relationships (***B***) showing activation with Diaz (green), block with 15 μM Thr101 (red), and attempted washout with 1T bath solution (blue). ***C***. Fractional block of Diaz-induced current (102.5 ± 44.4 pA/pF) by 15 μM Thr101 and attempted washout of Thr101. Thr101 blocked 86.2 ± 4.1% (n = 3, $P < 0.001$) of the current and failed to washout in 1T (n = 3, $P = 0.269$; *ns*). ***D***. Time-course of the experiment; time of break in indicated by open blue square.

3.5.2(b) Thr101 blocked downstream of H_2O_2

To determine if Thr101 blocked distal to H_2O_2, the effect of exogenous H_2O_2 (11-52 min) following Thr101 inhibition was also tested (Fig. 13). After blocking 83.8 ± 1.2% (*n* = 3, *P* < 0.001) of Diaz [in]-induced $I_{Cl,swell}$, H_2O_2 failed to reactivate $I_{Cl,swell}$ (vs. Thr101, *P* = 0.202, *ns*; vs. WO, *P* = 0.234, *ns*; *n* = 3 for both) and 86.5 ± 1.3% of current remained blocked (Fig. 13). As shown for Ebs (Fig. 8) and EbO (Fig. 11), Thr101 (Fig. 13) blocked downstream of exogenous H_2O_2. This implies that block of $I_{Cl,swell}$ with Thr101 is likely to be independent of NOX2- and mitochondrial ROS generation.

3.6 Mechanism of Block and Location of Binding Site

The apparent irreversibility and chemistry of Ebs and its congeners raise the possibility that these compounds act by forming Se-S (Glass et al., 1988; Sakurai et al., 2006) or S-S (Smith et al., 2012) bonds. Therefore, we decided to use classic impermeant MTS reagents to probe for the existence of thiol groups critical for the function of $I_{Cl,swell}$.

3.6.1 MTSES blocked $I_{Cl,swell}$

When negatively charged MTSES (Dunten et al., 1993; Yang et al., 1996; Chahine et al., 1997) was added to the bathing media following activation of $I_{Cl,swell}$ by Diaz [in], it blocked 81.5 ± 5.0 pA/pF (*n* = 3, *P* < 0.001) of the Diaz [in]-induced current (103.7 ± 11.3 pA/pF), as shown in Fig. 14. As expected for formation of a S-S bond by MTSES, block appeared to be irreversible upon washout of MTSES (8-37 min) in DI TNC1 astrocytes (*n* = 3, *P* = 0.233; *ns*). These experiments used a much lower concentration of MTSES than is often employed (e.g., 3.33 mM; Qiu et al., 2014), and 110 μM MTSES took >1 hr to fully suppress $I_{Cl,swell}$. Nevertheless, this demonstrates that free -SH groups accessible from the bathing solution are necessary to generate $I_{Cl,swell}$ but does not identify the responsible protein. To confirm this requirement was not cell-line specific, we repeated

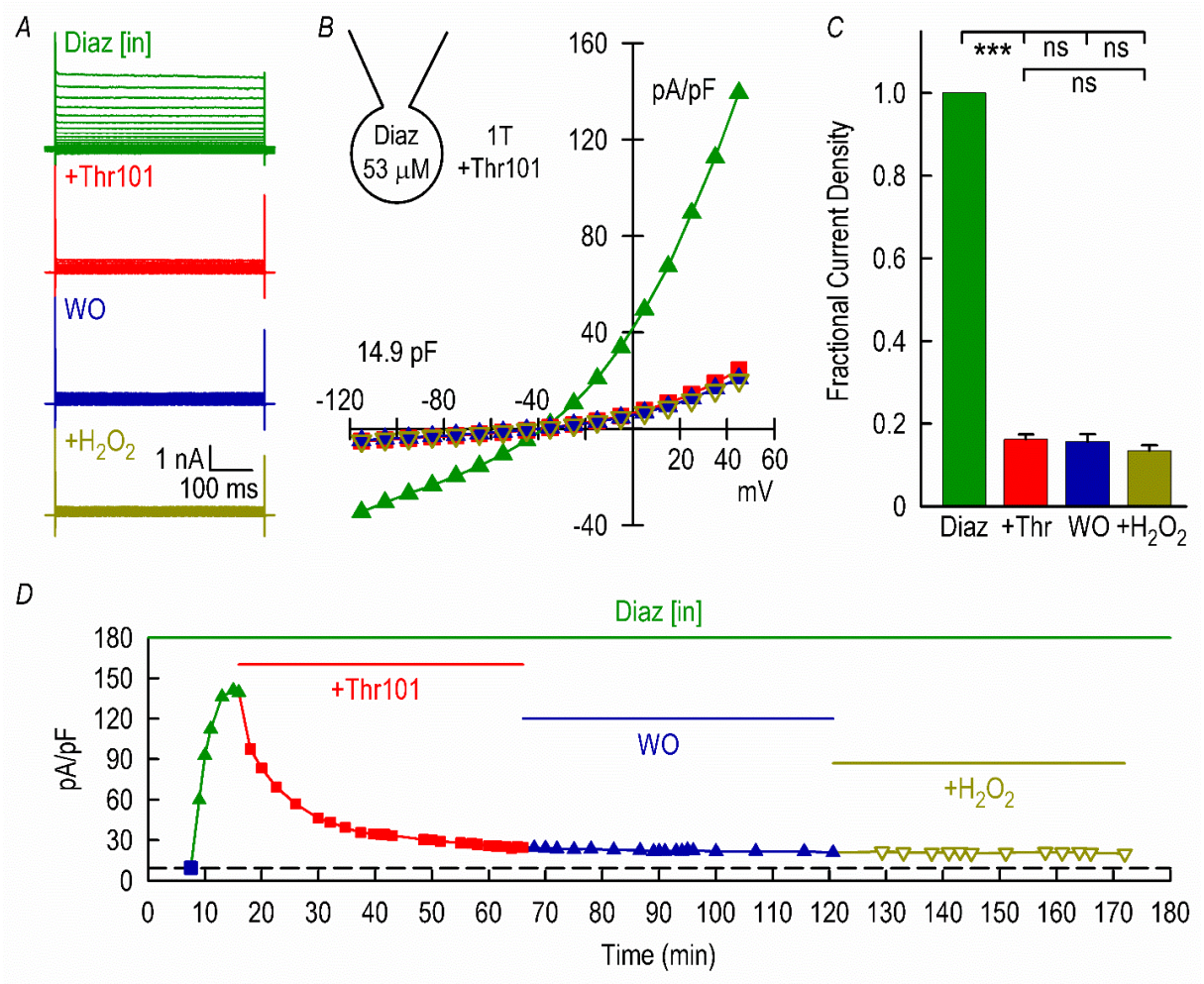

FIG. 13: H_2O_2 failed to activate $I_{Cl,swell}$ following block with Thr101. $I_{Cl,swell}$ was activated with Diaz [in], blocked with 15 µM Thr101, and washed out prior to H_2O_2 treatment. Current traces (***A***) and *I-V* relationships (***B***) showing activation with Diaz [in] (green), block with 15 µM Thr101 (red), washout of Thr101 (blue), and attempted activation with H_2O_2 (dark yellow). ***C***. Fractional block of Diaz-induced current (145.0 ± 3.3 pA/pF) by 15 µM Thr101, response to washout of Thr101, and attempted activation of $I_{Cl,swell}$ with H_2O_2. Thr101 (15 µM) blocked 83.8 ± 1.2% (n = 3, P < 0.001) of the normalized current and failed to washout in 1T (n = 3, P = 0.708; *ns*). Final treatment with H_2O_2 (500 µM) also failed to recover $I_{Cl,swell}$ compared to Thr101 block (n = 3, P = 0.202; *ns*) or washout (n = 3, P = 0.234; *ns*). ***D***. Time-course of the experiment; time of break in indicated by blue square.

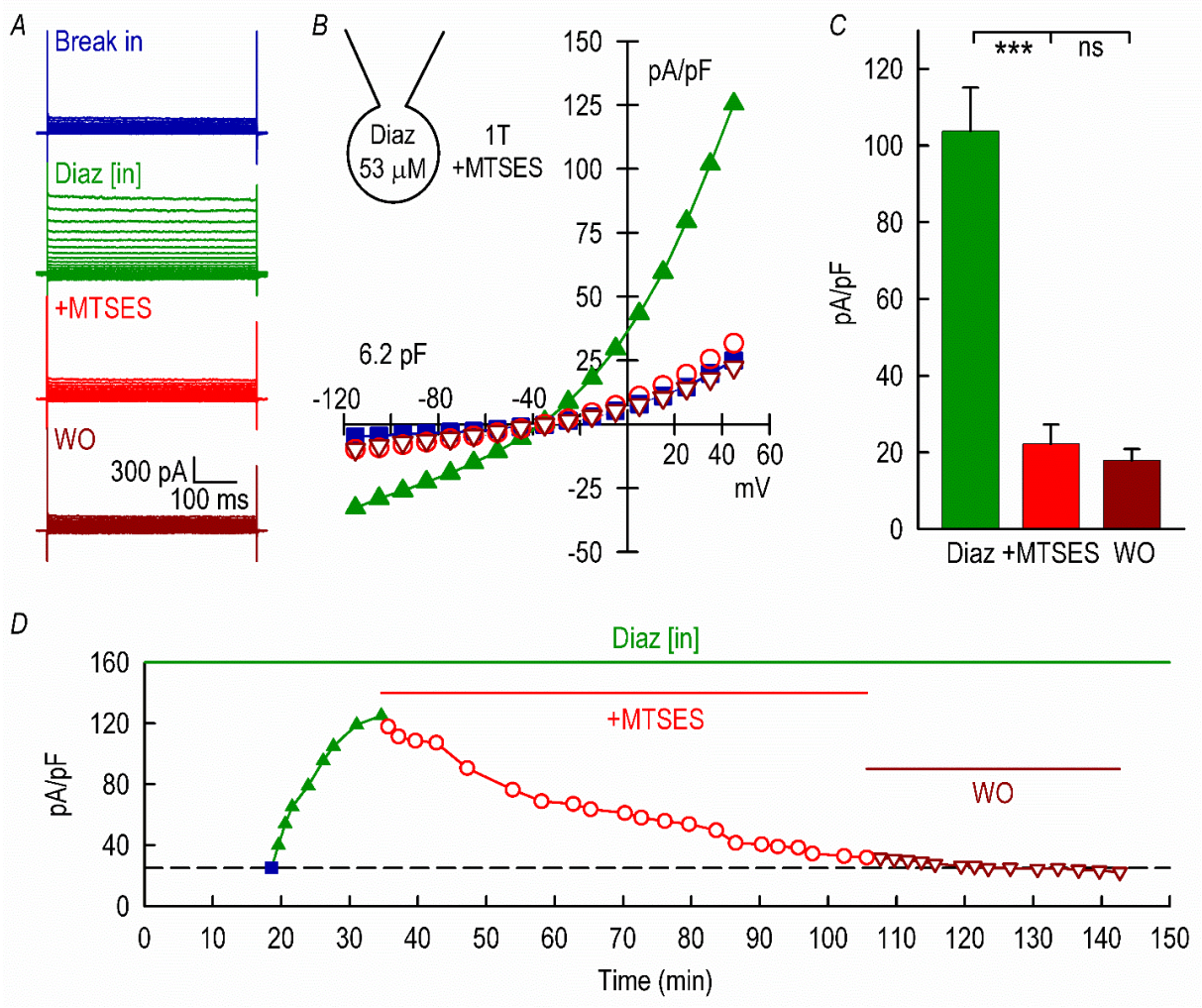

FIG. 14: MTSES blocked $I_{Cl,swell}$ and failed to washout in DI TNC1 astrocytes. $I_{Cl,swell}$ was activated in DI TNC1 astrocytes with Diaz [in] and was blocked with MTSES. Current traces (***A***) and *I-V* relationships (***B***) showing break in (blue), activation with Diaz [in] (green), block with 110 μM MTSES (red), and attempted washout in 1T (dark red). ***C***. Block of Diaz-induced raw current density (pA/pF) by MTSES and washout (WO). MTSES (110 μM) blocked 81.5 ± 5.0 pA/pF (n = 3, P < 0.001) of the Diaz-induced current (103.7 ± 11.3 pA/pF) and failed to washout in 1T (n = 3, P = 0.233; *ns*). ***D***. Time-course for the experiment; time of break in indicated by blue square.

the study using the HEK293 cell line. $I_{Cl,swell}$ in HEK293 cells was activated by including the same concentration of Diaz in the patch pipette, and MTSES was then added to the bathing media. As found for DI TNC1 cells, MTSES blocked 84.2 ± 5.7% (n = 3, P < 0.01) of Diaz [in]-induced $I_{Cl,swell}$ in HEK293 cells (Fig. 15).

3.6.2 MTSEA-biotin blocked $I_{Cl,swell}$

Another commonly used MTS reagent in ion channel studies is MTSEA. As MTSEA itself is uncharged and known to permeate the cell membrane, we used MTSEA-biotin (Traebert et al., 2000; Wagner and Czajkowski, 2001), an impermeant biotinylated derivative of MTSEA that would simultaneously test the importance of charge on an MTS reagent and the possibility of streptavidin-assisted pull down of the target channel or regulatory protein. Fig. 16 shows 82.5 ± 4.6% (n = 3, P < 0.001) block of Diaz [in]-induced $I_{Cl,swell}$ with 30 μM MTSEA-biotin. As with MTSES (Fig. 14), block with MTSEA-biotin appeared irreversible following 26-63 min washout and 83.6 ± 3.7% of the current remained blocked (n = 3, P = 0.775; *ns*). Time to full block was >1 hr with the low concentration of reagent. Moreover, positively charged MTSET fully blocked $I_{Cl,swell}$ and showed irreversibility upon washout (Appendix, Fig. 9). The complete block of natively expressed $I_{Cl,swell}$ by MTS reagents with different charge profile strongly suggests that a free -SH groups located extracellularly are required for current activation. Although block was not strictly MTS charge-dependent, we did not assess how MTS charge affected the kinetics of block or its voltage dependence.

3.7 Probing the Existence of Selenenylsulfide (Se-S) Bond with Reducing Agents

If free -SH groups with extracellular access are required for the activity of $I_{Cl,swell}$, then the best complimentary protocol to demonstrating block by Ebs, its congeners, and MTS reagents would be the use of specific reducing agents that can chemically cleave

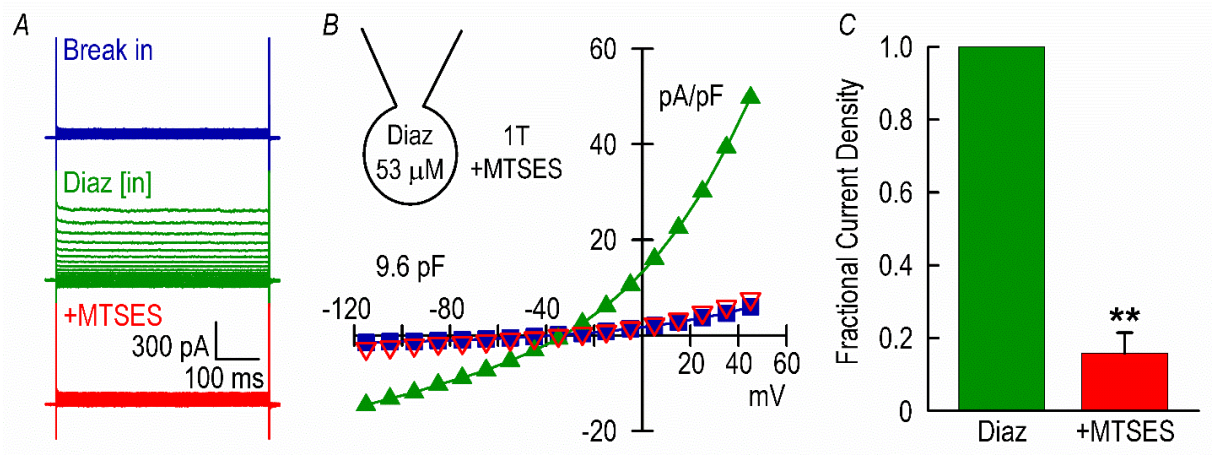

FIG. 15: MTSES blocked $I_{Cl,swell}$ and failed to washout in HEK293 cells. $I_{Cl,swell}$ was activated in HEK293 cells with Diaz [in] and was blocked with MTSES. Current traces (***A***) and *I-V* relationships (***B***) showing break in (blue), activation with Diaz [in] (green), and block with 2 mM MTSES (red). ***C***. Fractional block of Diaz-induced current (112.0 ± 68.8 pA/pF) by MTSES. MTSES (2 mM) blocked 84.2 ± 5.7% (n = 3, $P < 0.01$) of the normalized current.

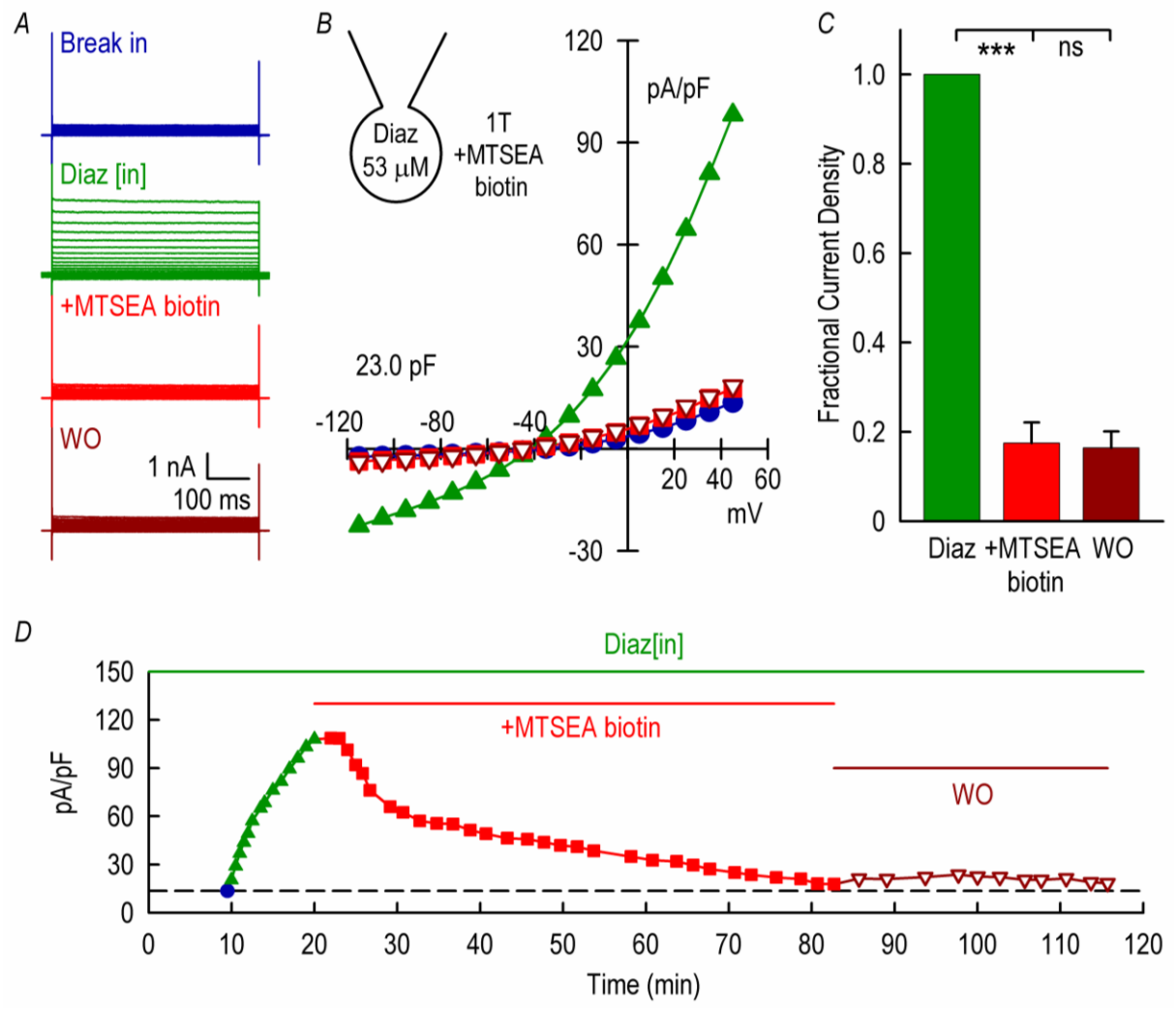

FIG. 16: MTSEA biotin blocked $I_{Cl,swell}$ and failed to washout. $I_{Cl,swell}$ was activated with Diaz [in] and blocked with MTSEA biotin prior to attempted washout (WO) in 1T. Current traces (***A***) and *I-V* relationships (***B***) showing break in (blue), activation with Diaz [in] (green), block with 30 μM MTSEA Biotin (red), and WO with 1T (dark red). ***C***. Fractional block of Diaz-induced current (90.7 ± 15.2 pA/pF) by MTSEA biotin and WO. MTSEA biotin (30 μM) blocked 82.5 ± 4.6% (n = 3, P < 0.001) of the current and failed to washout in 1T (n = 3, P = 0.775; *ns*). ***D***. Time-course for the experiment; time of break in denoted by filled blue circle.

Se-S or S-S bond to reactivate $I_{Cl,swell}$. We used Ebs, the only molecule with nanomolar affinity for $I_{Cl,swell}$, to first block ROS-induced activation of current prior to attempting reactivation with specific reducing agents, DTT and GSH.

3.7.1 DTT

Fig. 17 shows that following Diaz [in]-induced activation of $I_{Cl,swell}$, 15 μM Ebs fully blocked 93.5 ± 1.0% (n = 3, $P < 0.001$) of the current, and 5 mM DTT applied for 15-20 min duration failed to reactivate $I_{Cl,swell}$ (vs. Ebs, $P = 0.220$, *ns*; vs. WO, $P = 0.895$, *ns*; $n = 3$ for both) and 95.0 ± 0.4% of current remained blocked. To explore alternatives, in the experiment illustrated, we also resorted to sequential superfusion of 1 mM (>20 min) and 5 mM (~20 min) impermeant GSH and then a membrane permeable version of GSH, GSH-MEE ($n = 1$). After a total of ~130 min in various reducing, reactivation of the current did not occur.

3.7.2 GSH

To more rigorously test the ability of GSH to reduce the presumptive Se-S bond formed by Ebs, the experiment repeated challenging Ebs block of $I_{Cl,swell}$ with 1 to 10 mM GSH (Fig. 18). Following Ebs blocked of 93.8 ± 1.0% ($n = 5$, $P < 0.001$) of Diaz [in]-induced $I_{Cl,swell}$, Ebs was briefly washed out from the bath (2-3 min) and then GSH was superfused. Near the end of 10 mM GSH superfusion (3-14 min), a small but statistically significant partial recovery $I_{Cl,swell}$ after Ebs block was observed (vs. Ebs and WO, $P < 0.01$, $n = 5$ for both), although 89.0 ± 1.6% of the Diaz [in]-induced current remained blocked. Because this apparent recovery occurred at the end of the experiment, it is difficult to exclude the possibility that the integrity of the gigaohm seal was becoming compromised. Nevertheless, it is clear that reducing agents DTT and GSH agents failed to vigorously reverse block of $I_{Cl,swell}$ by Ebs. Two possibilities to explain these observations should be considered. First, it is possible that block of $I_{Cl,swell}$ by Ebs does

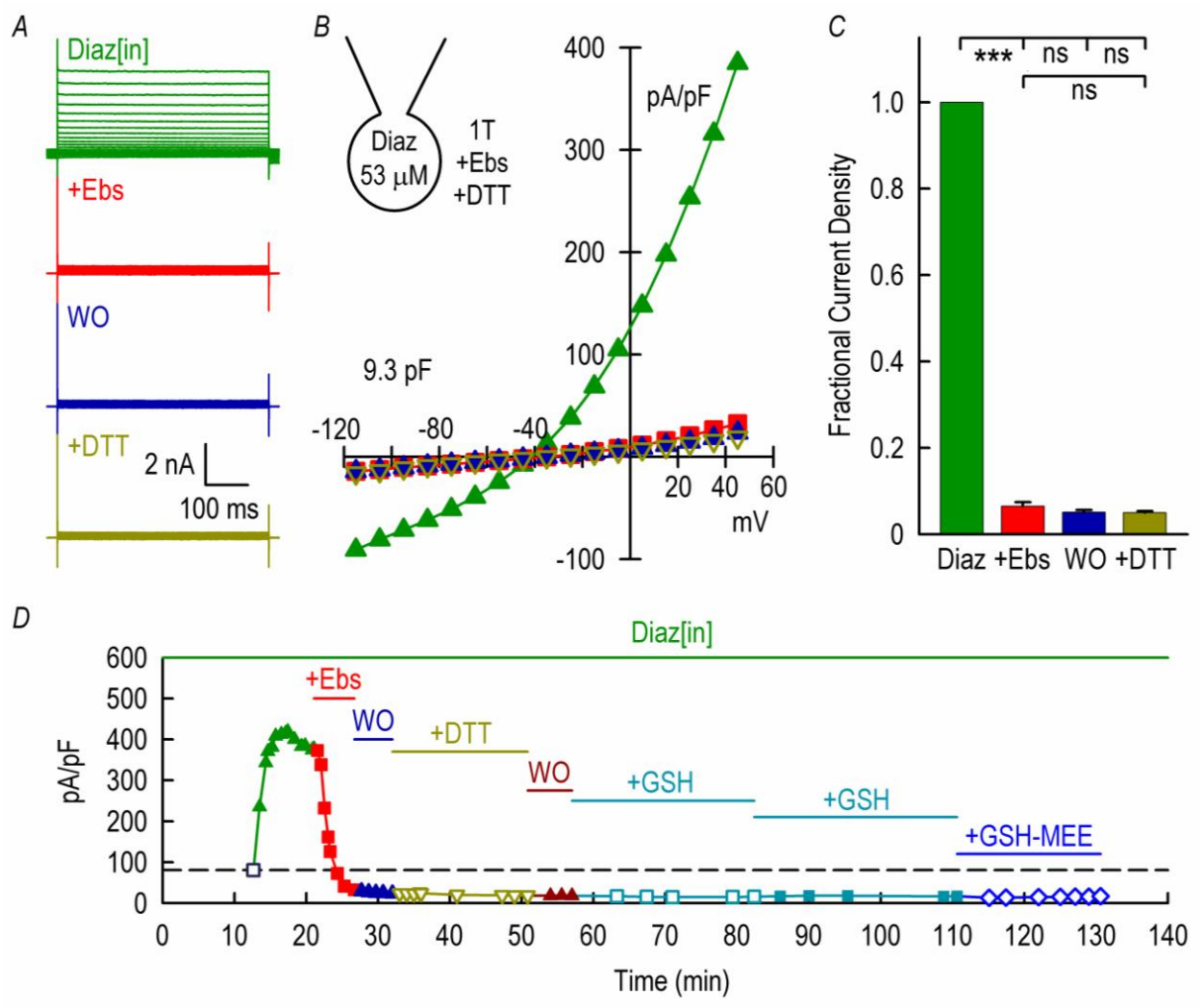

FIG. 17: DTT failed to activate $I_{Cl,swell}$ following block with Ebs. $I_{Cl,swell}$ was activated with Diaz [in], blocked with 15 µM Ebs, and washed out briefly before DTT treatment in bath. Current traces (***A***) and *I-V* relationships (***B***) showing activation with Diaz [in] (green), block with 15 µM Ebs (red), washout (WO) of Ebs (blue), and attempted recovery with 5 mM DTT (dark yellow). ***C***. Fractional block of Diaz-induced current (240.9 ± 77.6 pA/pF) by Ebs, WO of Ebs, and recovery with DTT. Ebs (15 µM) blocked 93.5 ± 1.0% (n = 3, $P < 0.001$) of the current and failed to washout in 1T (n = 3, $P = 0.183$; *ns*). Attempted recovery with DTT (5 mM) failed to turn on $I_{Cl,swell}$ compared to either Ebs block (*n* = 3, $P = 0.220$; *ns*) or washout (n = 3, $P = 0.895$; *ns*). ***D***. Time-course for the experiment; time of break in denoted by dark open gray square. For this experiment (*n* = 1), different concentrations of Glutathione (GSH: 1 mM, cyan open square; 5 mM, cyan filled square) were added in bath following 5 mM DTT; none of the GSH treatments recovered $I_{Cl,swell}$ including GSH-MEE (500 µM) (membrane permeable derivative).

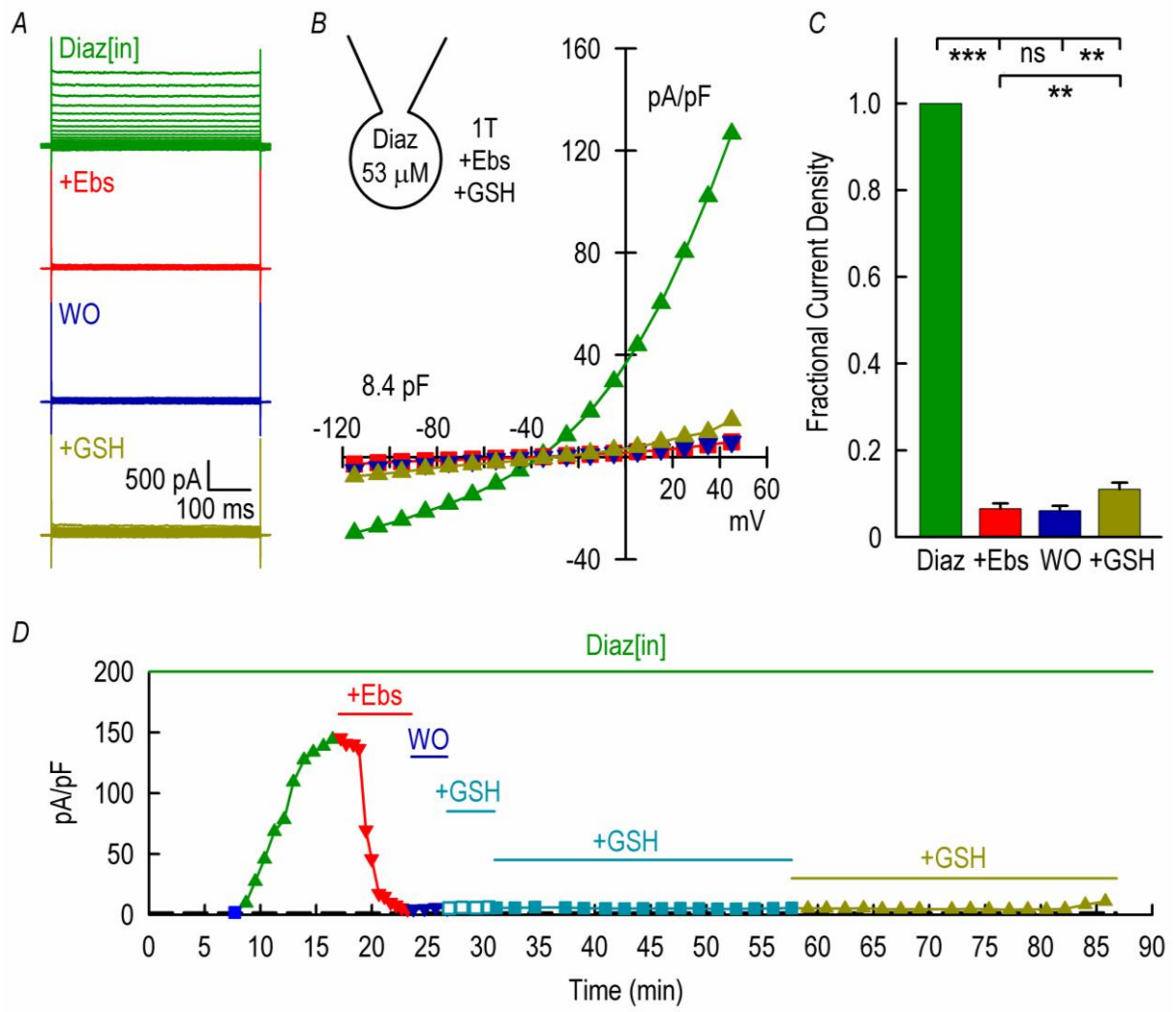

FIG. 18: GSH failed to activate $I_{Cl,swell}$ following block with Ebs. $I_{Cl,swell}$ was activated with Diaz [in], blocked with Ebs, and washed out briefly before GSSH treatment. Current traces (***A***) and *I-V* relationships (***B***) showing activation with Diaz [in] (green), block with 15 μM Ebs (red), washout (WO) of Ebs (blue), and recovery with 10 mM GSSH (dark yellow). ***C***. Fractional block of Diaz-induced current (141.3 ± 20.9 pA/pF) by Ebs, WO of Ebs, and recovery with GSH. Ebs (15 μM) blocked 93.8 ± 1.0% (n = 5, P < 0.001) of the current and failed to washout in 1T (n = 5, P = 0.838; *ns*). Attempted recovery with GSH (10 mM) partially recovered $I_{Cl,swell}$ compared to either Ebs block (n = 5, P < 0.01) or washout (n = 5, P < 0.01). ***D***. Time-course for the experiment; time of break in denoted by filled blue square. In this experiment, different concentrations of Glutathione (GSH: 1 mM, cyan open square; 5 mM, cyan filled square) were added in bath; only 10 mM GSH (dark yellow) appeared to elicit a slight recovery $I_{Cl,swell}$.

not involve a Se-S bond and there is nothing to reduce. Second, if a Se-S bound is required, access to the bond may be restricted thereby limiting the ability of reducing agents to act.

Because HEK293 cells were utilized in studies showing block by MTSES (Fig. 15), which is expected to be irreversible, we also wanted to characterize block of $I_{Cl,swell}$ by Ebs in this cell line. Fig. 19 shows that 15 μM Ebs blocked 96.6 ± 0.9% (n = 3, P < 0.001) of Diaz [in]-induced $I_{Cl,swell}$ in HEK293 cells. In contrast to studies in the astrocyte cell line, after 11-36 min of washout a small but statistically significant recovery of current was observed, 6.7 ± 1.4% (n = 3, P < 0.05). The mechanistic basis for partial recovery from Ebs block in this cell line was not explored.

3.8 Topology of $I_{Cl,swell}$ Block

Although the nature of irreversible block by impermeant MTS reagents suggest that $I_{Cl,swell}$ activation may involve free -SH groups located on the outside, it remains unclear whether Ebs functions in a similar manner from the outside or whether Ebs acts on cytosolic targets that critically modulate $I_{Cl,swell}$ apart from its action as a GPx-mimetic. If Ebs acts at an intracellular binding site, adding Ebs directly to the cytosol would be expected to have equal or greater potency and faster kinetics of block than adding Ebs to the bath solution. On the other hand, if Ebs and MTS reagents share a common binding site accessible from the extracellular face of the membrane, Ebs added to the cytosol might act with reduced potency and with slower kinetics because it would be more difficult for Ebs to reach its binding site. To test this idea, we back-filled the patch pipette with Ebs (30 μM; Ebs [in]) and activated DI TNC1 cells by osmotic swelling in 0.8T.

3.8.1 Ebs blocked $I_{Cl,swell}$ only from the outside

Fig. 20 shows that inclusion of 30 μM Ebs in the patch pipette (Ebs [in], inset),

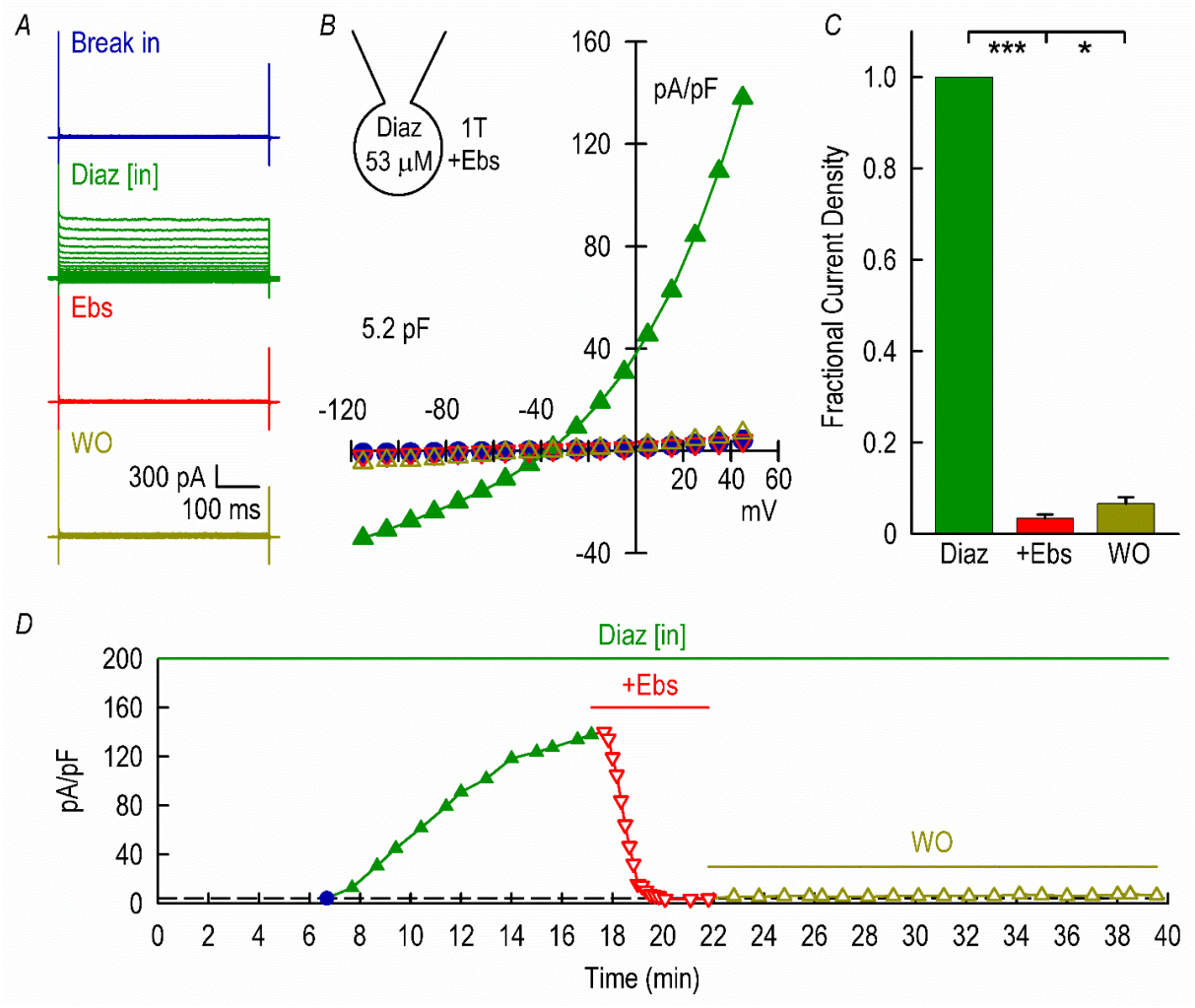

FIG. 19: Ebs blocked $I_{Cl,swell}$ and failed to washout fully in HEK293 cells. $I_{Cl,swell}$ was activated with Diaz [in] and was rapidly blocked with 15 μM Ebs prior to washout (WO). Current traces (***A***) and *I-V* relationships (***B***) showing break in (blue), activation with Diaz [in] (green), block with 15 μM Ebs (red), and WO (dark yellow). ***C***. Fractional block of Diaz-induced current (138.9 ± 10.4 pA/pF) by Ebs and WO of Ebs. Ebs (15 μM) blocked 96.6 ± 0.9% (n = 3, P < 0.001) of the current and showed partial washout in Ebs-free 1T (n = 3, P < 0.05). ***D***. Time-course for the experiment; time course denoted by filled blue circle.

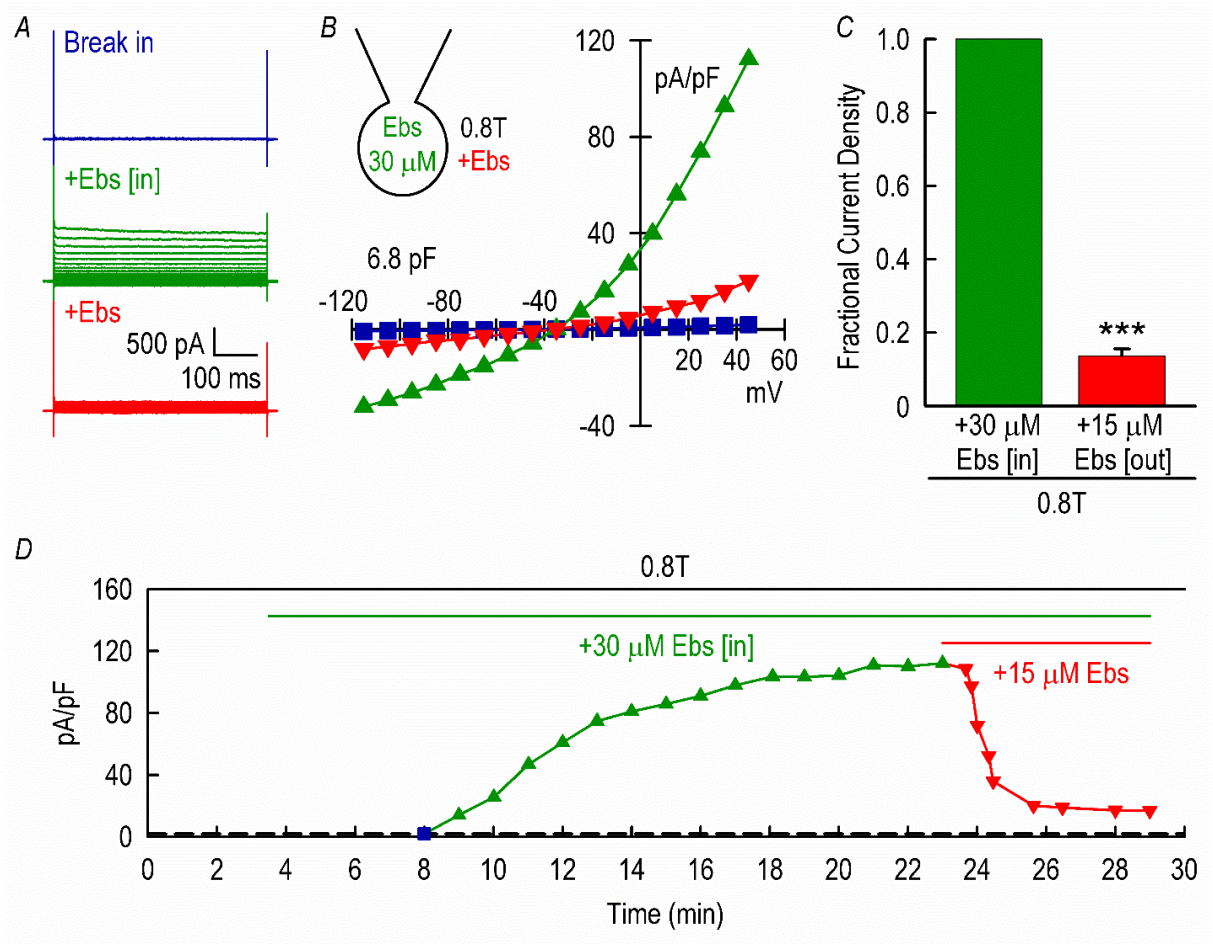

FIG. 20: Ebs blocked $I_{Cl,swell}$ only from the outside. $I_{Cl,swell}$ was activated with 0.8T with 30 μM Ebs back-filled in pipette (Ebs [in]; see inset) and was blocked by 15 μM external Ebs in 0.8T. Current traces (***A***) and *I-V* relationships (***B***) showing break in (blue), activation with 0.8T (green), and block with 15 μM Ebs (red) in 0.8T. ***C***. Fractional block of 0.8T-induced current (243.6 ± 52.1 pA/pF) by Ebs. Ebs (15 μM) blocked 86.3 ± 1.9% (n = 6, P < 0.001) of the current. ***D***. Time-course for the experiment; time of break in denoted by filled blue square.

twice the concentration shown to block from the outside, failed to block 0.8T-induced $I_{Cl,swell}$, and the swelling-induced current increased to ~112 pA/pF and was maintained without evidence of developing block. As a positive control, we added 15 μM Ebs to the bathing media in the continued presence of 30 μM Ebs [in]. External Ebs rapidly induced 86.3 ± 1.9% (n = 6, P <0.001) block of the swelling-induced current (Fig. 20). Time to full block with extracellular Ebs was 1-2 min, as shown previously for the Diaz [in]-activated current. One might argue that Ebs [in] prevented 0.8T-induced $I_{Cl,swell}$ from climbing higher. This possibility is difficult to rigorously exclude. Nevertheless, the mean current density of $I_{Cl,swell}$ in Fig. 20 was 243.6 ± 52.1 pA/pF (30 μM; Ebs [in]), greater by a factor of 7 than the swelling-induced current observed in the absence of Ebs [in], 33.3 ± 6.9 pA/pF (Fig. 2). These data suggest that Ebs blocked $I_{Cl,swell}$ only from the outside, analogous to the action of impermeant MTS reagents. Moreover, the data argue that cytosolic actions of Ebs as a GPx-mimetic and intracellular ROS scavenger are not required for block of $I_{Cl,swell}$. In a preliminary experiment, back-filling the patch pipette with Thr101 (30 μM; Thr101 [in]) also failed to suppress 0.8T-induced $I_{Cl,swell}$, whereas subsequent addition of external Thr101 (15 μM) blocked $I_{Cl,swell}$ in the same cell (Appendix, Fig. 10). Ebs [in] affected $I_{Cl,swell}$ in one condition (see Appendix, pp. 100-02).

3.8.2 DCPIB blocked $I_{Cl,swell}$ only from the outside

Our findings indicate that Ebs and MTS-reagents block $I_{Cl,swell}$ at a site accessible from the outside face of the membrane. This raises a question: Does block by DCPIB, the most selective blocker of $I_{Cl,swell}$ identified to date, occur with a similar topology and preferentially block from the outside? On the other hand, DCPIB inhibits K^+ channels with low PIP_2 affinity by binding to PIP_2 binding site on the inner face of the membrane (Deng et al., 2016), and block of $I_{Cl,swell}$ by DCPIB is reversible, suggesting it acts by a mechanism distinct from Ebs and MTS-reagents. To evaluate whether DCPIB displays sidedness of action, we tested the effect of directly applying 30 μM DCPIB to the cytosol

by back-filling the pipette. As shown in Fig. 21, DCPIB [in] (see inset) failed to suppress $I_{Cl,swell}$ in 0.8T. In contrast, bath superfusion of DCPIB (10 μM; DCPIB) blocked 77.3 ± 5.3% (n = 5, $P < 0.001$) of $I_{Cl,swell}$ in 5-15 min in the same cells. Although finding that DCPIB act with the same topology as Ebs and MTS-reagents is intriguing, the present studies do not provide evidence these two groups of compounds act at the same site.

3.9 Synthesis and Functionality of Ebs-biotin

As the molecular entity responsible for eliciting $I_{Cl,swell}$ has been controversial, we wanted to utilize the high affinity irreversible binding profile of Ebs to pull out binding site that regulates channel function. This site might be a component of the pore forming channel, a channel subunit, or a regulatory protein downstream from the site of $I_{Cl,swell}$ activation by H_2O_2. In addition to targeting -SH groups covalently (Sakurai et al., 2006), the Se in Ebs can serve as a unique spectroscopic marker (Aitkin et al., 2012) that fully inhibits the current at 45 nM, suggesting an IC_{50} of <5 nM. Although the characteristic Ebs extinction coefficient 340 nm (ε_{340}) is 5,000 M^{-1} cm^{-1} (Zhao et al., 2002), which may be useful for monitoring the oxidation state of Ebs and its substrates, spectroscopy by itself cannot be used to pull out the target of Ebs. An alternative, commercially available MTSEA-biotin is less than optimal for streptavidin-assisted pull down of the target protein that regulates $I_{Cl,swell}$ because block of $I_{Cl,swell}$ by MTSEA-biotin occurs with slow kinetics suggesting a lower affinity than Ebs for its –SH group target.

3.9.1 Organic synthesis of Ebs-biotin tag

With the assistance of Dr. Matthew C.T. Hartman (Dept. of Chemistry, VCU), we developed a biotin tagged Ebs compound (Ebs-biotin). Following synthesis of Ebs-*p*-yne (Appendix, Fig. 2) and verification of its structure by via ^{1}H-NMR (Appendix, Fig. 3 and 4), azide-alkyne Huisgen cycloadditon (click chemistry) of azido-PEG_3-biotin to Ebs-*p*-

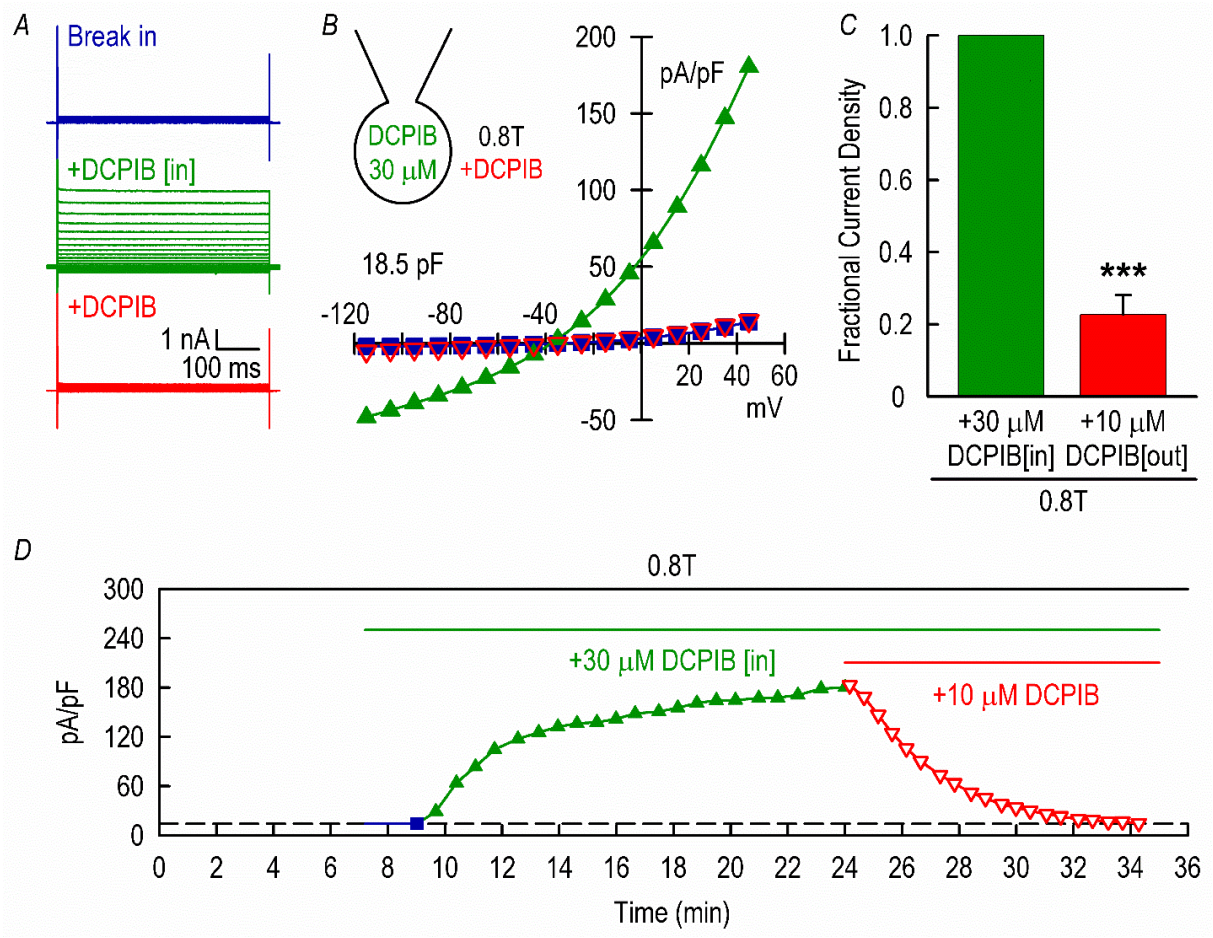

FIG. 21: DCPIB blocked $I_{Cl,swell}$ only from the outside. $I_{Cl,swell}$ was activated with 0.8T with 30 μM back-filled DCPIB (DCPIB [in]; see inset) and blocked with 10 μM external DCPIB in 0.8T. Current traces (***A***) and *I-V* relationships (***B***) showing break in (blue), activation with 0.8T (green), and block with 10 μM DCPIB (red) in 0.8T. ***C***. Fractional block of 0.8T-induced current (131.2 ± 32.6 pA/pF) by DCPIB. DCPIB [out] (10 μM) blocked 77.3 ± 5.3% (n = 5, P < 0.001) of the current. ***D***. Time-course for the experiment; time of break in denoted by filled blue square.

yne was performed to synthesize Ebs-biotin (Appendix, Fig. 5). The final structure of Ebs-biotin was then verified by MALDI-TOF, documenting an exact molecular weight (MW) of 743.20 g mol^{-1} (Appendix, Fig. 6).

3.9.2 Ebs-biotin demonstrated decreased affinity for $I_{Cl,swell}$

As drug properties tend to change following derivatization, it was critical to test whether Ebs-biotin retained the ability of Ebs to block $I_{Cl,swell}$ at nanomolar concentrations. Because addition of pegylated biotin (azido-PEG3-biotin) (Appendix, Fig. 5) with click chemistry increased the MW of Ebs from 274.18 to 743.20 g mol^{-1} (Appendix, Fig. 6), Ebs-biotin might block $I_{Cl,swell}$ with low affinity or not at all. Preliminary experiment showed that $I_{Cl,swell}$ elicited with Diaz [in], was fully blocked by adding 15 μM Ebs-biotin to the bathing media (n = 2; data not shown) and that block was irreversible (n = 1; data not shown). However, block by Ebs-biotin was slowed by a factor of ~20 compared to block by Ebs (1-2 min for full block by 15 μM Ebs). This suggests that the affinity of Ebs for its target was substantially reduced by addition of the biotin tag, limiting the utility of Ebs-biotin as a tool for selective protein isolation.

3.10 Ebs-*p*-yne: Alternative Tool for Identifying Molecular Entity Regulating $I_{Cl,swell}$

We also decided to closely analyze the penultimate compound, Ebs-*p*-yne, which has an additional ethynyl group (C≡C) placed on the para (*p*-) position of the benzene ring of Ebs (Appendix, Fig. 1). The ethynyl group is the reactive site required for click chemistry. Moreover, its addition to the benzene ring of Ebs alters the electron distribution and thereby may alter the chemistry responsible for Ebs forming covalent bonds with targeted –SH groups.

3.10.1 Ebs-*p*-yne blocked $I_{Cl,swell}$ with higher affinity than Ebs

In a preliminary study, we tested whether 150 nM Ebs-*p*-yne blocked $I_{Cl,swell}$. After activating $I_{Cl,swell}$ with Diaz [in], 150 nM Ebs-*p*-yne fully suppressed the current in <15 min and appeared to act much faster than 150 nM Ebs (n = 1 for both; data not shown). Therefore, we studied the kinetics of Ebs-*p*-yne at 5 nM, the predicted IC_{50} for Ebs. Fig. 22 demonstrates that 5 nM Ebs-*p*-yne successfully blocked 90.4 ± 1.7% (n = 3, P < 0.001) of Diaz [in]-elicited $I_{Cl,swell}$. In one experiment, we were able to demonstrate block by 5 nM Ebs-*p*-yne was irreversible with ~40 min of washout with 1T, and moreover, as for Ebs, ~25 min superfusion with H_2O_2 failed to reactivate the current. The complete block of $I_{Cl,swell}$ with 5 nM Ebs-*p*-yne suggests an apparent IC_{50} in the pM range.

3.10.2 Determination of rate constant (K) of block

We assessed the rate constants for block assuming 1:1 bimolecular pseudo-first order kinetics that binding to the receptor was proportional to block of current, and that block by Ebs and its congeners was irreversible over the time course studied. Binding to the receptors (R) and proportional block of current (-I) by drug (D) can be described by:

$$R + D \underset{k_{-1}}{\overset{k_1}{\rightleftarrows}} RD \xrightarrow{k_2} R\text{-}D$$

where k_1 is the initial rate constant for block, k_{-1} is the reverse rate constant which is assumed to be near 0, and k_2 is the rate constant for the irreversible process where RD goes to R-D. For simplicity the overall rate constant of block, K, does not distinguish whether RD or R-D is responsible for blocking the current. This gives:

$$-dI/dt = \{K\,[D]\}\,R$$

$$\tau^{-1} = K\,[D]$$

After fitting to a single exponential function, the time constants for block, τ, by 45 nM Ebs and 5 nM Ebs-*p*-yne were 33.9 ± 6.6 and 28.9 ± 3.0 min, respectively, strikingly similar despite the 9-fold difference in drug concentrations. The K values (in M^{-1} sec^{-1})

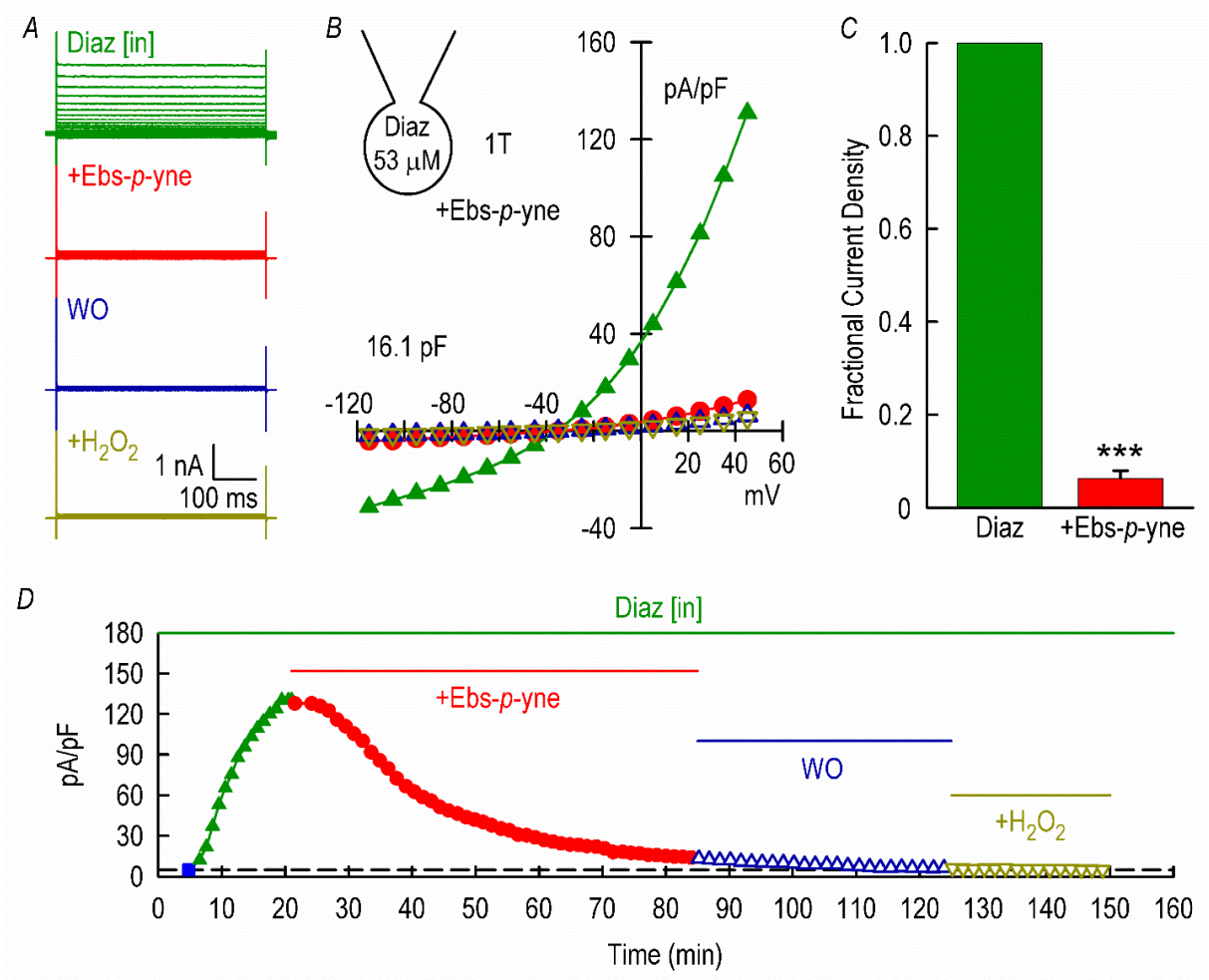

FIG. 22: Block of $I_{Cl,swell}$ by 5 nM Ebs-*p*-yne. $I_{Cl,swell}$ was activated by Diaz [in] and blocked by 5 nM Ebs-*p*-yne. Current traces (***A***) and *I-V* relationships (***B***) showing activation with Diaz (green), block with 5 nM Ebs-*p*-yne (red), washout (WO) (blue), and attempted recovery with 500 μM H_2O_2 (dark yellow). ***C***. The Diaz-induced current was 180.5 ± 62.2 pA/pF, and Ebs-*p*-yne (5 nM) blocked 90.4 ± 1.7% (n = 3, $P < 0.001$). ***D***. Time-course for the experiment; time of break in denoted by filled blue square. For this experiment ($n = 1$), H_2O_2 (500 μM) addition following ~40 min washout with Ebs-*p*-yne free 1T failed to recover $I_{Cl,swell}$.

were calculated for 45 nM Ebs and 5 nM Ebs-*p*-yne and are shown in Fig. 23. Ebs blocked with a K of 1.2 x 10^4 M^{-1} sec^{-1} while Ebs-*p*-yne blocked with a K of 11.8 x 10^4 (vs. Ebs, $P < 0.05$; $n = 3$ for both). Thus the K for Ebs-*p*-yne was 9.8-fold greater than that for Ebs. This surprising higher affinity of Ebs-*p*-yne is likely to make it useful as a tag for identifying the molecular entity that regulates $I_{Cl,swell}$.

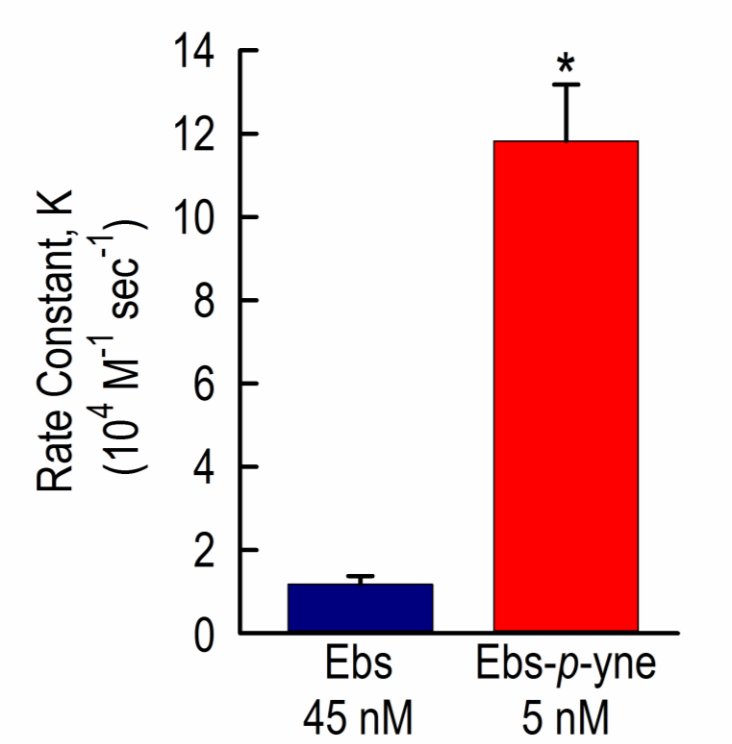

FIG. 23: Comparison of rate constants (K) of block for 45 nM Ebs and 5 nM Ebs-*p*-yne. The K for Ebs was 1.2 x 10^4, while that for Ebs-*p*-yne was 11.8 x 10^4 (n = 3, P < 0.05). K was calculated based on pseudo-first order kinetics assuming 1:1 irreversible binding and that binding was proportional to block of current.

CHAPTER 4

DISCUSSION

4.1 Identification of High Affinity Binding Molecular Tag of $I_{Cl,swell}$

We have identified ebselen (Ebs), ebselen oxide (EbO), Thr101, and MTS reagents as irreversible blockers of $I_{Cl,swell}$. We found several of these molecules to act at a site distal to H_2O_2, the most distal regulator of $I_{Cl,swell}$ identified to date. Nevertheless, we did not establish whether these agents directly blocked the channel protein, a regulatory subunit, or another regulator molecule downstream in the signaling pathway that activates $I_{Cl,swell}$. Common mechanism in blocking $I_{Cl,swell}$ most likely involves covalent modification of –SH groups which are critical for channel function. More importantly, Ebs demonstrated fast kinetics in blocking $I_{Cl,swell}$ relative to activation than what has been previously reported by Deng et al. (2010a). Ebs was also the fastest acting in blocking $I_{Cl,swell}$ among all agents tested. We showed complete block of $I_{Cl,swell}$ using 45 nM Ebs in addition to demonstrating that Ebs blocks $I_{Cl,swell}$ irreversibly at a site distal to H_2O_2. Furthermore, this predicts the IC_{50} of Ebs as <5 nM and suggests that Ebs may be a useful tool to identify the molecular basis of $I_{Cl,swell}$. Therefore, we synthesized a novel congener of Ebs known as ebselen-*para*-yne (Ebs-*p*-yne) with the help of Dr. Matthew C.T. Hartman (Dept. of Chemistry, VCU) to pull out the genetic basis behind $I_{Cl,swell}$. To our surprise, Ebs-*p*-yne demonstrated an even higher affinity in blocking $I_{Cl,swell}$ with an apparent IC_{50} ~pM range where K for Ebs-*p*-yne was 9.8-fold greater than that for Ebs. Ebs-*p*-yne is likely to be an important tool because tags can be directly attached to the molecule via standard click chemistry approaches. Although biotinylated Ebs (Ebs-biotin) and biotinylated MTS reagent (MTSEA-biotin) also inhibited $I_{Cl,swell}$ and were considered as useful tools, both molecules displayed slower blocking kinetics and lower apparent affinity for $I_{Cl,swell}$ than Ebs and Ebs-*p*-yne.

Prior to synthesizing Ebs-*p*-yne, Ebs persistently demonstrated high affinity block of $I_{Cl,swell}$, which turned out to be irreversible and downstream of H_2O_2, the most proximate regulator of $I_{Cl,swell}$. Based on reported claims that Ebs mainly functions in the scavenging of intracellular ROS, we decided to test EbO and Thr101, specific congeners

of Ebs lacking glutathione peroxidase (GPx) activity. To our surprise, these congeners completely suppressed the ROS-sensitive current. As with Ebs, the block was irreversible and downstream of H_2O_2. These observations led to the premise that Ebs and its congeners must be sharing a common mechanism irrespective of GPx profile. And based on structural chemistry of these molecules, we additionally proposed that Ebs and its congeners might function as sulfhydryl reagents.

To validate this proposal, we decided to bath perfuse classic membrane impermeant MTS reagents (MTSES and MTSEA biotin) following diazoxide-induced activation of $I_{Cl,swell}$. Both classic sulfhydryl reagents were fully capable of irreversibly suppressing the Cl^- current in native DI TNC1 astrocytes at much lower concentration than what is normally reported (Qiu et al., 2014). This was completely antithetic to earlier work by Qiu et al. (2014) involving SWELL1 (LRRC8A), the latest entity identified as $I_{Cl,swell}$, in which superfusion of 3.33 mM MTSES fails to suppress SWELLL1 after hyposmotically challenging their wild-type. The MTS-induced suppression of $I_{Cl,swell}$ in our experiments compared to Qiu et al. (2014) suggests an external binding site involving covalent modification of surface -SH moieties leading to disulfide (S-S) formation. We also have preliminary data with MTSET and NEM both demonstrating fully irreversible inhibition of $I_{Cl,swell}$ following current activation. Although the use of two specific reducing agents (DTT and GSH) failed to demonstrate the preexistence of the selenenylsulfide (Se-S) bond upon Ebs-induced block of $I_{Cl,swell}$, it is foreseeable that access to the bond may be restricted thereby limiting the ability of reducing agents to reactivate $I_{Cl,swell}$. In order to validate an external binding site and preclude the ROS quenching capability of Ebs as the primary cause of current suppression, we decided to directly expose the cytosolic compartment with Ebs by back-filling while under persistent hyposmotic challenge. As predicted, Ebs was inert from the inside since 0.8T-induced $I_{Cl,swell}$ persistently activated in the presence of intracellular Ebs. Only exogenously applied Ebs was able to rapidly suppress $I_{Cl,swell}$. We also tested DCPIB, the most selective blocker

of $I_{Cl,swell}$ structurally unrelated to either Ebs or MTS reagents, and found that DCPIB also blocked solely from the outside. External topological binding site seems to be required in block of $I_{Cl,swell}$.

And based on the rate constant (K) of block for Ebs relative to $I_{Cl,swell}$ and inability to washout downstream of H_2O_2, we synthesized a biotinylated derivative of Ebs (Ebs-biotin) with the intention of directly pulling out the channel or channel component responsible for the current via streptavidin-assisted pull down. Nonetheless, biotinylation caused a major loss of affinity toward $I_{Cl,swell}$. This led us to evaluate Ebs-*p*-yne, an intermediate in the synthesis of Ebs-biotin. To our surprise, we discovered that Ebs-*p*-yne possesses an even higher affinity than Ebs thus allowing complete block at 5 nM. Upon calculating the K value of Ebs-*p*-yne, we surprisingly discovered that Ebs-*p*-yne demonstrates 9.8 fold greater affinity for $I_{Cl,swell}$ compared to Ebs even when exogenous concentration employed was 9 fold less in block of $I_{Cl,swell}$.

4.2 Functional Mechanism of Ebselen and Its Congeners

4.2.1 Current knowledge about functional mechanism

Ebs has long been accepted to function primarily as a GPx-mimetic by diffusing through the cell membrane and functioning as a scavenger of ROS (Müller et al., 1984; Wendel et al., 1984; Sies and Masumoto, 1997; Nakamura et al., 2002; Deng et al., 2010a, 2010b). This selenium containing molecule is reported to decrease oxidative damage in tissues by reducing H_2O_2 and other hydroperoxides (Schewe, 1995). Cotgreave et al. (1989) reported IC_{50}s ~20-50 μM in neutrophils for blocking superoxide generation. Others reported that Ebs inhibits PKC at 20 μM in guinea pig alveolar macrophages (Leurs et al., 1989; Wakamura et al., 1990). In contrast, Ebs can inhibit purified PKC from broken cell preparations at sub-micomolar concentrations (Cotgreave et al., 1989). Therefore, Ebs also is implicated in preventing NOX2 assembly that involves

PKC-mediated phosphorylation of p47^{phox}. Smith et al. (2012), on the other hand, claim that Ebs disrupts the binding of the *bis*-SH3 domain of p47^{phox} to the PRD (proline-rich domain) of p22^{phox}. Nonetheless, our experiments demonstrating Ebs as a sulfhydryl reagent and the ability of Ebs to block $I_{Cl,swell}$ only from the outside will set out to argue against the relevance of these aforementioned mechanisms.

The first congener of Ebs that we chose to test is EbO. EbO can be readily produced when Ebs is oxidized in the presence of H_2O_2 (Glass et al., 1988); in addition, Sies and Masumoto (1997) mention EbO as a byproduct of reacting Ebs and peroxynitrite ($ONOO^-$). EbO is, therefore, cited in the literature as the most oxidized congener of Ebs (Glass et al., 1988; Daiber et al., 2000) and further oxidation is not possible under normal physiological condition. As a result, EbO is characterized as lacking the ability to scavenge ROS (Lass et al., 1996). Ultimately then EbO fails to demonstrate GPx activity, is inert to further cellular processes, and only occurs following the aftermath of quenching reactive oxygen species or reactive nitrogen species. Although mechanistically unknown at this time, EbO could by some unexplored mechanism end up reverting back to Ebs. Nevertheless, we are not aware of such reversion taking place under normal cellular processes.

Thr101 is the other congener of Ebs tested which contains sulfur (S) in place of selenium (Se) having additional fluoride (F) and ortho (*o*-) positioned methyl (CH_3-) group on the benzene ring of the molecule. Both S and Se belong to the chalcogen family on the periodic table with equal electronegativity values and share similar atomic property that often allows interchangeability in various biophysical uses. Thus, even if S replaces Se as part of the structural backbone, Thr101 is still classified as part of the Ebs family of drugs. Nevertheless, it is this Se to S substitution which disqualifies Thr101 as a GPx-mimetic (Leurs et al., 1989; Smith et al., 2012). However, this unique property of Thr101 allows the drug to share the same pharmacological profile of Ebs while failing to function in scavenging of ROS. Moreover, Thr101 can also target NOX2 by disrupting the

interaction of the *bis*-SH3 domain of p47^{phox} to the PRD of p22^{phox} as described for Ebs (Smith et al., 2012). Smith et al. (2012) also point out that Thr101 demonstrates higher selectivity for NOX2 compared to Ebs.

4.2.2 Alternative classification of Ebs and its congeners as sulfhydryl reagents

As mentioned, H_2O_2 has been characterized as the most distal in the $I_{Cl,swell}$ signaling cascade being downstream of NOX and mitochondrial ROS production (Deng et al., 2010a). This is clearly shown by Deng et al. (2010a) in freshly prepared rabbit ventricular myocytes. Even though the exact $I_{Cl,swell}$ regulatory cascade was never fully explored in DI TNC1 astrocytes as in the heart, our use of diazoxide and ability to turn on the current with exogenous H_2O_2 suggest that similar $I_{Cl,swell}$ signaling cascade seems intact in DI TNC1 astrocytes.

Whether Ebs works through scavenging of ROS or inhibiting NOX, exogenous H_2O_2 should have reactivated $I_{Cl,swell}$ downstream of block by Ebs after the current is elicited. As for EbO, the inert nature of the molecule toward further oxidation should have resulted in persistent demonstration of $I_{Cl,swell}$ following activation. However, both molecules behaved quite contrary to what was predicted. For Ebs, H_2O_2 was incapable of reactivating the current. On the other hand, EbO demonstrated full suppression of the current rather than being inert toward blocking $I_{Cl,swell}$.

Experiments with Thr101 is more complicated and requires more explanation. Because Thr101 shares the pharmacological profile of both Ebs and EbO, intervention by Thr101 should disrupt NOX2 assembly while demonstrating inability to scavenge ROS after eliciting $I_{Cl,swell}$. Assuming $I_{Cl,swell}$ regulatory cascade mentioned is intact in DI TNC1 astrocytes as in Deng et al. (2010a), this dual nature of Thr101 should lead to overall suppression of $I_{Cl,swell}$ but eventual reactivation with exogenous H_2O_2 if Thr101 blocks upstream of ROS and functions according to its classical nature. While Thr101 demonstrated complete block of $I_{Cl,swell}$, superfused H_2O_2 failed to re-elicit the ROS-

sensitive current thereby placing Thr101 distal to H_2O_2 regulation. The block by Thr101 also served to complimentarily validate EbO data.

Although Ebs had the highest apparent-affinity as an inhibitor of $I_{Cl,swell}$ of the three molecules tested demonstrating an estimated apparent IC_{50} <5 nM, all three molecules blocked $I_{Cl,swell}$ irreversibly and downstream of H_2O_2. In view of the apparent high affinity of Ebs, we searched the literature looking for potential targets with nanomolar affinity. We performed a detailed search of PubChem public database of chemical molecules (http://pubchem.ncbi.nlm.nih.gov) (search performed on June 25, 2016) and hit a total of 327 bioactivity profiles for Ebs. Top ten highest affinity targets of Ebs from this search are listed in TABLE 1 in the order of decreasing affinity. Interestingly, none of the 10 listed are extracellular in origin including UDP-glucose 4-epimerase, which is a validated drug target for African sleeping sickness (Urbaniak et al., 2006) with the highest binding affinity documented with an IC_{50} of 14 nM (TABLE 1).

We also identified two specific bacterial targets of Ebs not included as part of the PubChem list. First one identified is antigen 85 complex (Ag85c) (Favrot et al., 2013). According to Favrot et al. (2013), Ag85c in *Mycobacterium tuberculosis* is an emerging drug target where Ebs can covalently modify cysteine (C209) residue near the active site, therefore, leading to a covalent Se-S bond formation (Appendix, Fig. 7) with an observed K_i of 63 nM. Others have also reported such cysteine-targeted modification of thiols (-SH) by Ebs (Sakurai et al., 2006; Hanavan et al., 2015). Second is the cysteine protease domain (CPD) within the *Clostridium difficile* major virulence factor toxin B (TcdB) (Bender et al., 2015). Both bacterial paradigms report nanomolar binding affinities with IC_{50} ~100 nM for Ag85c (Favrot et al., 2013) and IC_{50} ~6.9-17.2 nM for TcdB (Bender et al., 2015).

We then theorized that irreversibility of Ebs and its congeners following block of $I_{Cl,swell}$ results from direct covalent modification of -SH groups on the channel or channel component responsible for the current. There are also reports of EbO-mediated rapid modification of -SH groups (Glass et al., 1988). For Thr101, very little information exists

TABLE 1

IC_{50}s and Potencies for Targets of Ebselen

Activity	[nM]	Target
IC_{50}	14	UDP-glucose 4-epimerase
Potency	63	15-lipoxygenase, partial
Potency	71	euchromatic histone-lysine N-methyltransferase 2
Potency	79	cytochrome P450 2C9 precursor
IC_{50}	111	PE/PC phosphatase isoform 1
Potency	126	aldehyde dehydrogenase 1 family, member A1
Potency	126	cytochrome P450 2C19 precursor
IC_{50}	190	MPI protein (phosphomannose isomerase type I)
Potency	224	aldehyde dehydrogenase 1 family, member A1
Potency	251	histone acetyltransferase KAT2A

regarding its mechanism other than disruption of *bis*-SH3 domain of p47^{phox} to the PRD of p22^{phox} as mentioned in Smith et al. (2012). No mechanism is ever proposed. However, other than additional F- and CH_3-groups on Thr101, structurally the molecule is very similar to Ebs although Se is replaced by elemental S in Thr101. Furthermore, both Se and S belong to the chalcogen family of electron acceptors having the same number of outer shell valence electrons including identical electronegativity (χ) values of roughly ~2.6 where $\chi = 4.0$ for F serves as a reference for being the most electronegative. Both chalcogens are often interchangeable during X-ray crystallography techniques. Based on such fact, we also proposed the existence of a Thr101-mediated covalent modification of -SH groups leading to disulfide (S-S) linkages and therefore, we postulated that Ebs, EbO, and Thr101 function as sulfhydryl reagents in blocking $I_{Cl,swell}$.

To verify this proposal, we decided to probe the existence of free -SH groups with use of classic sulfhydryl group modifying MTS reagents often used in ion channel physiology following SCAM (Akabas, 2015). The fact that cell impermeable MTS reagents demonstrated complete irreversible block regardless of charge on the MTS strengthens the idea that $I_{Cl,swell}$ is modulated by extracellular -SH groups. Unfortunately use of reducing agents such as DTT or GSH on Ebs did not demonstrate current recovery following block of $I_{Cl,swell}$ with Ebs. First possible reason for this inconsistency may be that as channels are embedded in membranes, these covalent modifications may not be fully accessible to various reducing agents once the bond forms and enters a hydrophobic pocket. Second possibility is that the channel or channel component responsible for eliciting $I_{Cl,swell}$ becomes internalized following covalent modification by Ebs and congeners. Garlid et al. (2009) describing cardioprotective signaling to mitochondria proposes such a mechanism involving ligand-activated G protein-coupled receptor internalization as part of multimeric signaling complexes gathered in caveolae. Third and final possible reason for this inconsistency may be that these covalent modifications really do not exist. In addition, we have further evidence from ongoing studies by Belkhayat et

al. (2016, Unpublished Data) from our laboratory that N-Ethylmaleimide (NEM), an organic molecule derived from maleic acid containing an imide functional group used commonly for modification of cysteines in proteins and peptide fragments, can also block $I_{Cl,swell}$ irreversibly downstream of H_2O_2.

Clearly the evidence for cysteine-targeted thiol modification by Ebs and its congeners is very strong based on MTS data while failed recovery attempts with reducing agents might simply involve access issue. This covalent modification would most likely serve as plausible explanation for why drug-free bathing media could not wash Ebs or its congeners off its intended target. While the actual site of action for H_2O_2-induced $I_{Cl,swell}$ is currently unknown, H_2O_2 is, nonetheless, a relatively strong cell permeable low molecular weight oxidizing agent capable of penetrating areas not normally accessed by larger molecules such as DTT or GSH. Since H_2O_2 does not oxidize preexisting covalent bonds, failed attempts to elicit $I_{Cl,swell}$ with exogenous H_2O_2 following block with Ebs and its congeners may be redox-related desensitization. To recapitulate, the fact that Ebs, EbO, and Thr101 along with MTS reagents all commonly demonstrate complete irreversible block of $I_{Cl,swell}$ strongly support the idea that these three molecules may be functioning as sulfhydryl modifying agents.

4.2.3 Topology: Ebs failed to block $I_{Cl,swell}$ from the inside

While ample evidence points to thiol-modified irreversible covalent bond formation from the outside, we could not with certainty preclude possible intracellular effects of these molecules because Ebs and its congeners are described as being cell permeable (Glass et al., 1988; Leurs et al., 1989; Schewe, 1995; Lass et al., 1996; Daiber et al., 2000; Zhao et al., 2002; Sakurai et al., 2006; Deng et al., 2010a; Aitken et al., 2012; Smith et al., 2012). When Ebs failed to block $I_{Cl,swell}$ from the inside in back-filling experiments, we searched the literature seeking measurements of Ebs permeability. Aitken et al. (2012) discussed the effective use of the Se atom of Ebs as a traceable isotopic marker.

According to Aitken et al. (2012), Se is a trace element having multiple isotopes found only in extremely low concentrations in cultured cells. Taking this isotopic approach, Aitken et al. (2012) based on evidence from synchrotron radiation induced X-ray emission (SRIXE) spectroscopy mapping of Ebs mention that only small traces of Se corresponding to drug uptake eventually localize to a discreet region of the cell after 1 h in differentiated ND15 cells. Rather than accumulation of intracellular Ebs within the timeframe coinciding with the block of $I_{Cl,swell}$ normally observed < 2 min, results by Aiken et al. (2012) raise the implication that Ebs might not be as permeable. In addition, Aiken et al. (2012) point to unexplained total dissipation of intracellular Ebs content following 4 h in ND15 cells not only casting doubt regarding the intracellular role of Ebs but also raising suspicion of its permeability. Irrespective of whether Ebs is found in its free form or bound to a specific target inside the cell, the X-ray methodology utilized by Aitken et al. (2012) should have detected the elemental Se of Ebs.

The fact that direct cytosolic exposure to Ebs (Ebs [in]; 30 μM) failed to block the current under constant hyposmotic challenge (0.8T) while demonstrating complete block of $I_{Cl,swell}$ <2 min with superfused Ebs (Ebs [out]; 15 μM) clarifies the presumption that both Ebs and MTS reagents share an external binding site and similar mechanism of action. If block was truly diffusion-limited, then immediate exposure of the cytosol to Ebs in back-filling studies should have resulted in rapid suppression of $I_{Cl,swell}$ despite the ability of Ebs to function as a scavenger of ROS or an inhibitor of NOX. Despite the property of Ebs ultimately responsible, an immediate block of $I_{Cl,swell}$ from the inside would have strongly argued in support of the canonically accepted intracellular functionality of the molecule. We also have evidence that Thr101 failed to block $I_{Cl,swell}$ from the inside while under hyposmotic challenge (n = 1). While the SRIXE study of Ebs does provide incontrovertible evidence that Ebs permeates through the cell membrane albeit slowly ~1 h (Aitken et al., 2012), the inability to block $I_{Cl,swell}$ from the cytosolic side as we demonstrated irrefutably also support the idea that Ebs topologically blocks from the

outside. Nonetheless, Ebs appears to demonstrate limited-diffusivity according to Aitken et al., 2012. Multiple connotations (Müller et al., 1984; Wendel et al., 1984; Glass et al., 1988; Leurs et al., 1989; Schewe, 1995; Lass et al., 1996; Sies and Masumoto, 1997; Daiber et al., 2000; Nakamura et al., 2002; Zhao et al., 2002; Sakurai et al., 2006; Deng et al., 2010a; Aitken et al., 2012; Smith et al., 2012) to Ebs as a fully membrane permeable molecule might, therefore, be slightly misleading. Furthermore, Ebs has mostly been used in cell-free condition (Zhao et al., 2002; Smith et al., 2012) where diffusion through the membrane becomes irrelevant. With permeability aside, our aforementioned data clearly indicate that Ebs-induced block of $I_{Cl,swell}$ undeniably takes place topologically from the outside and completely lacks function from the inside under intact whole cell patch-clamp parameter.

With inability of Ebs to demonstrate block from the inside, question was also raised regarding DCPIB topology in blocking $I_{Cl,swell}$. The fact that DCPIB failed to block $I_{Cl,swell}$ from the inside while mirroring the effect of Ebs from the outside, points to the importance of outer topology in the mechanism of block. As DCPIB cannot function as a sulfhydryl reagent, we cannot make the claim that DCPIB and Ebs share a common mechanism nor a common binding site. But it is critical to mention that both binding sites are located on the outside. DCPIB is also a butanoic acid derivative having a carboxylic acid functionality. Under physiological pH 7.4, the acidic proton becomes deprotonated and the molecule becomes negatively charged. It is well known that charged molecules have difficulty crossing the cell membrane unless traversed in through an ion channel or somehow transported inside. Based on this alone, DCPIB most likely works from the outside as our back-filling data seem to suggest. This outer topology is in stark contrast to inwardly rectifying K^+ (Kir) channels with weak affinity for PIP_2 (Deng et al., 2016). Deng et al. (2016) mentions that DCPIB can directly compete for PIP_2 binding site as long PIP_2 interaction is relatively weak compared to Kir channels demonstrating higher PIP_2 binding affinity. Thus, as long as PIP_2 is bound relatively weak, then DCPIB must

compete with PIP_2 from the cytosolic side. Since we are dealing with two completely different channels that pass ions of the opposite charge, both binding topologies are likely to be correct as DCPIB can have off-target effects other than selective inhibition of $I_{Cl,swell}$. In fact, recent publication on DCPIB pharmacology validates some of these off-target effects of DCPIB. According to Bowens et al. (2012), several glutamate transport pathways in glial cells are sensitive to block by DCPIB. In rat glial cells, for instance, DCPIB can potently inhibit glutamate release through connexin hemichannels (Cx43) and glutamate uptake via the glutamate transporter (GLT-1). Although topology of block is never mentioned in Bowens et al. (2012), evidence for such non-$I_{Cl,swell}$ targets certainly lends credibility to DCPIB- PIP_2 competition in Kir channels. Additional studies will be needed prior to drawing any conclusion regarding DCPIB, but it is clear at the moment that DCPIB is the most selective for inhibition of $I_{Cl,swell}$ under patch clamp conditions that isolate the anionic currents. As DCPIB can competitively knock off PIP_2 from its binding site in certain Kir channels, it is not far-fetched to postulate the effect of PIP_2 on $I_{Cl,swell}$. While our lab has not studied this issue, Yamamoto et al. (2008) have suggested PIP_3 as the key important player in restoring $I_{Cl,swell}$ where PIP_2 mainly functions as a substrate of PI-3K for generating PIP_3. The fact that DCPIB blocked only from the outside, although in sharp contrast to Kir channels with weak affinity for PIP_2, offers more assurance for Ebs blocking only from the outside and more importantly demonstrates that topological preference in block of ion channels is not unique to $I_{Cl,swell}$.

4.3 Implications for SWELL1 (LRRC8A)

SWELL1 (Qiu et al., 2014) or LRRC8A (Voss et al., 2014) was originally identified through the use of a high-throughput cell-based fluorescence assay screening for $I_{Cl,swell}$ activity in HEK293T cells persistently expressing the halide (I^-)-sensitive yellow fluorescent protein (YFP) in accompaniment with genome-wide RNAi screen ultimately

using swelling as the primary stimulus for activating $I_{Cl,swell}$. Out of 17,631 known and 4,837 predicted human genes, choice was narrowed down to 51 candidates before identifying SWELL1 siRNA as the most likely candidate responsible for $I_{Cl,swell}$ based on I^- quenching response in the presence of DCPIB (Qiu et al., 2014). When HeLa cells expressing stable SWELL1 knockdown were co-transfected with RNAi-insensitive wild-type (WT) SWELL1, bath applied MTSES (0.1-3.33 mM) failed to block hyposmotically elicited $I_{Cl,swell}$. It was only through systematically placing T44C mutation into transmembrane domain (TMD) 1 of LRRC8A via SCAM that the candidate entity responded to ~20% block with MTSES following hyposmotic challenge. This was completely opposite to our MTSES data. Our results demonstrated that MTSES was fully capable of inhibiting the native current at a set concentration of 110 μM compared to a wider concentration range required of SWELL1. There may be several plausible explanations for such inconsistency. First and foremost, current elicited by SWELL1 may not explicitly be identical to what is measured in native DI TNC1 astrocytes. While DCPIB suppressed SWELL1 with an IC_{50} of 20.9 μM, normally complete suppression of $I_{Cl,swell}$ can be achieved at 10 μM with our protocol which places the IC_{50} ~1-2 μM much closer to values reported in literature; therefore, at a concentration 10-20 fold greater, DCPIB can foreseeably bind to other targets similarly to what Bowens et al. (2013) and Deng et al. (2016) have reported. Second explanation is that different stimuli activate completely different Cl^- currents. While hyposmotic media was used to activate the current in HeLa cells, our work utilized intracellular diazoxide for directly eliciting $I_{Cl,swell}$ proximate to the source independent of swelling-activated regulatory cascade. Although the work in cardiac myocytes by Deng et al. (2010a) shows a serial relationship of swelling-induced mitochondrial ROS release that elicit $I_{Cl,swell}$, this was never explored in HeLa cells by Qiu et al. (2014) whereas we demonstrated direct activation of $I_{Cl,swell}$ with exogenous H_2O_2 which was fully blocked by DCPIB in DI TNC1 astrocytes in addition to hyposmotically activating the current followed by block with DCPIB in the same cell line. Final reason for

the disparity might be the existence of multiple unidentified $I_{Cl,swell}$ isoforms giving rise to $I_{Cl,swell}$ not to mention variations that might even exist within single cell type. Therefore, the differences may arise from off-target effects of agents used to characterize the current, $I_{Cl,swell}$ signaling cascade, and variable isoforms from cell type to cell type. Nonetheless, as MTSES also provided complete inhibition of intracellular diazoxide-induced $I_{Cl,swell}$ in native HEK293 cells, the cell type argument is yet to hold.

Perhaps the biggest inconsistency for SWELL1 is the lack of inhibition by MTSES for WT SWELL1 in contrast to complete inhibition of $I_{Cl,well}$ with three different MTS reagents in DI TNC1 astrocytes. The fact based on responses to MTSES is clear in that non-selective $I_{Cl,swell}$ modulatory components are likely involved as our data point to; however, inability to demonstrate any response to MTSES in SWELL1 clearly remains problematic and deserves a second look. It is also noteworthy to mention that overexpression of WT SWELL1 does not lead to more current. Qiu et al. (2014) contributes this phenomenon to the existence of multiple subunits where only proper assembly of the multimeric channel can elicit $I_{Cl,swell}$. We, nevertheless, have preliminary data showing that siRNA directed against SWELL1 failed to substantially knockdown $I_{Cl,swell}$ in DI TNC1 astrocytes implicating that SWELL1 might not be the true molecular identity responsible for modulating $I_{Cl,swell}$; however, at the same time we cannot preclude the involvement of different $I_{Cl,swell}$ subunits currently unknown to us that might be a critical factor in eliciting $I_{Cl,swell}$.

4.4 Significance and Future Studies

The novel property of Ebs-*p*-yne with its predicted IC_{50} ~pM along with its sulfhydryl modifying property based on the parent compound Ebs opens the door for the first time to perform unique click chemistry reactions while serving as a blocker of $I_{Cl,swell}$ with the highest affinity ever reported to date. Although selectivity of Ebs-*p*-yne was not

explored in detail, we have evidence at least in *Xenopus oocytes* that calcium-activated chloride channels are unaffected by Ebs (n = 4; data not shown). Moreover, pM binding affinity tends to be very selective as shown in certain bacterial toxins such as the cholera toxin in its ability to bind cerebral gangliosides (Kuziemko et al., 1996). While the usefulness of Ebs-biotin originally intended for streptavidin-assisted pull down of $I_{Cl,swell}$ or channel component is yet to be elucidated from what can only be characterized as loss of high affinity toward $I_{Cl,swell}$ following biotinylation, Ebs-*p*-yne, on the other hand, may be used in biotin/streptavidin-free click chemistry reactions where alkyne-tagged proteins may be eluded directly off azide-columns. Furthermore, fluorescent tags can now be directly attached to Ebs-*p*-yne to be studied in confocal imaging under various pathological models. As Ebs is currently in clinical trials and under investigation as a treatment for reperfusion injury, stroke, bipolar disorder, traumatic brain injury (TBI), cancer, and bacterial infections, the higher affinity of Ebs-*p*-yne over the parent compound has tremendous implications on all of these disease states.

REFERENCES

Aitken, J.B., P.A. Lay, T.T. Duong, R. Aran, P.K. Witting, H.H. Harris, B. Lai, S. Vogt, and G.I. Giles. 2012. Synchrotron radiation induced X-ray emission studies of the antioxidant mechanism of the organoselenium drug ebselen. *J Biol Inorg Chem*. 17:589-598.

Akabas, M.H. 2015. Cysteine Modification: Probing Channel Structure, Function and Conformational Change. *Adv Exp Med Biol*. 869:25-54.

Akita, T., S.V. Fedorovich, and Y. Okada. 2011. Ca^{2+} nanodomain-mediated component of swelling-induced volume-sensitive outwardly rectifying anion current triggered by autocrine action of ATP in mouse astrocytes. *Cell Physiol Biochem*. 28:1181-1190.

Allen, M.C., C. Newland, M.A. Valverde, and S.P. Hardy. 1998. Inhibition of ligand-gated cation-selective channels by tamoxifen. *Eur J Pharmacol*. 354:261-269.

Baumgarten, C.M., D.M. Browe, and Z. Ren. 2005. Swelling- and Stretch-activated Chloride Channels in the Heart: Regulation and Function. *In* Mechanosensitivity in Cells and Tissues. A. Kamkin and I. Kiseleva, editors, Moscow.

Baumgarten, C.M., and H.F. Clemo. 2003. Swelling-activated chloride channels in cardiac physiology and pathophysiology. *Prog Biophys Mol Biol*. 82:25-42.

Bender, K.O., M. Garland, J.A. Ferreyra, A.J. Hryckowian, M.A. Child, A.W. Puri, D.E. Solow-Cordero, S.K. Higginbottom, E. Segal, N. Banaei, A. Shen, J.L. Sonnenburg, and M. Bogyo. 2015. A small-molecule antivirulence agent for treating Clostridium difficile infection. *Sci Transl Med*. 7:306ra148.

Bourke, R.S., J.B. Waldman, H.K. Kimelberg, K.D. Barron, B.D. San Filippo, A.J. Popp, and L.R. Nelson. 1981. Adenosine-stimulated astroglial swelling in cat cerebral cortex in vivo with total inhibition by a non-diuretic acylaryloxyacid derivative. *J Neurosurg*. 55:364-370.

Bowens, N.H., P. Dohare, Y.H. Kuo, and A.A. Mongin. 2013. DCPIB, the proposed selective blocker of volume-regulated anion channels, inhibits several glutamate transport pathways in glial cells. *Mol Pharmacol*. 83:22-32.

Browe, D.M., and C.M. Baumgarten. 2004. Angiotensin II (AT_1) receptors and NADPH oxidase regulate Cl^- current elicited by β1 integrin stretch in rabbit ventricular myocytes. *J Gen Physiol*. 124:273-287.

Browe, D.M., and C.M. Baumgarten. 2006. EGFR kinase regulates volume-sensitive chloride current elicited by integrin stretch via PI-3K and NADPH oxidase in ventricular myocytes. *J Gen Physiol*. 127:237-251.

Cahalan, M.D., and R.S. Lewis. 1988. Role of potassium and chloride channels in volume regulation by T lymphocytes. *Soc Gen Physiol Ser*. 43:281-301.

Chahine, M., I. Deschenes, E. Trottier, L.Q. Chen, and R.G. Kallen. 1997. Restoration of fast inactivation in an inactivation-defective human heart sodium channel by the cysteine modifying reagent benzyl-MTS: analysis of IFM-ICM mutation. *Biochem Biophys Res Commun*. 233:606-610.

Chen, B., D.M. Jefferson, and W.K. Cho. 2010. Characterization of volume-activated chloride currents in regulatory volume decrease of human cholangiocyte. *J Membr Biol*. 235:17-26.

Chen, L., L. Wang, L. Zhu, S. Nie, J. Zhang, P. Zhong, B. Cai, H. Luo, and T.J. Jacob. 2002. Cell cycle-dependent expression of volume-activated chloride currents in nasopharyngeal carcinoma cells. *Am J Physiol Cell Physiol*. 283:C1313-1323.

Chung, M.K., and H. Kim. 2002. Volume-activated chloride currents from human fibroblasts: blockade by nimodipine. *Gen Physiol Biophys*. 21:85-101.

Clemo, H.F., B.S. Stambler, and C.M. Baumgarten. 1999. Swelling-activated chloride current is persistently activated in ventricular myocytes from dogs with tachycardia-induced congestive heart failure. *Circ Res*. 84:157-165.

Cole, M.P., C.T. Jones, and I.D. Todd. 1971. A new anti-oestrogenic agent in late breast cancer. An early clinical appraisal of ICI46474. *Br J Cancer*. 25:270-275.

Cotgreave, I.A., S.K. Duddy, G.E.N. Kass, D. Thompson, and P. Moldeus. 1989. Studies on the Anti-Inflammatory Activity of Ebselen - Ebselen Interferes with Granulocyte Oxidative Burst by Dual Inhibition of Nadph Oxidase and Protein Kinase-C. *Biochemical Pharmacology*. 38:649-656.

Cragoe, E.J., Jr., N.P. Gould, O.W. Woltersdorf, Jr., C. Ziegler, R.S. Bourke, L.R. Nelson, H.K. Kimelberg, J.B. Waldman, A.J. Popp, and N. Sedransk. 1982. Agents for the treatment of brain injury. 1. (Aryloxy)alkanoic acids. *J Med Chem*. 25:567-579.

Daiber, A., M.H. Zou, M. Bachschmid, and V. Ullrich. 2000. Ebselen as a peroxynitrite scavenger in vitro and ex vivo. *Biochem Pharmacol*. 59:153-160.

Decher, N., H.J. Lang, B. Nilius, A. Bruggemann, A.E. Busch, and K. Steinmeyer. 2001. DCPIB is a novel selective blocker of $I_{Cl,swell}$ and prevents swelling-induced shortening of guinea-pig atrial action potential duration. *Br J Pharmacol*. 134:1467-1479.

Deng, W., L. Baki, and C.M. Baumgarten. 2010a. Endothelin signalling regulates volume-sensitive Cl^- current via NADPH oxidase and mitochondrial reactive oxygen species. *Cardiovasc Res*. 88:93-100.

Deng, W., L. Baki, J. Yin, H. Zhou, and C.M. Baumgarten. 2010b. HIV protease inhibitors elicit volume-sensitive Cl^- current in cardiac myocytes via mitochondrial ROS. *J Mol Cell Cardiol*. 49:746-752.

Deng, W., R. Mahajan, C.M. Baumgarten, and D.E. Logothetis. 2016. The $I_{Cl,swell}$ inhibitor DCPIB blocks Kir channels that possess weak affinity for PIP_2. *Pflug Arch Eur J Phy*. 468:817-824.

Dick, G.M., A.C. Hunter, and K.M. Sanders. 2002. Ethylbromide tamoxifen, a membrane-impermeant antiestrogen, activates smooth muscle calcium-activated large-conductance potassium channels from the extracellular side. *Mol Pharmacol*. 61:1105-1113.

Dick, G.M., I.D. Kong, and K.M. Sanders. 1999. Effects of anion channel antagonists in canine colonic myocytes: comparative pharmacology of Cl^-, Ca^{2+} and K^+ currents. *Br J Pharmacol*. 127:1819-1831.

Du, X.L., Z. Gao, C.P. Lau, S.W. Chiu, H.F. Tse, C.M. Baumgarten, and G.R. Li. 2004. Differential effects of tyrosine kinase inhibitors on volume-sensitive chloride current in human atrial myocytes: evidence for dual regulation by Src and EGFR kinases. *J Gen Physiol*. 123:427-439.

Duan, D., J.R. Hume, and S. Nattel. 1997. Evidence that outwardly rectifying Cl^- channels underlie volume-regulated Cl^- currents in heart. *Circ Res*. 80:103-113.

Duan, D., L. Ye, F. Britton, B. Horowitz, and J.R. Hume. 2000. A novel anionic inward rectifier in native cardiac myocytes. *Circ Res*. 86:E63-71.

Dunten, R.L., M. Sahin-Toth, and H.R. Kaback. 1993. Cysteine scanning mutagenesis of putative helix XI in the lactose permease of Escherichia coli. *Biochemistry*. 32:12644-12650.

Egee, S., B.J. Harvey, and S. Thomas. 1997. Volume-activated DIDS-sensitive whole-cell chloride currents in trout red blood cells. *J Physiol*. 504 (Pt 1):57-63.

Favrot, L., A.E. Grzegorzewicz, D.H. Lajiness, R.K. Marvin, J. Boucau, D. Isailovic, M. Jackson, and D.R. Ronning. 2013. Mechanism of inhibition of Mycobacterium tuberculosis antigen 85 by ebselen. *Nat Commun*. 4:2748.

Garlid, K.D., and A.P. Halestrap. 2012. The mitochondrial K_{ATP} channel--fact or fiction? *J Mol Cell Cardiol*. 52:578-583.

Glass, R.S., F. Farooqui, M. Sabahi, and K.W. Ehler. 1988. Formation of Thiocarbonyl Compounds in the Reaction of Ebselen Oxide with Thiols. *Abstr Pap Am Chem S*. 196:373-Orgn.

Grinstein, S., C.A. Clarke, A. Dupre, and A. Rothstein. 1982. Volume-induced increase of anion permeability in human lymphocytes. *J Gen Physiol*. 80:801-823.

Hagiwara, N., H. Masuda, M. Shoda, and H. Irisawa. 1992. Stretch-activated anion currents of rabbit cardiac myocytes. *J Physiol*. 456:285-302.

Hall, S.K., J.P. Zhang, and M. Lieberman. 1997. An early transient current is associated with hyposmotic swelling and volume regulation in embryonic chick cardiac myocytes. *Experimental Physiology*. 82:43-54.

Hanavan, P.D., C.R. Borges, B.A. Katchman, D.O. Faigel, T.H. Ho, C.T. Ma, E.A. Sergienko, N. Meurice, J.L. Petit, and D.F. Lake. 2015. Ebselen inhibits QSOX1 enzymatic activity and suppresses invasion of pancreatic and renal cancer cell lines. *Oncotarget*. 6:18418-18428.

Haydon, P.G., and G. Carmignoto. 2006. Astrocyte control of synaptic transmission and neurovascular coupling. *Physiol Rev*. 86:1009-1031.

Hazama, A., and Y. Okada. 1988. Ca^{2+} sensitivity of volume-regulatory K^+ and Cl^- channels in cultured human epithelial cells. *J Physiol*. 402:687-702.

Herbst, A.L., C.T. Griffiths, and R.W. Kistner. 1964. Clomiphene Citrate (Nsc-35770) in Disseminated Mammary Carcinoma. *Cancer Chemother Rep*. 43:39-41.

Hoffmann, E.K., L.O. Simonsen, and I.H. Lambert. 1984. Volume-induced increase of K^+ and Cl^- permeabilities in Ehrlich ascites tumor cells. Role of internal Ca^{2+}. *J Membr Biol*. 78:211-222.

Hume, J.R., D. Duan, M.L. Collier, J. Yamazaki, and B. Horowitz. 2000. Anion transport in heart. *Physiol Rev*. 80:31-81.

Jackson, P.S., and K. Strange. 1993. Volume-sensitive anion channels mediate swelling-activated inositol and taurine efflux. *Am J Physiol*. 265:C1489-1500.

Jentsch, T.J., V. Stein, F. Weinreich, and A.A. Zdebik. 2002. Molecular structure and physiological function of chloride channels. *Physiol Rev*. 82:503-568.

Kistner, R.W., and O.W. Smith. 1960. Observations on the use of a non-steroidal estrogen antagonist: MER-25. *Surg Forum*. 10:725-729.

Kunzelmann, K. 2015. TMEM16, LRRC8A, bestrophin: chloride channels controlled by Ca^{2+} and cell volume. *Trends Biochem Sci*. 40:535-543.

Kuziemko, G.M., M. Stroh, and R.C. Stevens. 1996. Cholera toxin binding affinity and specificity for gangliosides determined by surface plasmon resonance. *Biochemistry*. 35:6375-6384.

Lange, S., J. Heger, G. Euler, M. Wartenberg, H.M. Piper, and H. Sauer. 2009. Platelet-derived growth factor BB stimulates vasculogenesis of embryonic stem cell-derived endothelial cells by calcium-mediated generation of reactive oxygen species. *Cardiovasc Res*. 81:159-168.

Lass, A., P. Witting, R. Stocker, and H. Esterbauer. 1996. Inhibition of copper- and peroxyl radical-induced LDL lipid oxidation by ebselen: antioxidant actions in addition to hydroperoxide-reducing activity. *Biochim Biophys Acta*. 1303:111-118.

Leurs, R., H. Timmerman, and A. Bast. 1989. Inhibition of superoxide anion radical production by ebselen (PZ51) and its sulfur analogue (PZ25) in guinea pig alveolar macrophages. *Biochem Int*. 18:295-299.

Li, X., K. Shimada, L.A. Showalter, and S.A. Weinman. 2000. Biophysical properties of ClC-3 differentiate it from swelling-activated chloride channels in Chinese hamster ovary-K1 cells. *J Biol Chem*. 275:35994-35998.

Mongin, A.A. 2015. Volume-regulated anion channel-a frenemy within the brain. *Pflugers Arch*.

Müller, A., E. Cadenas, P. Graf, and H. Sies. 1984. A Novel Biologically-Active Organoselenium Compound-1: Glutathione Peroxidase-Like Activity In vitro and Antioxidant Capacity of PZ-51 (Ebselen). *Biochemical Pharmacology*. 33:3235-3239.

Nakamura, Y., Q. Feng, T. Kumagai, K. Torikai, H. Ohigashi, T. Osawa, N. Noguchi, E. Niki, and K. Uchida. 2002. Ebselen, a glutathione peroxidase mimetic seleno-organic compound, as a multifunctional antioxidant. Implication for inflammation-associated carcinogenesis. *J Biol Chem*. 277:2687-2694.

Nilius, B., J. Eggermont, T. Voets, G. Buyse, V. Manolopoulos, and G. Droogmans. 1997. Properties of volume-regulated anion channels in mammalian cells. *Prog Biophys Mol Biol*. 68:69-119.

Pacher, P., J.S. Beckman, and L. Liaudet. 2007. Nitric oxide and peroxynitrite in health and disease. *Physiol Rev*. 87:315-424.

Park, S.J., C.M. McKay, Y. Zhu, and J.D. Huizinga. 2005. Volume-activated chloride currents in interstitial cells of Cajal. *Am J Physiol Gastrointest Liver Physiol*. 289: G791-797.

Parkerson, K.A., and H. Sontheimer. 2003. Contribution of chloride channels to volume regulation of cortical astrocytes. *Am J Physiol Cell Physiol*. 284:C1460-1467.

Parpura, V., M.T. Heneka, V. Montana, S.H. Oliet, A. Schousboe, P.G. Haydon, R.F. Stout, Jr., D.C. Spray, A. Reichenbach, T. Pannicke, M. Pekny, M. Pekna, R. Zorec, and A. Verkhratsky. 2012. Glial cells in (patho)physiology. *J Neurochem*. 121:4-27.

Qiu, Z., A.E. Dubin, J. Mathur, B. Tu, K. Reddy, L.J. Miraglia, J. Reinhardt, A.P. Orth, and A. Patapoutian. 2014. SWELL1, a plasma membrane protein, is an essential component of volume-regulated anion channel. *Cell*. 157:447-458.

Queliconi, B.B., A.P. Wojtovich, S.M. Nadtochiy, A.J. Kowaltowski, and P.S. Brookes. 2011. Redox regulation of the mitochondrial K_{ATP} channel in cardioprotection. *Biochim Biophys Acta*. 1813:1309-1315.

Radany, E.H., M. Brenner, F. Besnard, V. Bigornia, J.M. Bishop, and C.F. Deschepper. 1992. Directed establishment of rat brain cell lines with the phenotypic characteristics of type 1 astrocytes. *Proc Natl Acad Sci U S A*. 89:6467-6471.

Ren, Z., and C.M. Baumgarten. 2005. Antagonistic regulation of swelling-activated Cl^- current in rabbit ventricle by Src and EGFR protein tyrosine kinases. *Am J Physiol Heart Circ Physiol*. 288:H2628-2636.

Ren, Z., F.J. Raucci, Jr., D.M. Browe, and C.M. Baumgarten. 2008. Regulation of swelling-activated Cl^- current by angiotensin II signalling and NADPH oxidase in rabbit ventricle. *Cardiovasc Res*. 77:73-80.

Sakaguchi, M., H. Matsuura, and T. Ehara. 1997. Swelling-induced Cl^- current in guinea-pig atrial myocytes: inhibition by glibenclamide. *J Physiol*. 505 (Pt 1):41-52.

Sakurai, T., M. Kanayama, T. Shibata, K. Itoh, A. Kobayashi, M. Yamamoto, and K. Uchida. 2006. Ebselen, a seleno-organic antioxidant, as an electrophile. *Chem Res Toxicol*. 19:1196-1204.

Sarkadi, B., E. Mack, and A. Rothstein. 1984. Ionic events during the volume response of human peripheral blood lymphocytes to hypotonic media. I. Distinctions between volume-activated Cl^- and K^+ conductance pathways. *J Gen Physiol*. 83:497-512.

Sarkadi, B., E. Mack, and A. Rothstein. 1984. Ionic events during the volume response of human peripheral blood lymphocytes to hypotonic media. II. Volume- and time-dependent activation and inactivation of ion transport pathways. *J Gen Physiol*. 83:513-527.

Satterwhite, C.M., M. Hermoso, S. Wilson, B. Horowitz, and J.R. Hume. 2002. Inhibition of native volume-senstive chloride currents and RVD in HeLa cells and Xenopus laevis oocytes by ClC-3 antisense. *Biophysical Journal*. 82:242a-242a.

Scheel, O., A.A. Zdebik, S. Lourdel, and T.J. Jentsch. 2005. Voltage-dependent electrogenic chloride/proton exchange by endosomal CLC proteins. *Nature*. 436:424-427.

Schewe, T. 1995. Molecular actions of ebselen--an antiinflammatory antioxidant. *Gen Pharmacol*. 26:1153-1169.

Seifert, G., K. Schilling, and C. Steinhauser. 2006. Astrocyte dysfunction in neurological disorders: a molecular perspective. *Nat Rev Neurosci*. 7:194-206.

Shimizu, T., T. Numata, and Y. Okada. 2004. A role of reactive oxygen species in apoptotic activation of volume-sensitive Cl^- channel. *Proc Natl Acad Sci U S A*. 101:6770-6773.

Shuba, L.M., T. Ogura, and T.F. McDonald. 1996. Kinetic evidence distinguishing volume-sensitive chloride current from other types in guinea-pig ventricular myocytes. *J Physiol*. 491 (Pt 1):69-80.

Sies, H. 1993. Ebselen, a selenoorganic compound as glutathione peroxidase mimic. *Free Radic Biol Med*. 14:313-323.

Sies, H., and H. Masumoto. 1997. Ebselen as a glutathione peroxidase mimic and as a scavenger of peroxynitrite. *Adv Pharmacol*. 38:229-246.

Smith, S.M., J. Min, T. Ganesh, B. Diebold, T. Kawahara, Y. Zhu, J. McCoy, A. Sun, J.P. Snyder, H. Fu, Y. Du, I. Lewis, and J.D. Lambeth. 2012. Ebselen and congeners inhibit NADPH oxidase 2-dependent superoxide generation by interrupting the binding of regulatory subunits. *Chem Biol*. 19:752-763.

Smitherman, K.A., and H. Sontheimer. 2001. Inhibition of glial Na^+ and K^+ currents by tamoxifen. *J Membr Biol*. 181:125-135.

Sorota, S. 1994. Pharmacologic properties of the swelling-induced chloride current of dog atrial myocytes. *J Cardiovasc Electrophysiol*. 5:1006-1016.

Stielow, C., R.A. Catar, G. Muller, K. Wingler, P. Scheurer, H.H. Schmidt, and H. Morawietz. 2006. Novel Nox inhibitor of oxLDL-induced reactive oxygen species formation in human endothelial cells. *Biochem Biophys Res Commun*. 344:200-205.

Stobrawa, S.M., T. Breiderhoff, S. Takamori, D. Engel, M. Schweizer, A.A. Zdebik, M.R. Bosl, K. Ruether, H. Jahn, A. Draguhn, R. Jahn, and T.J. Jentsch. 2001. Disruption of ClC-3, a chloride channel expressed on synaptic vesicles, leads to a loss of the hippocampus. *Neuron*. 29:185-196.

Sun, Q.A., D.T. Hess, B. Wang, M. Miyagi, and J.S. Stamler. 2012. Off-target thiol alkylation by the NADPH oxidase inhibitor 3-benzyl-7-(2-benzoxazolyl)thio-1,2,3-triazolo[4,5-d]pyrimidine (VAS2870). *Free Radic Biol Med*. 52:1897-1902.

Szucs, G., G. Buyse, J. Eggermont, G. Droogmans, and B. Nilius. 1996. Characterization of volume-activated chloride currents in endothelial cells from bovine pulmonary artery. *J Membr Biol*. 149:189-197.

Traebert, M., K. Kohler, G. Lambert, J. Biber, I. Forster, and H. Murer. 2001. Investigating the surface expression of the renal type IIa Na^+/P_i-cotransporter in Xenopus laevis oocytes. *J Membr Biol*. 180:83-90.

Tseng, G.N. 1991. Cell swelling activates a membrane Cl^- channel in canine cardiac myocytes. *Biophys. J.* 59:91a.

Tseng, G.N. 1992. Cell swelling increases membrane conductance of canine cardiac cells: evidence for a volume-sensitive Cl^- channel. *Am J Physiol*. 262:C1056-1068.

Urbaniak, M.D., J.N. Tabudravu, A. Msaki, K.M. Matera, R. Brenk, M. Jaspars, and M.A.J. Ferguson. 2006. Identification of novel inhibitors of UDP-Glc 4'-epimerase, a validated drug target for African sleeping sickness. *Bioorganic & Medicinal Chemistry Letters*. 16:5744-5747.

Vandenberg, J.I., A. Yoshida, K. Kirk, and T. Powell. 1994. Swelling-activated and isoprenaline-activated chloride currents in guinea pig cardiac myocytes have distinct electrophysiology and pharmacology. *J Gen Physiol*. 104:997-1017.

Varela, D., F. Simon, A. Riveros, F. Jorgensen, and A. Stutzin. 2004. NAD(P)H oxidase-derived H_2O_2 signals chloride channel activation in cell volume regulation and cell proliferation. *J Biol Chem*. 279:13301-13304.

Verdon, B., J.P. Winpenny, K.J. Whitfield, B.E. Argent, and M.A. Gray. 1995. Volume-activated chloride currents in pancreatic duct cells. *J Membr Biol*. 147:173-183.

Verrecchia, F., and J. Herve. 1997. Reversible inhibition of gap junctional communication by tamoxifen in cultured cardiac myocytes. *Pflugers Arch*. 434:113-116.

Voss, F.K., F. Ullrich, J. Munch, K. Lazarow, D. Lutter, N. Mah, M.A. Andrade-Navarro, J.P. von Kries, T. Stauber, and T.J. Jentsch. 2014. Identification of LRRC8 heteromers as an essential component of the volume-regulated anion channel VRAC. *Science*. 344:634-638.

Wagner, D.A., and C. Czajkowski. 2001. Structure and dynamics of the GABA binding pocket: A narrowing cleft that constricts during activation. *J Neurosci*. 21:67-74.

Wakamura, K., T. Ohtsuka, N. Okamura, S. Ishibashi, and H. Masayasu. 1990. Mechanism for the Inhibitory Effect of a Selenoorganic Compound, Ebselen, and Its Analogs on Superoxide Anion Production in Guinea-Pig Polymorphonuclear Leukocytes. *J Pharmacobio-Dynam*. 13:421-425.

Wang, L., L. Chen, and T.J. Jacob. 2000. The role of ClC-3 in volume-activated chloride currents and volume regulation in bovine epithelial cells demonstrated by antisense inhibition. *J Physiol*. 524 Pt 1:63-75.

Ward, H.W. 1973. Anti-oestrogen therapy for breast cancer: a trial of tamoxifen at two dose levels. *Br Med J*. 1:13-14.

Wendel, A., M. Fausel, H. Safayhi, G. Tiegs, and R. Otter. 1984. A Novel biologically-active organoselenium Compound-2: Activity of Pz-51 in Relation to Glutathione-Peroxidase. *Biochemical Pharmacology*. 33:3241-3245.

Wind, S., K. Beuerlein, M.E. Armitage, A. Taye, A.H. Kumar, D. Janowitz, C. Neff, A.M. Shah, K. Wingler, and H.H. Schmidt. 2010. Oxidative stress and endothelial dysfunction in aortas of aged spontaneously hypertensive rats by NOX1/2 is reversed by NADPH oxidase inhibition. *Hypertension*. 56:490-497.

Yamamoto, S., K. Ichishima, and T. Ehara. 2008. Regulation of volume-regulated outwardly rectifying anion channels by phosphatidylinositol 3,4,5-trisphosphate in mouse ventricular cells. *Biomed Res-Tokyo*. 29:307-315.

Yamamoto-Mizuma, S., G.X. Wang, L.L. Liu, K. Schegg, W.J. Hatton, D. Duan, T.L. Horowitz, F.S. Lamb, and J.R. Hume. 2004. Altered properties of volume-sensitive osmolyte and anion channels (VSOACs) and membrane protein expression in cardiac and smooth muscle myocytes from Clcn3-/- mice. *J Physiol*. 557:439-456.

Yamazaki, J., and J.R. Hume. 1997. Inhibitory effects of glibenclamide on cystic fibrosis transmembrane regulator, swelling-activated, and Ca^{2+}-activated Cl^- channels in mammalian cardiac myocytes. *Circ Res*. 81:101-109.

Yang, N., A.L. George, Jr., and R. Horn. 1996. Molecular basis of charge movement in voltage-gated sodium channels. *Neuron*. 16:113-122.

Ye, Z.C., N. Oberheim, H. Kettenmann, and B.R. Ransom. 2009. Pharmacological "cross-inhibition" of connexin hemichannels and swelling activated anion channels. *Glia*. 57:258-269.

Zhang, F., S.S. Lau, and T.J. Monks. 2011. The cytoprotective effect of N-acetyl-L-cysteine against ROS-induced cytotoxicity is independent of its ability to enhance glutathione synthesis. *Toxicol Sci*. 120:87-97.

Zhang, J., R.L. Rasmusson, S.K. Hall, and M. Lieberman. 1993. A chloride current associated with swelling of cultured chick heart cells. *J Physiol*. 472:801-820.

Zhao, R., H. Masayasu, and A. Holmgren. 2002. Ebselen: a substrate for human thioredoxin reductase strongly stimulating its hydroperoxide reductase activity and a superfast thioredoxin oxidant. *Proc Natl Acad Sci U S A*. 99:8579-8584.

APPENDIX

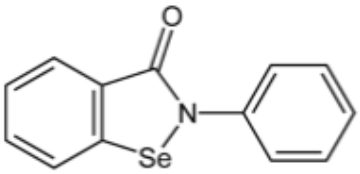

Ebselen (Ebs)

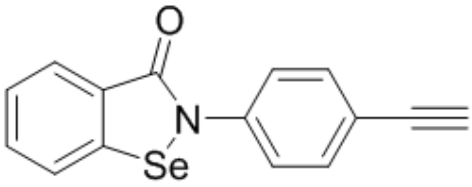

Ebselen-*para*-yne (Ebs-*p*-yne)

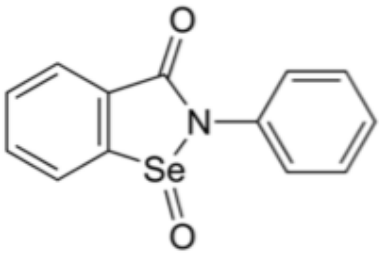

Ebselen Oxide (EbO)

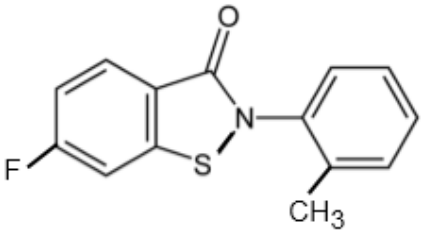

Thr101

FIG. 1: Structures of Ebs and its congeners

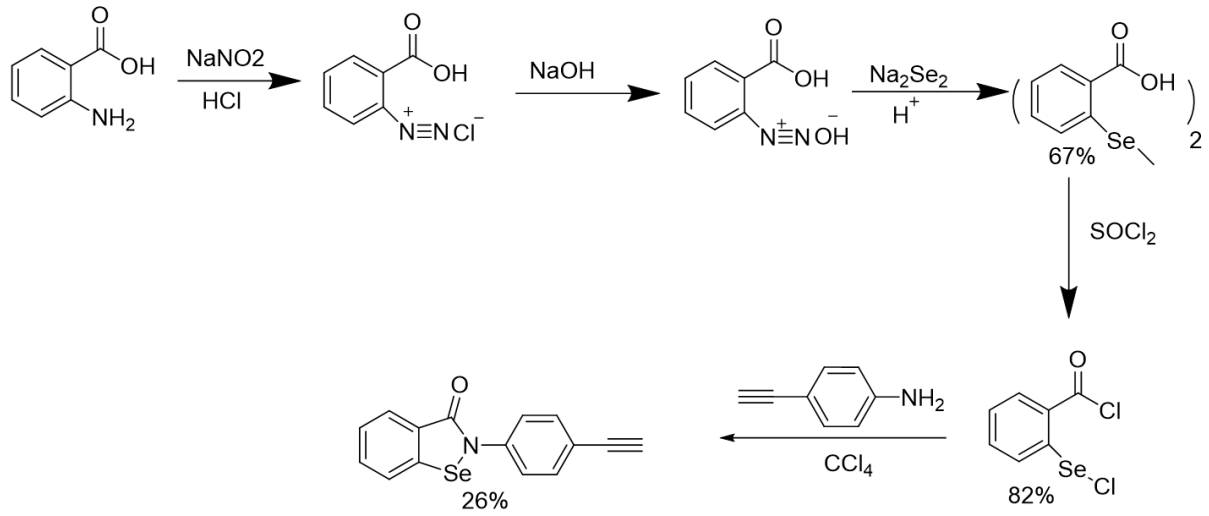

FIG. 2: Steps for organic synthesis of Ebs-*p*-yne (Hartman Lab).
Step 1: Antranillic acid was first dissolved in water. HCl was then added and cooled down to -18 ˚C for proper formation of nitronium ion, which only exists below -15 ˚C. Once properly cooled, addition of sodium nitrate dissolved in water lead to nitronium ion generation. Using Rongalite and NaOH, the solution was then made basic for stabilizing diselenide species. The reaction mixture was stirred under reflux for 1 h. The mixture was then reacidified and the precipitate was filtered prior to redissolving under basic condition. This basic mixture was once more filtered and made acidic prior to final filtration. The intermediate (67% yield) compound was then obtained from hot ethanol.

Step 2: Thionyl chloride was added as solvent/reagent, refluxed for 3 h under inert condition, and removed under decreased pressure. The remaining solid was then crystalized with hexanes to generate a chlorinated intermediate (82% yield).

Step 3: This chlorinated intermediate was then dissolved in CCl_4 and corresponding 2-, 3-, or 4-Ethynylaniline dissolved in CCl_4 was added using a syringe. Final mixture was stirred for ~45 min – 1 h before purifying via column chromatography. For generating Ebs-*p*-yne [para (*p*)-Ebs derivative] with a 26% yield, 4-Ethynylaniline/ CCl_4 was added. Adding either 2-Ethynylaniline or 3-Ethynylaniline would analogously lead to Ebs-*o*-yne (ortho) or Ebs-*m*-yne (meta) derivatives, respectively.

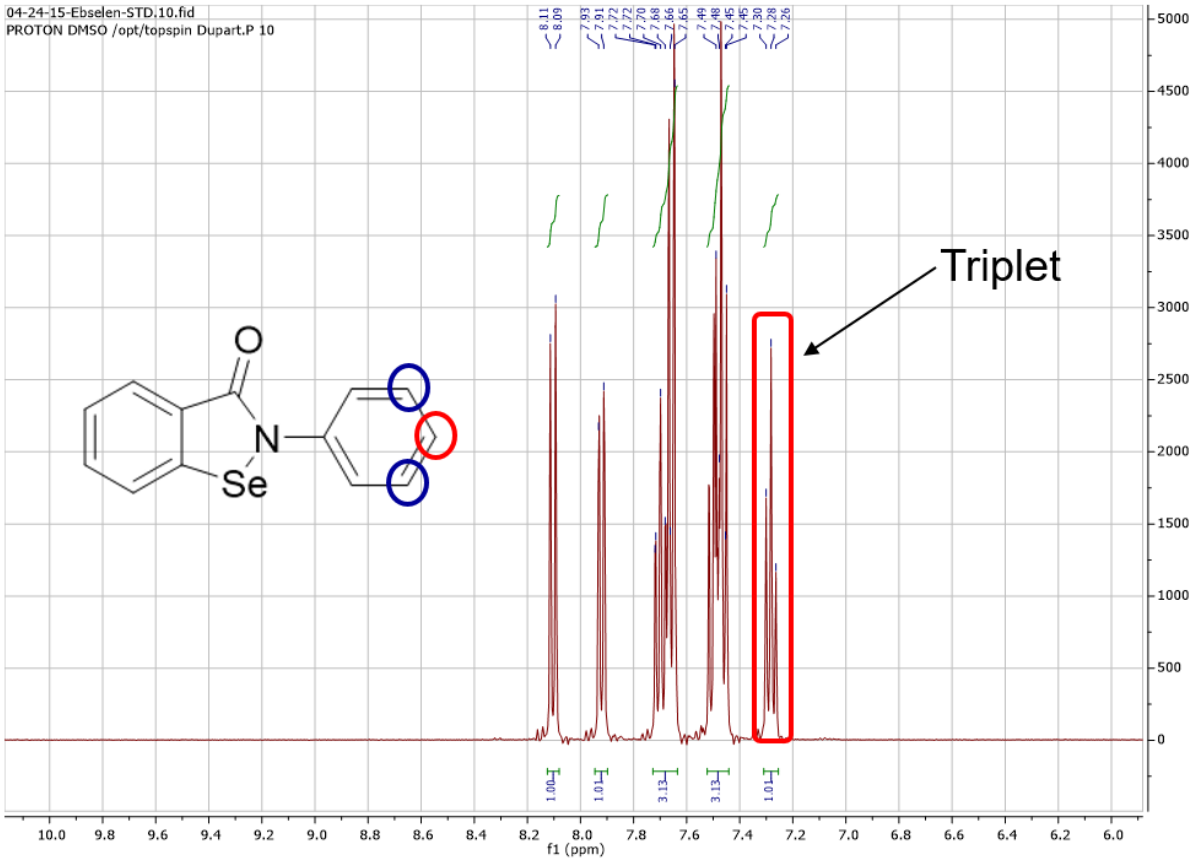

FIG. 3: ^{1}H-NMR spectrum of Ebselen (Ebs) prior to derivatization (Hartman Lab). Structure of Ebs is shown as reference along with five specific peaks each with appropriate splitting. Prior to derivatization, chemical shift at 7.3 ppm (triplet) due to proton (red circle) on the para position of benzene ring of Ebs each split by adjacent protons (blue circles) is noticeably prominent.

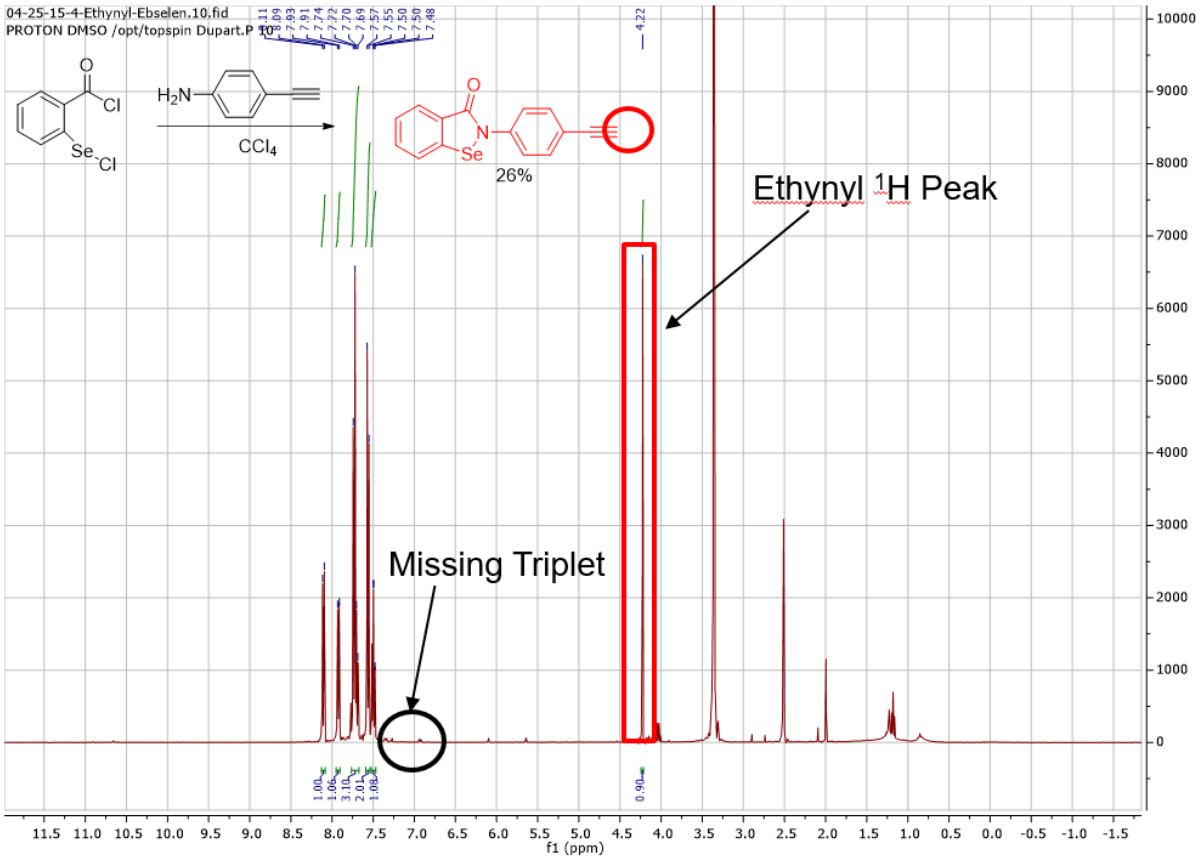

FIG. 4: ^{1}H-NMR spectrum of Ebs-*p*-yne (Hartman Lab). Upon adding 4-Ethynylaniline to last step of synthesis, prominent chemical shift at 7.3 ppm (missing triplet) normally observed in Ebs disappeared with the appearance of an ethynyl proton (red circle) peak at 4.2 ppm.

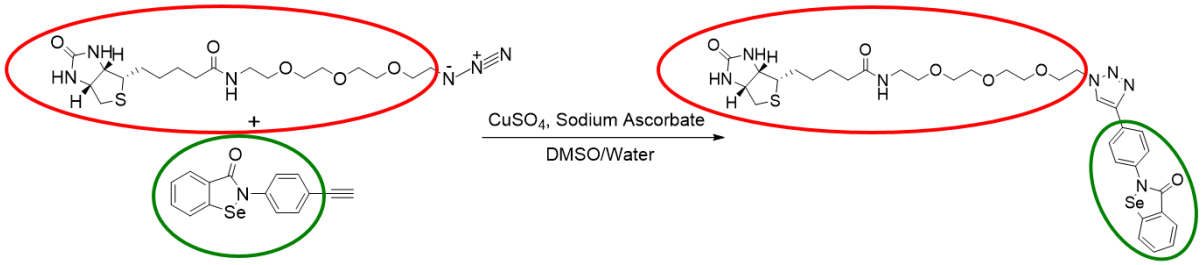

FIG. 5: Huisgen cycloaddition (click chemistry) of azido-PEG$_3$-biotin and Ebs-*p*-yne for synthesizing Ebs-PEG$_3$-biotin (Ebs-biotin) (Hartman Lab).

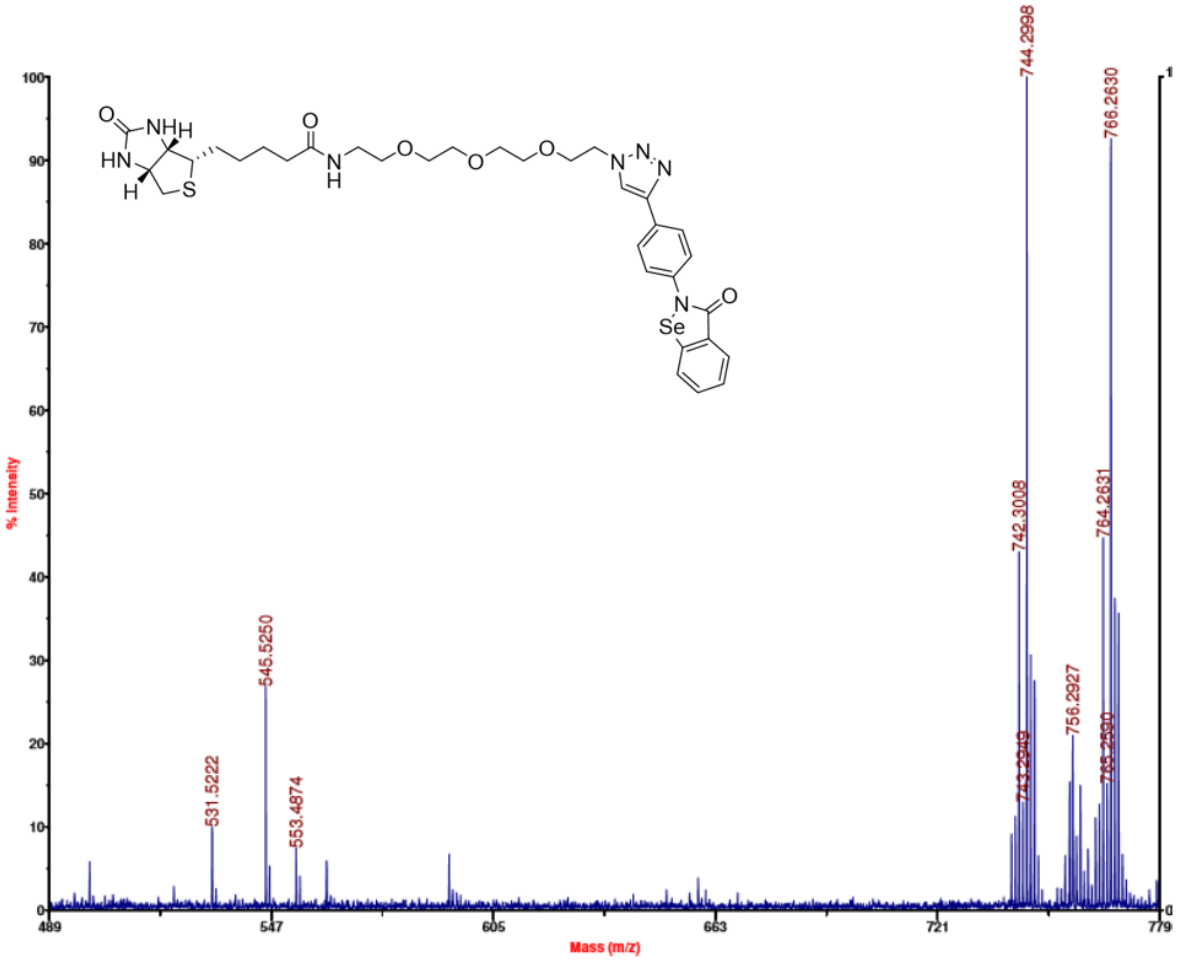

FIG. 6: Matrix-assisted laser desorption/ionization-Time of flight (MALDI-TOF) (Hartman Lab). Proper synthesis of Ebs-PEG3-Biotin was verified showing an exact mass of 743.20 Daltons. Due to existence of various selenium isotopes found in nature, multiple peaks were found and are shown on the right (742.3008; 743.2949; 744.2998).

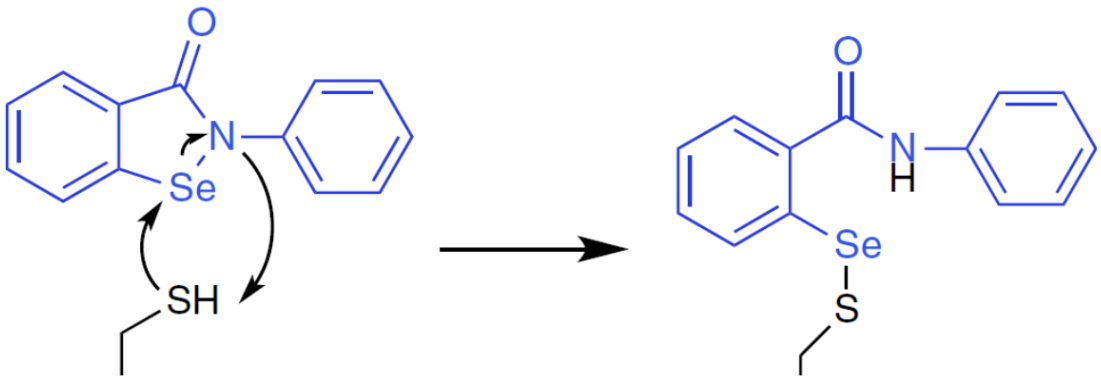

FIG. 7: Thiol-mediated nucleophilic attack of Ebs. Free -SH groups can directly attack the Se of Ebs leading to the formation of S-Se bond as shown. The figure has been adapted from Favrot et al. (2013).

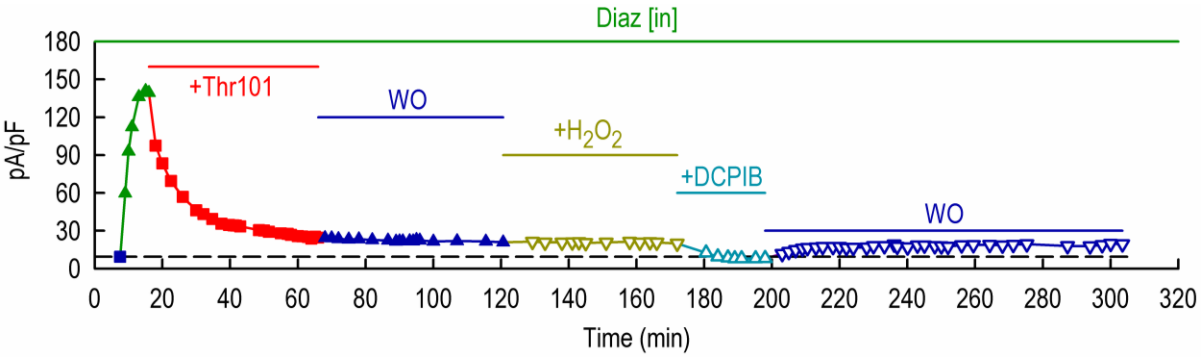

FIG. 8: Effect of DCPIB fully reversed. This is the extension of the time-course shown in Fig. 13 (*D*) of Results. $I_{Cl,swell}$ was elicited with 53 μM back-filled diazoxide (Diaz [in]). After failure of 500 μM H_2O_2 (dark yellow) to recover $I_{Cl,swell}$ following block with 15 μM Thr101 (red), 10 μM DCPIB (cyan) completely blocked the remaining current down to initial basal level (~10 pA/pF) in ~10 min. However, following <10 min of washout (WO) with 1T, DCPIB fully reversed and current reached ~25 pA/pF, the original current density reached with 10 μM Thr101 block near ~65 min, and remained for the next ~95 min. This demonstrated that DCPIB is more efficacious than Thr101; nonetheless, unlike Thr101, DCPIB block is fully reversible.

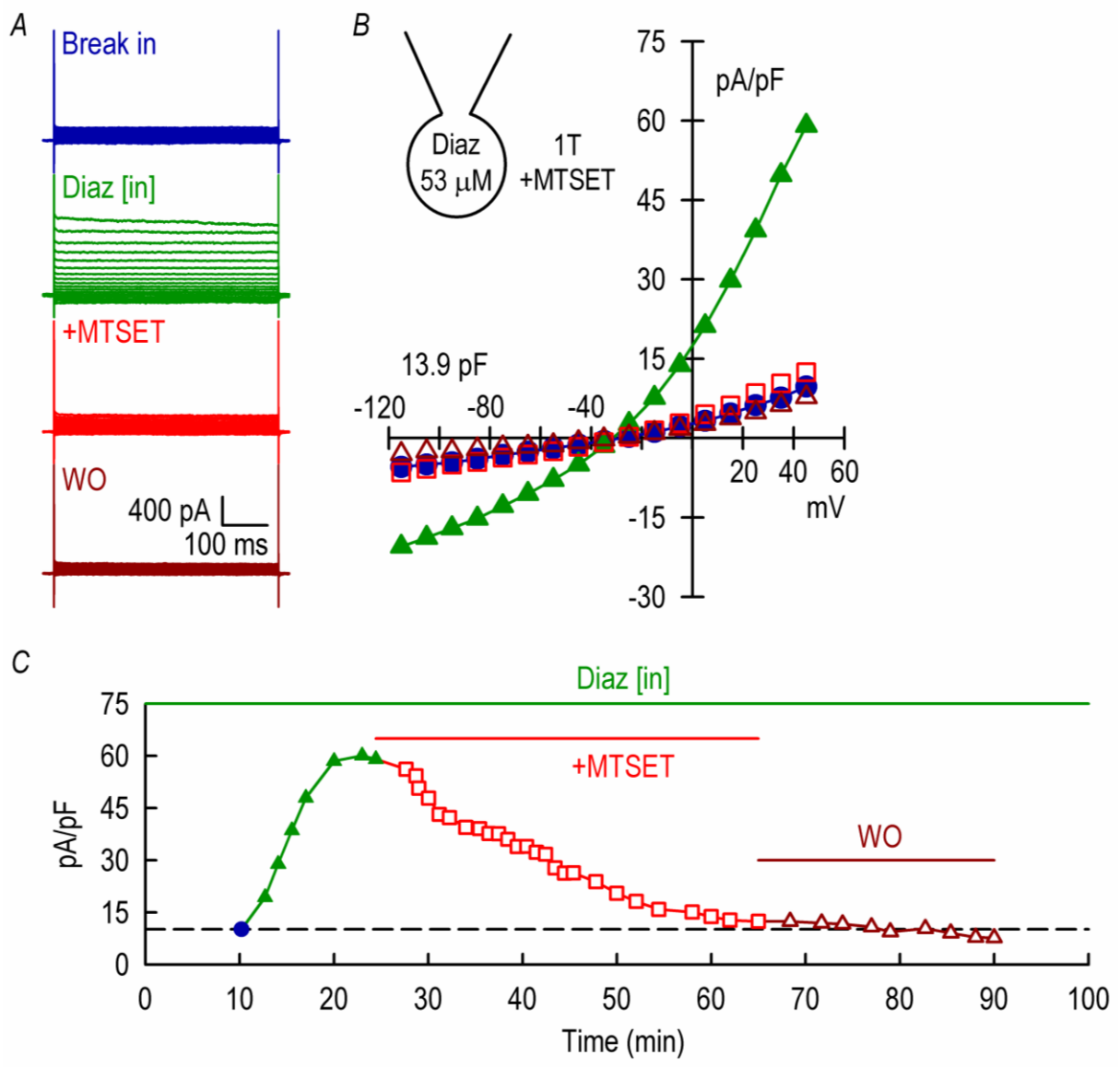

FIG. 9: MTSET blocked $I_{Cl,swell}$ and failed to washout. $I_{Cl,swell}$ was activated with Diaz [in] and blocked with MTSET prior to attempted washout (WO) in 1T. Current traces (***A***) and *I-V* relationships (***B***) showing break in (blue), activation with Diaz [in] (green), block with 110 μM MTSET (red), and WO with 1T (dark red). ***C***. Time-course for the experiment; time of break in denoted by filled blue circle.

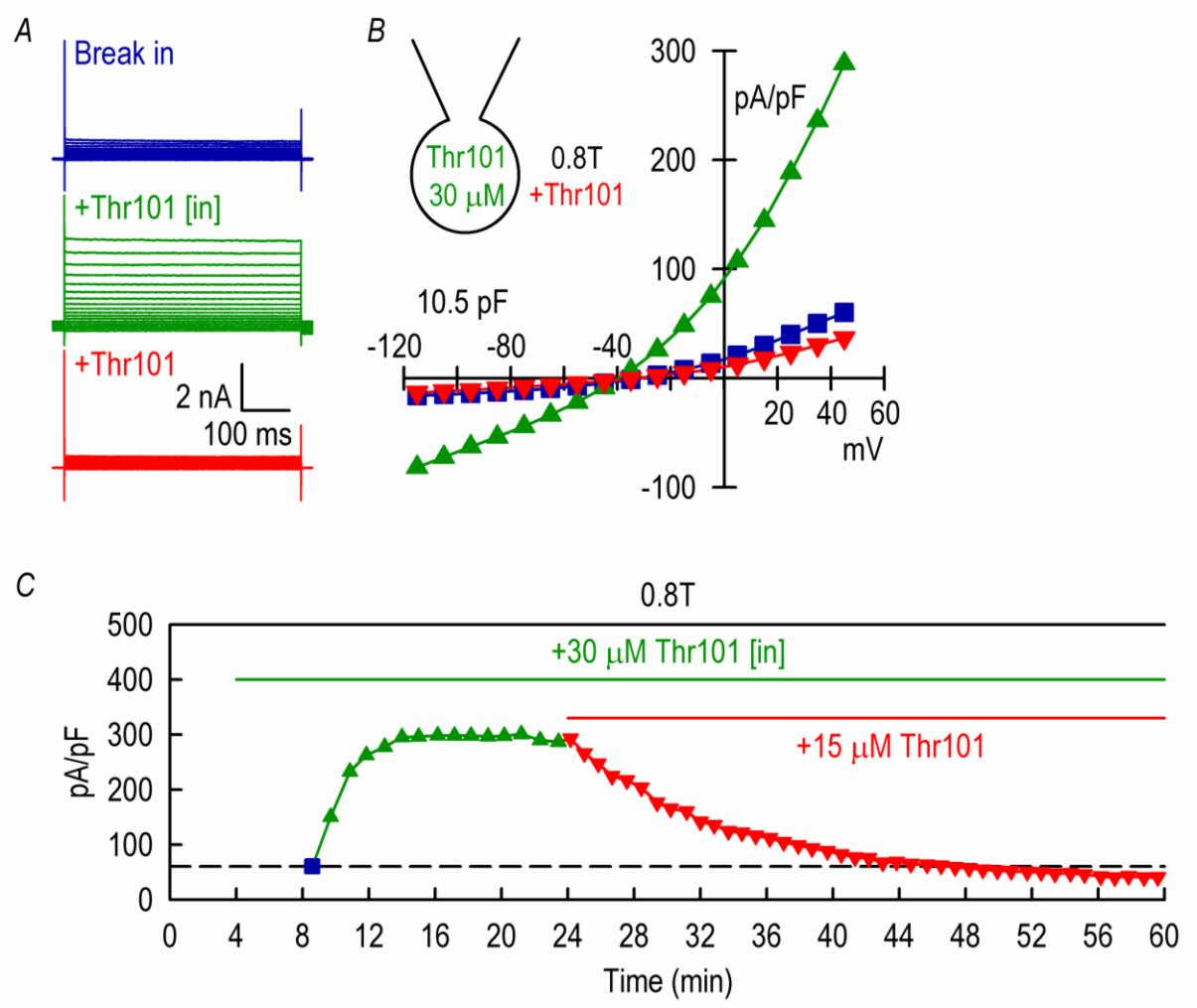

FIG. 10: Thr101 blocked $I_{Cl,swell}$ only from the outside. $I_{Cl,swell}$ was activated with 0.8T with 30 μM Thr101 back-filled in pipette (Thr101 [in]; see inset) and was blocked by 15 μM external Thr101 in 0.8T. Current traces (***A***) and *I-V* relationships (***B***) showing break in (blue), activation with 0.8T (green), and block with 15 μM Thr101 (red) in 0.8T. ***C***. Time-course for the experiment; time of break in denoted by filled blue square.

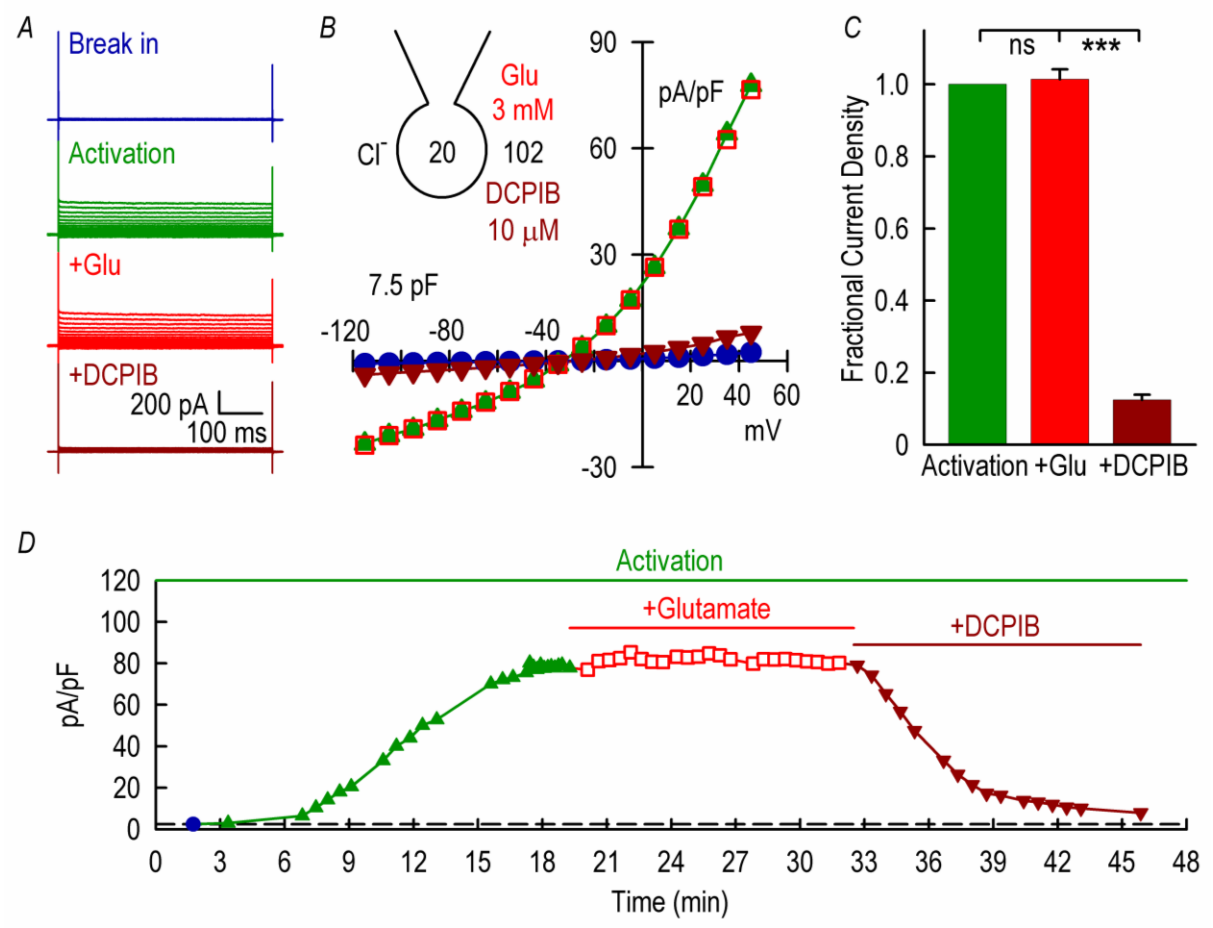

FIG. 11: Glutamate failed to block $I_{Cl,swell}$. After activation of $I_{Cl,swell}$, 3 mM glutamate (Glu) failed to block the current compared to full block by 10 μM DCPIB. Current traces (***A***) and *I-V* relationships (***B***) showing break in (blue), activation of $I_{Cl,swell}$ (green), 3 mM Glu (red), and 10 μM DCPIB (dark red). ***C***. Glu (3 mM) failed to block (n = 4, P = 0.490; *ns*) the activated current (83.1 ± 26.3 pA/pF) compared to 98.5 ± 1.5% block by DCPIB (n = 4, P < 0.001). ***D***. Time-course for activation, Glu addition, and block by DCPIB; time of break in indicated by filled circle (blue).

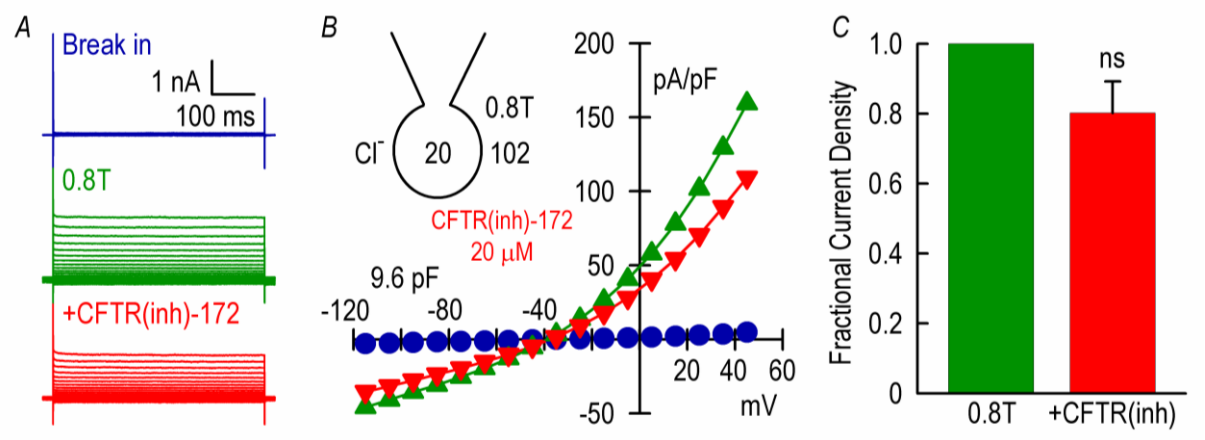

FIG. 12: CFTR(inh)-172 failed to block $I_{Cl,swell}$. After activation of $I_{Cl,swell}$ with 0.8T, 20 μM CFTR(inh)-172 failed to block the current. Current traces (***A***) and *I-V* relationships (***B***) showing break in (blue), 0.8T-induced activation of $I_{Cl,swell}$ (green), and 20 μM CFTR(inh)-172 (red). ***C***. CFTR(inh)-172 (20 μM) failed to block 80.2 ± 9.0% (*n* = 6, *P* = 0.079; *ns*) of the activated current (189.1 ± 39.2 pA/pF).

Ebs [in] Affected $I_{Cl,swell}$ Block by VAS2870

VAS2870 (3-Benzyl-7-(2-benzoxazolyl)thio-1,2,3-triazolo(4,5-d)pyrimidine) is a cell-permeable NOX inhibitor with an IC_{50} in the micromolar range widely used in studies involving NOX-dependent ROS generation in multiple cell types (Wind et al., 2010; Lange et al., 2009; Stielow et al., 2006). When 6 μM VAS2870 was superfused following 0.8T-induced steady-state activation of $I_{Cl,swell}$, VAS2870 failed to block the current during a 15-min exposure. In contrast, in the same cell, $I_{Cl,swell}$ was fully blocked by 15 μM Ebs in ~1-2 min (Appendix, Fig. 13). However, when the same experiment was repeated with back-filled Ebs (Ebs [in], 15 μM; Appendix, Fig. 14; see inset), 6 μM VAS2870 superfusion in 0.8T gradually but only partially blocked the current in ~25 min (Appendix, Fig. 14).

This study points to an as yet undefined role for Ebs [in] when cell-permeable VAS2870 is superfused. We previously showed the inability of Ebs [in] (30 μM) to block $I_{Cl,swell}$ from the inside in 0.8T bath solution (Results, Fig. 20). Therefore, Ebs [in] alone was not primarily responsible for block shown in Fig. 14 of Appendix. This then leaves VAS2870, the common component of both Fig. 13 and 14 of Appendix, as the key player leading to $I_{Cl,swell}$ block in the presence of intracellular Ebs (Ebs [in]). Although the mechanism is uncertain, one possibility is that VAS2870 permeated the membrane and bound to Ebs [in] generating a product with distinct properties. Alternatively, the action of VAS2870 may have sensitized steps involved in the activation of $I_{Cl,swell}$ so that they now could be blocked by Ebs [in]. In fact, an off-target interaction of VAS2870 with GSH previously was demonstrated by Sun et al. (2012) using mass spectrometric analysis (LC-ESI-MS). In each of these examples, we can be assured that back-filled Ebs [in] successfully diffused into the cytoplasm, ruling out the possibility that Ebs [in] failed to inhibit $I_{Cl,swell}$ due to absorption by the inner walls of the borosilicate glass pipette as has been suggested (D.E. Logothetis, personal communication).

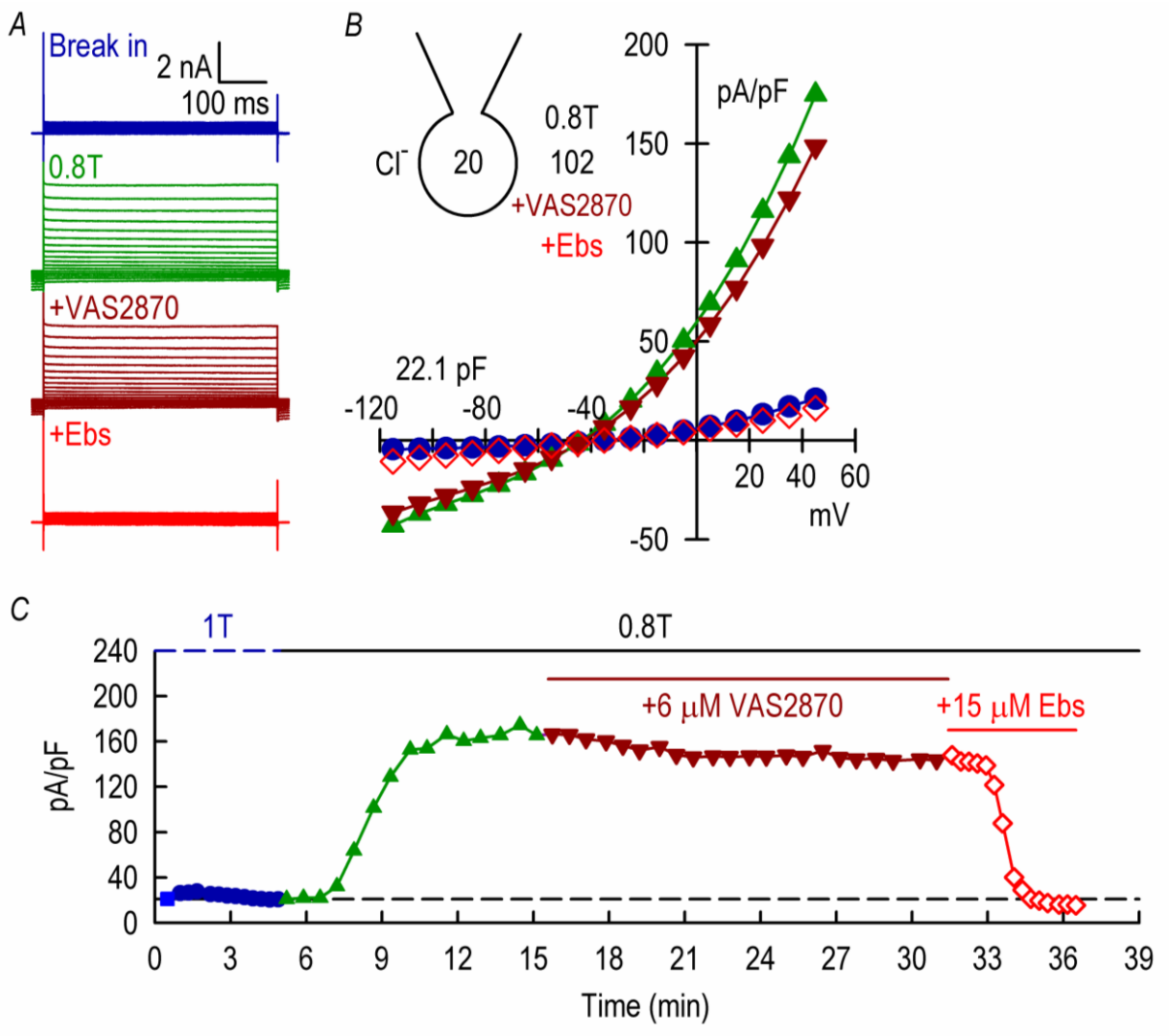

FIG. 13: VAS2870 failed to block $I_{Cl,swell}$. After activation of $I_{Cl,swell}$ with 0.8T, 6 μM VAS2870 superfusion failed to block the current compared to 15 μM Ebs. Current traces (***A***) and *I-V* relationships (***B***) showing break in (blue), 0.8T-induced activation of $I_{Cl,swell}$ (green), 6 μM VAS2870 (dark red), and 15 μM Ebs (red). ***C***. Time-course for the experiment; time of break in denoted by filled blue square.

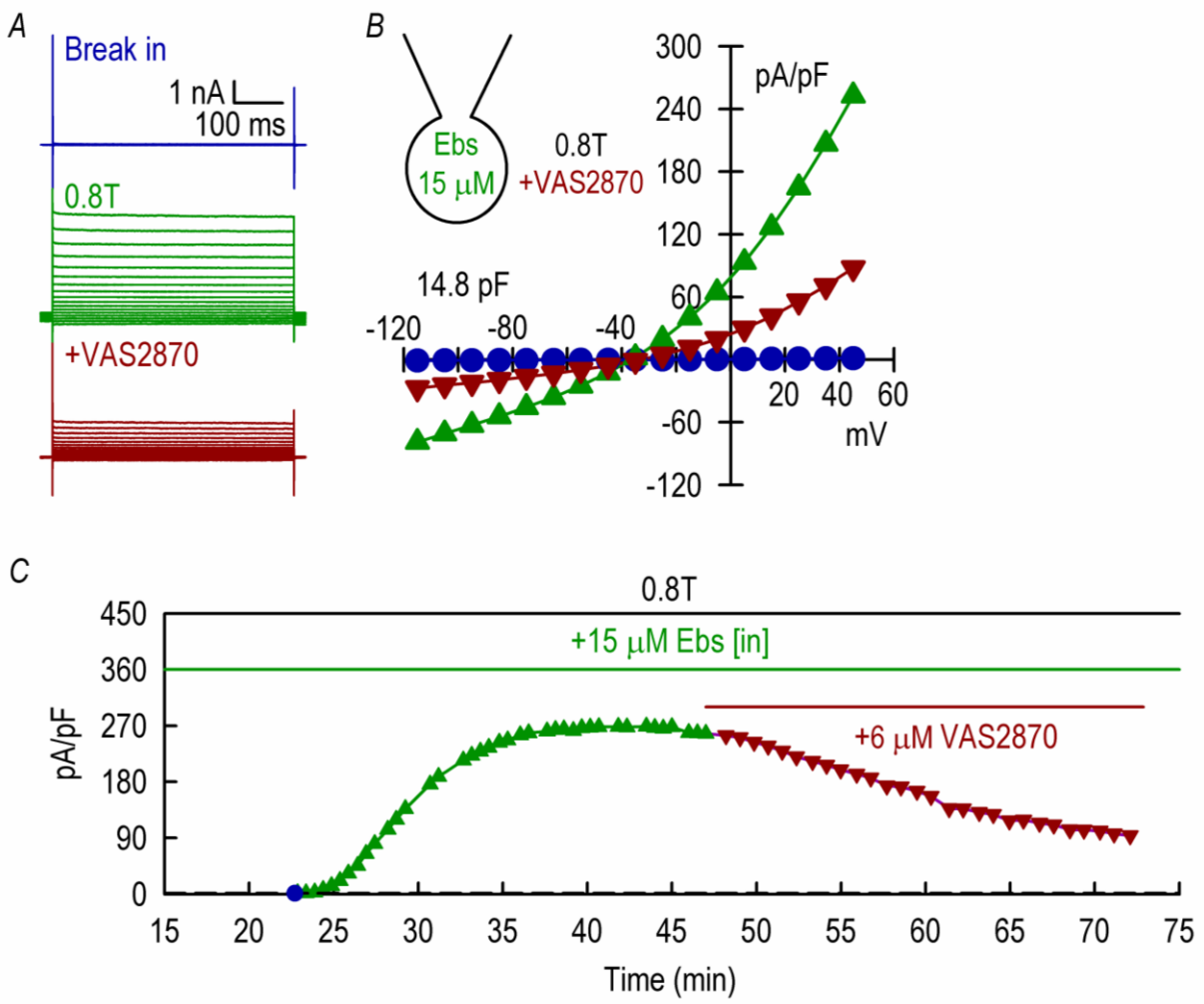

FIG. 14: VAS2870 blocked $I_{Cl,swell}$ in the presence of Ebs [in]. $I_{Cl,swell}$ was activated with 0.8T with Ebs back-filled in pipette (Ebs [in], 15 μM; see inset) and was blocked by 6 μM external VAS2870 in 0.8T. Current traces (***A***) and *I-V* relationships (***B***) showing break in (blue), activation with 0.8T (green), and slow block with 6 μM VAS2870 (dark red) in 0.8T. ***D***. Time-course for the experiment; time of break in denoted by filled blue circle.

VITA

Sung Hoon Park (Korean: 박성훈) was born January 1, 1972 in Seoul, S. Korea. He immigrated to the United States with his father and sister (Amy Eui Seong Park) to join his mother already living in Los Angeles, CA. He graduated from Westlake High School in Westlake Village, CA in 1990 prior to attending University of California at Los Angeles from 1990-1996. He earned his B.Sc. in Biochemistry in 1996. While attending a M.Sc. program at University of San Francisco from 2007 through 2010, he accepted entrance into Medical College of Virginia (MCV) Ph.D. program via the Biomedical Portal in 2010. In 2013, Sung was awarded the Ramsey Award, which is awarded to the most outstanding doctoral student. He successfully defended his Ph.D. Defense in July 20, 2016 at MCV. His project lead to the discovery of ebselen-*para*-yne (Ebs-*p*-yne) which demonstrated the highest affinity for the swelling-activated chloride current ($I_{Cl,swell}$) ever reported to date. His project demonstrating complete block of $I_{Cl,swell}$ with 5 nM Ebs-*p*-yne made the cover page of the yearly Departmental Physiology and Biophysics summer retreat booklet. Several manuscripts are under preparation regarding his research project including a first author paper.